



UNIVERSIDADE FEDERAL DE SERGIPE
PRÓ-REITORIA DE PÓS-GRADUAÇÃO E PESQUISA

***QUÍMICA MINERAL DE CRISTAIS DE BIOTITA EM
ENCLAVES SIENÍTICOS EM GRANITOS DO STOCK
GRANÍTICO GLÓRIA SUL, DOMÍNIO MACURURÉ,
SUL DA PROVÍNCIA BORBOREMA***

Asayuki Rodrigues de Menezes

Orientador: Dr. Herbet Conceição

Coorientadora: Dra. Maria de Lourdes da Silva Rosa

DISSERTAÇÃO DE MESTRADO

Programa de Pós-Graduação em Geociências e Análise de Bacias

São Cristóvão-SE
– 2022 –

Asayuki Rodrigues de Menezes

***QUÍMICA MINERAL DE CRYSTALS DE BIOTITA EM
ENCLAVES SIENÍTICOS EM GRANITOS DO STOCK
GRANÍTICO GLÓRIA SUL, DOMÍNIO MACURURÉ,
SUL DA PROVÍNCIA BORBOREMA***

Dissertação apresentada ao Programa de Pós-Graduação
em Geociências e Análise de Bacias da Universidade
Federal de Sergipe, como requisito para obtenção do título
de Mestre em Geociências.

Orientador: Dr. Herbet Conceição

Coorientadora: Dra. Maria de Lourdes da Silva Rosa

**FICHA CATALOGRÁFICA ELABORADA PELA BIBLIOTECA CENTRAL
UNIVERSIDADE FEDERAL DE SERGIPE**

S237p	Menezes, Asayuki Rodrigues QUÍMICA MINERAL DE CRISTAIS DE BIOTITA EM ENCLAVES SIENÍTICOS EM GRANITOS DO STOCK GLÓRIA, DOMÍNIO MACURURÉ, SUL DA PROVÍNCIA BORBOREMA/ Asayuki Rodrigues de Menezes; orientador Herbet Conceição. – São Cristóvão, SE, 2022. 105 f. : il.
Dissertação (mestrado em Geociências e Análise de Bacias) – Universidade Federal de Sergipe, 2022.	
1. Geociências. 2. Petrologia. 3. Rochas Ígneas. 4. Magmatismo. I. Conceição, Herbet orient. II. Título.	
CDU 552.321(813.7)	

***QUÍMICA MINERAL DE CRYSTALS DE BIOTITA EM
ENCLAVES SIENÍTICOS EM GRANITOS DO STOCK
GRANÍTICO GLÓRIA, DOMÍNIO MACURURÉ,
SUL DA PROVÍNCIA BORBOREMA***

por:

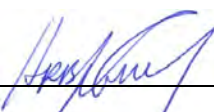
Asayuki Rodrigues de Menezes
(Geólogo, Universidade Federal de Sergipe – 2021)

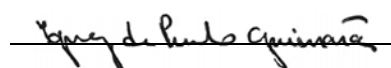
DISSERTAÇÃO DE MESTRADO

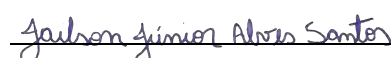
Submetida em satisfação parcial dos requisitos ao grau de:

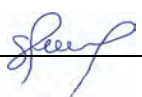
MESTRE EM GEOCIÊNCIAS

BANCA EXAMINADORA:

 Dr. Herbet Conceição [Orientador - UFS]

 Dra. Ignez de Pinho Guimarães [UFPE]

 Dr. Jailson Júnior Alves Santos [UFBA]

 Dra. Simone Cerqueira Pereira Cruz [UFBA]

Data da Defesa: 21/12/2022

DEDICATÓRIA

A minha vó Antonieta.

AGRADECIMENTOS

À Coordenação de Aperfeiçoamento de Pessoal de Nível Superior (CAPES), pela concessão bolsa de mestrado e incentivo a ciência.

Ao programa de Pós-Graduação em Geociências e Análise de Bacias e ao Condomínio de Laboratórios de Multusuários das Geociências da Universidade Federal de Sergipe (CLGeo-UFS) por toda a infraestrutura disponibilizada para a realização desta pesquisa.

À Superintendência de Salvador do Serviço Geológico do Brasil pelo apoio recebido na confecção de lâminas delgadas polidas e moagem de amostras.

Aos meus orientadores doutores Herbet Conceição e Maria de Lourdes da Silva Rosa por todo suporte, ensinamentos, apoio, confiança e paciência.

Aos companheiros do LAPA Diego, Vinícius, Jailson, Rayane, Carlos, Hiakan e Rodolfo pelas conversas, apoio e hamburguers.

Aos meus amigos Carlos Alves, Bruno, Danielle, Mariana, Sinthia, Ananda, João Pedro e Isabela.

A minha família, em especial aos meus pais Anorio e Vanusia por todo suporte e apoio.

O meu sincero agradecimento a todos!

EPÍGRAFE

*"Life ... is a tale
Told by an idiot, full of sound and fury,
Signifying nothing."*

William Shakespeare

RESUMO

A biotita é um constituinte importante nos enclaves microgranulares sieníticos hospedados em granitos do Stock Glória Sul, localizado na região central do Sistema Orogênico Sergipano. Estes enclaves são centimétricos, arredondados e elipsoides, têm granulação mais fina que os granitos encaixantes e são constituídos por ortoclásio, microclina, albita-oligoclásio, diopsídio, quartzo, hornblenda, titanita, apatita, zircão, magnetita, ilmenita e pirita. As texturas presentes nos enclaves evidenciam rápido resfriamento (granulação fina, apatita e zircão aciculares e zonação em plagioclásio). Os dados químicos permitiram classificar a mica marrom destes enclaves como Mg-biotita e Fe-biotita. A evolução composicional dos cristais de biotita investigados é essencialmente controlada por duas substituições (${}^{VI}R^{2+} + 2 {}^{VI}Al^{3+} = {}^{VI}\square + 2 {}^{VI}Si^{4+}$ e ${}^{VI}R^{2+} + {}^{VI}Ti = 2 {}^{VI}Al^{3+}$) que refletem a diminuição do alumínio e titânio. A química da biotita dos enclaves indica cristalização de magma da série magnetita de natureza cálcio-alcalina. A assinatura química dos cristais estudados indica igualmente que o magma que a formou teve evolução complexa e resulta da mistura entre magma mantélico (traquítico) e crustal (riolítico). A termobarometria indicou que a cristalização da biotita nos enclaves microgranulares sieníticos ocorreu a aproximadamente a 6,3 km entre as temperaturas 788-975 °C. A similaridade dos dados termobarométricos da biotita dos enclaves e dos granitos encaixantes sugerem que estes valores correspondam ao das condições físicas da interação entre os magmas traquítico (enclaves) e riolítico (granito). A petrogênese estabelecida para os enclaves é coerente com o ambiente colisional estabelecido para o Sistema Orogênico Sergipano.

Palavras-Chave: Micas; Mineraloquímica; Sistema Orogênico Sergipano.

ABSTRACT

Biotite is an important constituent in the syenitic microgranular enclaves hosted in granites of the Glória Sul Stock, located in the central region of the Sergipano Orogenic System. These enclaves are centimetric, rounded and ellipsoidal, have finer grain size than the surrounding granites and are composed of microcline, orthoclase, albite-oligoclase, diopside, quartz, hornblende, titanite, apatite, zircon, magnetite, ilmenite, and pyrite. The textures present in the enclaves imply to rapid cooling (fine-grained, acicular apatite and zircon and zonation in plagioclase). The chemical data allowed the brown mica from these enclaves to be classified as Mg-biotite and Fe-biotite. The compositional evolution of the investigated biotite crystals is essentially controlled by two substitutions (${}^{VI}R^{2+} + 2 {}^{VI}Al^{3+} = {}^{VI}\square + 2 {}^{VI}Si^{4+}$ and ${}^{VI}R^{2+} + {}^{VI}Ti = 2 {}^{VI}Al^{3+}$) that reflect aluminum and titanium decrease. The biotite chemistry of the enclaves indicates magma crystallization of the magnetite series of calcium-alkaline nature. The chemical signature of the crystals studied also indicates that the magma that formed it has a complex evolution and results from the mixture between mantle (trachytic) and crustal (rhyolitic) magma. Thermobarometry indicated that crystallization of biotite in the syenitic microgranular enclaves occurred at approximately 6.3 km between temperatures 788-975 °C. The similarity of the thermobarometric data of biotite from the enclaves and the surrounding granites suggests that these values correspond to that of the physical conditions of the interaction between trachytic (enclaves) and rhyolitic (granite) magmas. The petrogenesis established for the enclaves are coherent with the collisional environment established for the Sergipe Orogenic System.

Keywords: Micas; Mineralochemistry; Sergipano Orogenic System.

ÍNDICE DE FIGURAS

Capítulo 1

Introdução

Figura 1.	Mapa de localização e acesso à área de estudo	16
-----------	---	----

Capítulo 2

Chemical-memory of biotite crystals preserves the temperature and pressure conditions of the mixing process between trachytic and rhyolitic magmas in the Glória Sul Stock, Sergipano Orogenic System, Northeast Brazil

Figure 1.	Regional and local geological maps. (A) Geological map of the Borborema Province. (B) Geological map of the Sergipano Orogenic System. (C) Simplified geological map of Glória Sul Stock.	26
Figure 2.	Photographs A and B correspond to biotite-granite outcrops where the studied enclaves occur. High abundance of microgranular enclaves characterize of these granites.	29
Figure 3.	Images of microgranular enclaves hosted in biotite-granite from Glória Sul Stock.	30
Figure 4.	Textures present in the microgranular syenitic enclaves (A-L) and the host biotite-granite (M-S).	32
Figure 5.	Mg-Li versus Fe+Mn+Ti- VIAL diagram for the classification of micas from Tischendorf et al. (1997).	36
Figure 6.	Cation correlation diagrams used to illustrate the chemical evolution of the studied biotite crystals..	36
Figure 7.	Discriminating chemical diagrams for biotite. (A) MgO - (FeO+MnO) - (10.TiO ₂) diagram Nachit et al. (2005) to discriminate magmatic, magmatic, re-equilibrated and non-magmatic biotite applied to the analyzed crystals. (B) (FeO+MnO+ MgO)/(FeO+MnO) versus TiO ₂ proposed to note the variation of these oxides in the analyzed crystals.	38
Figure 8.	Temperature (oC) - Pressure (kbar) diagram with thermobarometric determinations, calculated using the Li and Zhang. (2022) algorithm, of the biotite crystals from the enclaves and studied biotita-granites.	41
Figure 9.	Fe ₂₊ - Fe 3+ - Mg 2+ diagram of the Wones and Eugster (1965) for inferring oxygen fugacity conditions, applied to the studied biotite crystals.	42
Figure 10.	Diagrams for magmatic affinity inferences based on chemical data from biotite crystals. (A) Fe/(Fe+Mg) - total Al diagram of the Anderson (2008). (B) Triangular diagram FeO* - MgO – Al ₂ O ₃ with fields of crystallized biotite in alkaline, calc-alkaline, and peraluminous magmas (Abdel Raman 1994). (C) Total Al - Mg diagram Nachit et al. (1985), with crystallized biotite fields in alkaline, calc-alkaline, aluminopotassic and peraluminous magmas.	43
Figure 11.	FeO/(FeO+MgO) versus MgO diagram Sousa et al. (2019) modified from Zhou (1986) for inference on the nature of the biotite-forming magma applied to the biotite crystals studied from Glória Sul Stock..	43

ÍNDICE DE TABELAS

Table 1.	Comparação entre as composições dos padrões de minerais fornecidos pela Astimex e dos padrões internos do laboratório, obtidos com microssonda eletrônica, e os resultados com EDS-MEV neste estudo.	28
Table 2.	Representative chemical analyses of the biotite crystals studied. Structural formula calculated for 22 oxygens. Microgranular enclaves (EMs) and biotite-granite (BG).	35
Table 3.	Maximum and minimum temperature and pressure values obtained in this study. Temperature values were calculated using P saturation in whole rock (Harrison and Watson, 1984), after the data from Conceição et al. (2016). Temperature and pressure values were calculated using chemical data from biotite crystals with a high titanium content from enclaves (MEs) and magmatic biotite from biotite-granites (BG).	39

SUMÁRIO

DEDICATÓRIA	v
AGRADECIMENTOS	vi
EPÍGRAFE	vii
RESUMO	viii
ABSTRACT	ix
ÍNDICE DE FIGURAS	x
ÍNDICE DE TABELAS	xi
CAPÍTULO 1 – INTRODUÇÃO	13
1.1 APRESENTAÇÃO	14
1.2 OBJETO E OBJETIVOS	15
1.3 LOCALIZAÇÃO E ACESSO A ÁREA DE ESTUDO	16
1.4 METODOLOGIAS	17
1.5 REFERÊNCIAS	19
CAPÍTULO 2 – CHEMICAL-MEMORY OF BIOTITE CRYSTALS PRESERVES THE TEMPERATURE AND PRESSURE CONDITIONS OF THE MIXING PROCESS BETWEEN TRACHYTIC AND RHYOLITIC MAGMAS IN THE GLÓRIA SUL STOCK, SERGIPANO OROGENIC SYSTEM, NORTHEAST BRAZIL	22
ABSTRACT	23
INTRODUCTION	24
GEOLOGICAL BACKGROUND	25
GLÓRIA SUL STOCK	27
SAMPLING AND ANALYTICAL METHODS	27
RESULTS	29
DISCUSSION	36
FINAL CONSIDERATIONS	43
ACKNOWLEDGMENTS	44
REFERENCES	45
CAPÍTULO 3 – CONSIDERAÇÕES FINAIS	51
3.1 CONCLUSÕES GERAIS	52
ANEXO – COMPROVANTE DE SUBMISSÃO DO ARTIGO	53
APÊNDICE – ANÁLISES QUÍMICAS DOS CRISTAIS DE BIOTITA	55

CAPÍTULO 1: Introdução

1.1 APRESENTAÇÃO

Os granitos são normalmente ricos em inclusões de outras rochas e estas são nomeadas genericamente como enclave. O termo “enclave” foi utilizado pela primeira vez por Lacroix (1890).

No presente texto o foco são os cristais de biotita de enclaves microgranulares. Este tipo de enclave é interpretado como “gotas” de magmas máficos ou hibridizados que foram resfriados mais rapidamente que os granitos encaixantes (Didier e Barbarin, 1991). Bonin (2004) considera os enclaves microgranulares (EMs) em granitos (*lato sensu*) como os representantes de magmas mantélicos envolvidos na formação dos complexos plutônicos félsicos.

Os enclaves microgranulares em granitos (*l.s.*) têm sido utilizados para ampliar a compreensão dos processos físicos e químicos presentes durante a evolução dos magmas em sistemas plutônicos. Eles permitem identificar a natureza das fontes dos magmas máfico e félsico, grau de hibridização, momento(s) da(s) chegada(s) do(s) pulsos de magma(s) máfico(s) dentre outros aspectos petrológicos importantes (e.g. Weindedorfer et al., 2014)

No Sistema Orogênico Sergipano (SOS) a presença de EMs nas intrusões é uma feição comum (e.g. Silva, 2014; Lisboa et al., 2019; 2020; Fernandes et al., 2020; Sousa, 2020; Sousa et al., 2022). O SOS está situado ao sul da Província Borborema em contato o Cráton do São Francisco. A evolução geológica do setor sul da PB é complexa (Van Schmus et al., 2008). Neste contexto formou-se o SOS da colisão entre a placa Sanfranciscana e o Superterreno Pernambuco-Alagoas (650-500 Ma – Van Schmus et al., 1995; Brito Neves e Silva Filho, 2019).

O SOS é constituído por sete domínios geológicos, que de sul para norte são: Estância, Vaza-Barris, Macururé (DM), Marancó, Poço Redondo, Canindé e Rio Coruripe (Davison e Santos, 1998; Silva Filho e Torres, 2002).

No Domínio Macururé ocorrem cerca de 60 intrusões nas quais enclaves são abundantes (Conceição et al., 2016). Este fato tem levado vários autores (e.g. Silva, 2014; Conceição et al., 2016; Fontes et al., 2018; Lisboa et al., 2019; 2020; Fernandes et al., 2020; Oliveira 2020; Sousa, 2020; Lima, 2021; Santos, 2021) a proporem a coexistência e interação entre magmas ultramáficos-máficos-intermediários com magmas félsicos na geração de granitos.

O Stock Glória Sul (SGS) constitui uma das intrusões do Domínio Macururé e contém inúmeros enclaves microgranulares.

O SGS tem forma arredondada, possui área de 41 km², é intrusivo em rochas metassedimentares do Grupo Macururé e está localizado na porção central do DM. Ele é constituído por granitos cinza e róseo, de granulação fina a média e contém xenólitos de rochas do DM e enclaves microgranulares. Conceição (2019) descreve o SGS como formado por biotita sienogranito, muscovita sienogranito, sienogranito com biotita e muscovita e monzogranito com granada.

Os EMs são mais abundantes na fácies biotita-sienogranito. Eles apresentam dimensões centimétricas a decimétricas, exibem contatos bem definidos e são abundantes. Eles ocorrem hospedados nos granitos encaixantes e podem exibir borda de coloração mais escura devido ao maior volume de biotita. As formas do EMs elípticas ou arredondadas e mostram-se orientados pelo fluxo magmático.

1.2 OBJETO E OBJETIVOS

O objeto desse estudo foi a biotita presente nos enclaves microgranulares em biotita-sienogranitos que ocorrem no Stock Granítico Gloria Sul. O objetivo geral desta dissertação foi compreender a petrologia dos enclaves presentes no SGS. A pesquisa envolveu as seguintes etapas:

- Realizar etapa de campo para obtenção de amostras de enclaves e dos granitos encaixantes.
- Realizar descrição petrográfica macroscópica e microscópica de amostras representativas.
- Determinar a composição química pontual de cristais de biotita.
- Discutir e interpretar os dados obtidos no estudo petrográfico e de química mineral.
- Inferir as condições de colocação e cristalização dos enclaves investigados.

1.3 LOCALIZAÇÃO E ACESSO A ÁREA DE ESTUDO

A área estudada está situada na porção nordeste do Estado de Sergipe, distando aproximadamente 113 km da capital Aracaju. Esta região, está inserida na Folha Topográfica Gracho Cardoso (SC.24-Z-B-I), sendo delimitada pelas coordenadas geográficas 10°12' – 10°20' S e 37°50' – 37°41' W (Figura 1).

O acesso a área estudada, dá-se partindo da capital de Sergipe (Aracaju) através da BR-235 até a cidade Itabaiana, e de Itabaiana até o município de Nossa Senhora da Glória é feito pela rodovia estadual SE-175. A partir dessa cidade o acesso aos afloramentos é feito pela SE-230 e estradas carroçáveis.

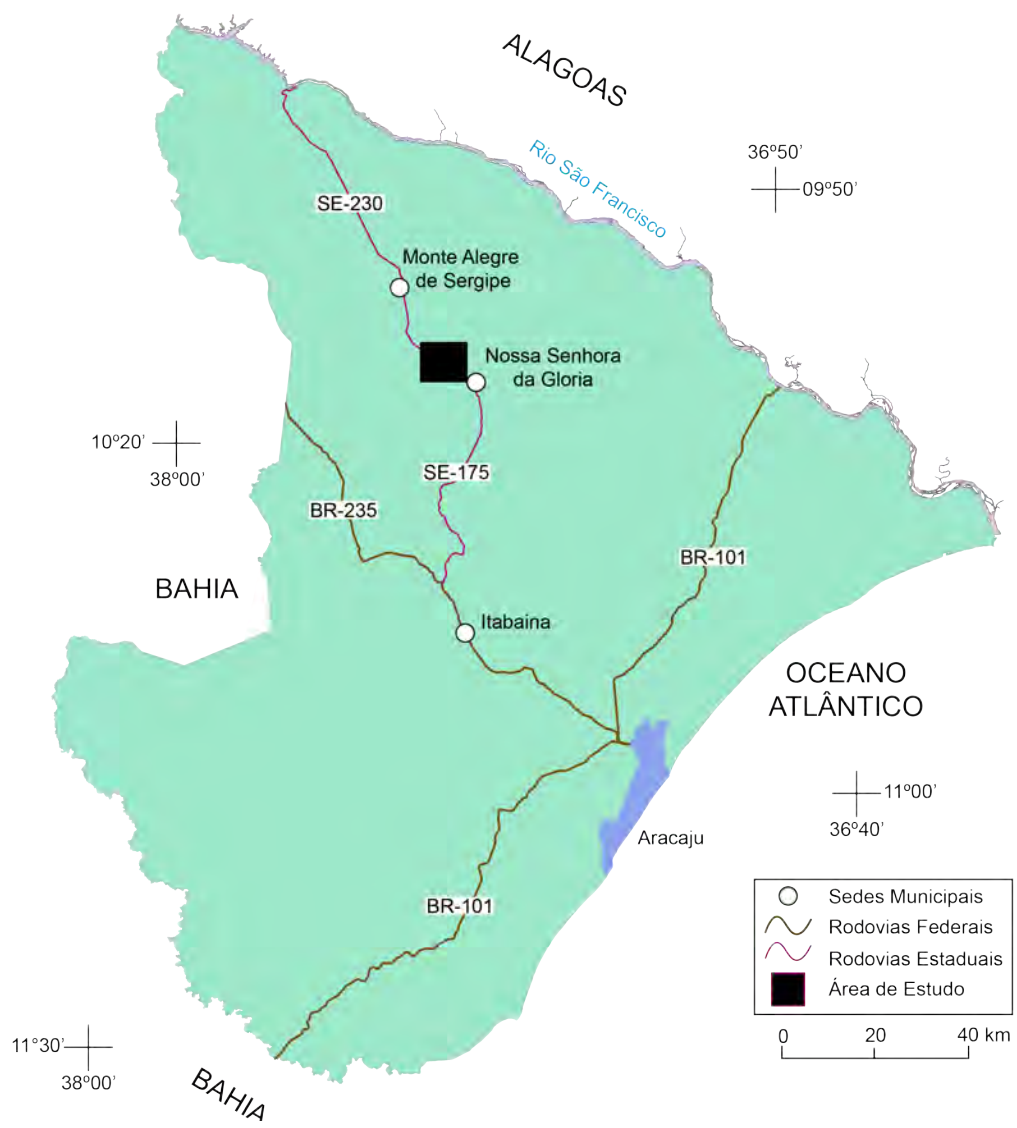


Figura 1. Mapa de localização e acesso à área de estudo.

1.4 METODOLOGIAS

Levantamento Bibliográfico

O Levantamento Bibliográfico constou da integração dos dados geológicos disponíveis sobre gênese e relações de enclaves microgranulares em granitos, assim como o magmatismo presente no SOS. Para tal propósito, foram consultados artigos científicos, dissertações, teses, projetos de mapeamento e anais de eventos que abordassem esses temas, esse levantamento foi realizado utilizando-se do Portal de Periódicos da CAPES (<https://www.periodicos.gov.br>), na Rede de Biblioteca Ametista do Serviço Geológico do Brasil (SGB/CPRM; <https://www.cprm.gov.br/publique/Redes-Institucionais/Rede-de-Bibliotecas---Rede-Ametista-263>), Agência Nacional de Mineração (ANM) e em sites de cursos de pós-graduação de universidades.

Trabalhos de Campo

Realizou-se missões de campo no SGS, com duração total de três dias, objetivando identificar a variação dos tipos de rochas e coletar amostras representativas. Foram visitados três afloramentos e coletadas 13 amostras sendo onze dos enclaves e duas dos biotita-sienogranito encaixantes.

Preparação de Amostras

Das rochas coletadas onze foram preparadas para os estudos petrográfico, mineraloquímico (lâmina delgado-polida), dessas foram cortados tabletos de tamanhos próximos de um punho cerrado (5 x 8 cm). Estas lâminas foram gentilmente confeccionadas no Laboratório de Laminação da Superintendência Regional de Salvador do Serviço Geológico do Brasil (SGB/CPRM).

Petrografia e Mineraloquímica

A análise petrográfica em luz transmitida e refletida foi realizada utilizando-se de microscópio trinocular, da marca Opton®, modelo TNP-09T. Nessas descrições foram coletadas informações sobre as rochas (e.g. identificar e nomear os minerais presentes, descrever as suas formas e tamanhos, a existência de inclusões, tipos de contatos e orientações preferenciais). A posteriori, para serem analisadas com o microscópio eletrônico de varredura (MEV), metalizou-se estas lâminas com ouro (espessura de 8-10 µm) com o metalizador da marca *Quorum*® modelo Q150R ES.

As composições químicas pontuais da biotita de onze amostras 9 dos enclaves e dos sienogranitos encaixante (Anexo I) foram obtidas como o espectrômetro de energia dispersiva (EDS), modelo X-Act, da *Oxford Instruments*[®]. Esse espectrômetro está acoplado ao microscópio eletrônico de varredura (MEV) Tescan-Vega LMU3 presente no laboratório de microanálises do Condômino de Laboratórios Multiusuários das Geociências da Universidade Federal de Sergipe (CLGeo-UFS).

Tratamento dos Dados

Os dados químicos pontuais de cristais de biotita foram reduzidos em planilhas do *software Excel*[®] pertencente ao pacote Microsoft Office[®] 365. Programou-se as planilhas para realização dos cálculos da fórmula estrutural da biotita com base em 22 oxigênios como sugerido por Deer et al. (1992). O conteúdo de H₂O foi estimado com assumindo que o preenchimento total do sítio (OH + F + Cl = 4). O Li₂O foi calculado com base na equação empírica (Li₂O = 0,287 x SiO₂ - 9,552), segundo as sugestões presentes nos apêndices de Tischendorf et al. (2004).

As estimativas dos conteúdos de ferro nas valências 2 e 3 foram realizadas segundo a normalização proposta por Dymek (1983) onde: (Total de Cátions) - (K+Na+Ca+Ba) + Ti + 1/2^{VI}Al_{xc} = 7,0; onde ^{VI}Al_{xc} = ^{VI}(Al+Cr) - ^{IV}Al + (K+Na+2Ca+2Ba)]. O total do ferro Fe³⁺ é obtido pela diferença entre 22 - (somatório das cargas dos elementos químicos dosados). O valor do Fe²⁺ é obtido pela diferença entre (Fe_{total} normalizado - Fe³⁺).

Os valores de fugacidade de oxigênio foram calculados utilizando os cálculos da tabela confeccionada por Gündüz et al. (2022), que utiliza o algoritmo proposto por Wones (1989).

A planilhas confeccionadas para o presente trabalho foram configuradas para, também, gerarem e alocarem dos dados em diagramas comumente utilizados como por exemplo: Mg-Li vs Fe + Mn + Ti - ^{VI}Al – classificação das micas (Tischendorf et al. (1997); ^{VI}vacância + 2 Si vs R²⁺ + 2^{IV}Al, Ti + R²⁺ vs 2^{VI}Al (substituições); FeO + MnO – 10TiO₂ – MgO, avaliação do caráter magmático, magmático-reequilibrado e não magmático de cristais de biotita (Nachit et al. 2005); Fe²⁺ - Fe³⁺ - Mg²⁺ inferência de fugacidade de oxigênio (Wones e Eugster; 1965); Fe/(Fe+Mg) vs Al_{Total} inferência sobre a biotita ser cristalizada em magma das series Magnetita e Ilmenita (Anderson; 2008);

FeO – MgO – Al₂O₃ inferência sobre a biotita ser formada por magmas cálcio-alcalino, alcalino e peraluminoso (Abdel Raman, 1994); Al_{Total} vs Mg inferência sobre a biotita ser formada por magmas cálcio-alcalino, alcalino e peraluminoso (Nachit et al., 1985); FeO*/(FeO* + MgO) vs MgO infere sobre a natureza mantélica, mantélica + crustal e crustal do magma que a biotita se cristalizou (Zhou et al., 1986).

O cálculo da pressão foi feito segundo a equação de Uchida et al. (2007): P (kbar)= 3,03×Al-6,53 (com erro de ± 0,33), onde P= pressão (kbar) e Al= (^{VI}Al + ^{IV}Al).

A temperatura foi calculada com o algoritmo segundo o modelo empírico de Henry et al. (2005) cuja equação é: T= {[ln(Ti) – a - c (X_{Mg})] / b} ^{0,333} (com erro de ± 24 °C). Onde: T = temperatura (°C), X_{Mg} = Mg / (Mg + Fe); a= -2,3594; b = 4,6482 x 10⁻⁹ e c= -1,7283.

1.5 REFERÊNCIAS

- Abdel-Rahman, A. M. (1994). Nature of biotites from alkaline, calc-alkaline, and peraluminous magmas. *Journal of Petrology*, 35(2), 525-541. <https://doi.org/10.1093/petrology/35.2.525>
- Anderson, J. L., Barth, A. P., Wooden, J. L., Mazdab, F. (2008). Thermometers and Thermobarometers in Granitic Systems. *Reviews in Mineralogy and Geochemistry*, 69 (1), 121–142. <https://doi.org/10.2138/rmg.2008.69.4>
- Bonin B. (2004). Do coeval mafic and felsic magmas in post-collisional to within-plate regimes necessarily imply two contrasting, mantle and crustal, sources? A review. *Lithos*, 78(1-2):1–24. doi:10.1016/j.lithos.2004.04.042
- Brito Neves, B. B., Silva Filho, A. F. (2019). Superterreno Pernambuco-Alagoas (PEAL) na Província Borborema: ensaio de regionalização tectônica. *Geologia USP. Série Científica*, 19(2), 3-28. <https://doi.org/10.11606/issn.2316-9095.v19-148257>
- Conceição, J. A. (2019). Magmatismo Leucogranítico do Domínio Macururé, Sistema Orogênico Sergipano, Província Borborema, NE do Brasil. Tese (Doutorado). Salvador: Instituto de Geociências – UFBA.
- Conceição, J. A., Rosa, M. L. S, Conceição, H. (2016). Sienogranitos leucocráticos do Domínio Macururé, Sistema Orogênico Sergipano: Stock Glória Sul. *Brazilian Journal of Geology*, 46(1), 63-77. <https://doi.org/10.1590/2317-4889201620150044>
- Davison, I., Santos, R. A. (1989). Tectonic evolution of the Sergipano Fold Belt, NE Brazil, during the Brasiliano Orogeny. *Precambrian Research*, 45(4), 319-342. [https://doi.org/10.1016/0301-9268\(89\)90068-5](https://doi.org/10.1016/0301-9268(89)90068-5)
- Deer, W. A., Howie, R. A., Zussman, J. (1992). *An introduction to the rock-forming minerals* (2^a ed.). Londres: Longman.
- Didier, J., Barbarin, B. (1991). *Enclaves and Granite Petrology*. Elsevier.
- Dymek, R. F. (1983). Titanium, aluminium and interlayer cation substitutions in biotite from high-grade gneisses, West Greenland. *American Mineralogist*, 68(9-10), 880-899.

- Fernandes, D. M., Lisboa, V. A. C., Rosa, M. L. S., Conceição, H. (2020). Petrologia e idade do Stock Fazenda Lagoas, Domínio Macururé, Sistema Orogênico Sergipano, NE-Brasil. *Geologia USP. Série Científica*, 20(1), 39-60. <https://doi.org/10.11606/issn.2316-9095.v20-160040>
- Fontes, M. P., Conceição, H., Rosa, M. L. S., Lisboa, V. A. C. (2018). Minettes do Stock Monzonítico Glória Norte: evidência de magmatismo ultrapotássico pós-orogênico, com assinatura de subducção, no Sistema Orogênico Sergipano. *Geologia USP. Série Científica*, 18(1), 51-66. <https://doi.org/10.11606/issn.2316-9095.v18-133599>
- Gündüz, M., Asan, K. (2022). MagMin_PT: An Excel-based mineral classification and geothermobarometry program for magmatic rocks. *Mineralogical Magazine*, 1-25. <https://doi.org/10.1180/mgm.2022.113>
- Henry, D. J. (2005). The Ti-saturation surface for Low-to-Medium Pressure Metapelitic Biotites: Implications for Geothermometry and Ti-Substitution Mechanisms: Implications For geothermometry and Ti-Substitution Mechanisms. *American Mineralogist*, 90(2–3), 316–328. <https://doi.org/10.2138/am.2005.1498>
- Lacroix, A. (1890). Sur les enclaves du trachyte de Menet (Cantal), sur leurs modifications et leur origin. *Paris: CR Academy of Science*, 11, 1003–1006.
- Lima, A. L. R. (2021). Petrologia do Stock Altos Verdes, Domínio Macururé, Província Borborema. Dissertação (Mestrado). Programa de Pós-Graduação em Geociências e Análises de Bacias-UFS.
- Lisboa, V. A. C., Conceição, H., Rosa, M. L. S., Fernandes, D. M. (2019). The onset of post-collisional magmatism in the Macururé Domain, Sergipano Orogenic System: the Glória Norte Stock. *Journal of South American Earth Sciences*, 89, 173-188. <https://doi.org/10.1016/J.JSAMES.2018.11.005>
- Lisboa, V. A. C., Conceição, H., Rosa, M. L. S., Marques, G. T., Lamarão, C. N., Lima, A. L. R. (2020). Amphibole crystallization conditions as record of interaction between ultrapotassic enclaves and monzonitic magmas in the Glória Norte Stock, South of Borborema Province. *Brazilian Journal of Geology*, 50(2), e20190101. <https://doi.org/10.1590/2317-4889202020190101>
- Nachit, H., Ibhi, A., Abia, E. H., Ohoud, M. B. (2005). Discrimination between primary magmatic biotites, reequilibrated biotites and neoformed biotites. *Comptes Rendus Geoscience*. 337:1415-1420. <https://doi.org/10.1016/j.crte.2005.09.002>
- Nachit, H., Razafimahefa, N., Stussi, J. M., Caron, J. P. (1985). Composition chimique des biotites et typologie magmatique des granitoïdes. *Comptes rendus l'Académie des Sci*, 301, 813–818.
- Santos, L. Q. S. (2021). Petrogênese do Stock Fazenda Alvorada, Domínio Macururé, Sistema Orogênico Sergipano. Dissertação (Mestrado). São Cristóvão: Universidade Federal de Sergipe.
- Silva Filho, M. A., Torres H. H. F. (2002). A New Interpretation on the Sergipano Belt domains. *Anais da Academia Brasileira de Ciências*, 74(3), 556-557. <https://doi.org/10.1590/S0001-37652002000300049>

- Silva, C. C. (2014). Petrologia e geocronologia do stock granodiorítico Lagoa do Roçado, Domínio Macururé, Faixa Sergipana-SE. Dissertação (Mestrado). São Cristóvão: Universidade Federal de Sergipe.
- Sousa, C. S., Conceição, H., Soares, H. S., Fernandes, D. M., Rosa, M. L. S. (2022). Injection of enriched lithospheric mantle magmas explains the formation of microgranular enclaves in the Rio Jacaré Batholith, Borborema Province, Brazil. *Journal of South American Earth Sciences*, v. 52(4), e2022033. <https://doi.org/10.1016/j.jsames.2022.103942>
- Sousa, E. S. (2020). Petrologia do Magmatismo Ediacarano na Porção Central do Domínio Macururé: Stocks Graccho Cardoso e Queimadinha. Dissertação (Mestrado). São Cristóvão: Universidade Federal de Sergipe.
- Tischendorf, G., Gottesmann, B., Förster, H. J., Trumbull, R. B. (1997). On Li-bearing Micas: Estimating Li From Electron-Microprobe Analyses and an Improved Diagram For Graphical Representation. *Mineralogical Magazine*, 61, 809–834. <https://doi.org/10.1180/minmag.1997.061.409.05>
- Tischendorf, G., Rieder, M., Forster, H. J., Gottesmann, B., Guidotti, C. V. (2004). A New Graphical Presentation and Subdivision of Potassium Micas. *Mineralogical Magazine*, 68, 649-667. <https://doi.org/10.1180/0026461046840210>
- Uchida, E., Endo, S., Makino, M. (2007). Relationship Between Solidification Depth of Granitic Rocks and Formation of Hydrothermal Ore Deposits. *Resource Geology*, 57(1), 47–56. <https://doi.org/10.1111/j.1751-3928.2006.00004.x>
- Van Schmus, W. R., Brito Neves, B. B., Hackspacher, P., Babinski, M. (1995). U/Pb and Sm/Nd geochronologic studies of the eastern Borborema Province, northeastern Brazil: initial conclusions. *Journal of South American Earth Sciences*, 8, 267-288. DOI: [https://doi.org/10.1016/0895-9811\(95\)00013-6](https://doi.org/10.1016/0895-9811(95)00013-6)
- Van Schmus, W. R., Oliveira, E. P., Silva Filho, A. F., Toteu, S. F., Penaye, J., Guimarães, I. P. (2008). Proterozoic links between the Borborema Province, NE Brazil, and the Central African Fold Belt. *Geol. Soc. London, Spec. Publ.* 294, 69–99. <https://doi.org/10.1144/SP294.5>
- Weidendorfer, D., Mattson H. B., Ulmer, P. (2014). Dynamics of Magma Mixing in Partially Crystallized Magma Chambers: Textural and Petrological Constraints From the Basal Complex of the Austurhorn Intrusion (SE Iceland). *Journal of Petrology*, 55(9), 1865-1903. <https://doi.org/10.1093/petrology/egu044>
- Wones, D. R. (1989). Significance of the Assemblage Titanite+Magnetite+Quartz In Granitic Rocks. *American Mineralogist*. 74 (7-8), 744–749.
- Wones, D. R., Eugster, H. P. (1965). Stability of Biotite Experiment Theory and Application. *American Mineralogist*, 50(9), 1228–1272.
- Zhou, Z. (1986). The origin of intrusive mass in Fengshandong, Hubei province. *Acta Petrologica Sinica*, 2(2), 56-70.

***CAPÍTULO 2: Chemical-memory of biotite crystals
preserves the temperature and pressure conditions
of the mixing process between trachytic and rhyolitic
magmas in the Glória Sul Stock, Sergipano
Orogenic System, Northeast Brazil***

Chemical-memory of biotite crystals preserves the temperature and pressure conditions of the mixing process between trachytic and rhyolitic magmas in the Glória Sul Stock, Sergipano Orogenic System, Northeast Brazil

Asayuki Rodrigues Menezes¹, Joane Almeida da Conceição², Maria Lourdes Silva Rosa¹, Gisele Tavares Marques³, Cláudio Nery Lamarão³, Herbet Conceição¹

¹Programa de Pós-Graduação em Geociências e Análise de Bacias, Universidade Federal de Sergipe – São Cristóvão (SE), Brazil. E-mails: asayukirm@outlook.com; herbet@academico.ufs.br; lrosa@academico.ufs.br

²Universidade Federal do Oeste da Bahia, Barreiras (BA), Brazil. E-mail: joane.conceicao@ufob.edu.br

³Universidade Federal do Pará – Belém (PA), Brazil. E-mails: gisele.ufpa@gmail.com; lamarao@ufpa.br

ABSTRACT

Biotite is an important constituent in the microgranular syenitic enclaves of the Glória Sul Stock, located in the central region of the Sergipano Orogenic System, Northeast Brazil. These enclaves are centimeter-sized, rounded, and ellipsoidal, finer-grained than the surrounding granites. They are composed of microcline, orthoclase, albite-oligoclase, diopside, quartz, hornblende, titanite, apatite, zircon, epidote, magnetite, ilmenite, thorite, and pyrite. The textures present in the enclaves indicate mixing between magmas and rapid cooling of the trachyte magma that formed the microgranular enclaves (fine-grained texture, acicular apatite and zircon, blade-shaped biotite). The studied biotite exhibits a magmatic texture and is chemically classified as Fe- and Mg-biotite, particularly those with $\text{TiO}_2 > 2.3\%$. The chemical evolution of biotite is controlled by two substitutions (${}^{VI}\text{R}^{2+} + 2 {}^{VI}\text{Al}^{3+} = {}^{VI}\square + 2 {}^{VI}\text{Si}^{4+}$ and ${}^{VI}\text{R}^{2+} + {}^{VI}\text{Ti} = 2 {}^{VI}\text{Al}^{3+}$) reflecting a decrease in titanium and an increase in aluminum. The chemical data of biotite crystals indicate that they crystallized from Type I magma, with calc-alkaline affinity, suggesting that the rocks of Gloria Sul Stock were formed by the interaction between mantle- and crustal-derived magmas. Thermobarometry of magmatic biotite (enclaves and granites) provided crystallization temperatures between 900-800 °C and a depth of 36 -13 km. The interaction between trachytic (enclave) and rhyolitic (granite) magmas in Glória Sul Stock at occurred at about 26 km depth and at a temperature about 800°C.

Keywords: Mica; Mineral chemistry; Sergipano Orogenic System; biotite chemistry; magma mixing/mingling.

1. INTRODUCTION

In orogenic regions, geologic terrains with complex evolution are marked by various magmatic events, where mixing processes between magmas are common (e.g., Clark 1992, Pitcher 1993, Cobbing 2000, Faure 2001, Nédélec and Bouchez, 2011). Evidence of magma mixing is easier to identify when it involves magmas of contrasting compositions, such as mafic and felsic. In many of these interactions, enclaves form because the magmas have different viscosities and temperatures, preventing complete mixing (e.g., Didier and Barbarin 1991; Perugini and Poli, 2011). The internal dynamics of magma reservoirs tend to disaggregate the flows of mafic magmas, generating microgranular enclaves if the host magma has a low crystallization rate (e.g., Vernon et al. 1988; Fernandez and Barbarin 1991; Barbarin 2005; Weidendorfer et al. 2014; Kumar 2020).

The granitic stocks and batholiths of the Sergipano Orogenic System, northeastern Brazil have abundant enclaves, with most of them being microgranular (Conceição et al., 2016; Lisboa et al., 2019, 2020; Fernandes et al., 2020; Sousa et al., 2019, 2022, 2022a; Oliveira et al., 2021; Soares et al., 2022; Pereira et al., 2023; Oliveira et al., 2023). The structures and textures of these intrusions indicate a complex petrological evolution marked by the presence of mixing processes between mafic and felsic magmas, that have generated granites, monzonites and syenites. The relationships between the enclaves and the host magmatic rocks suggest that these enclaves were formed by several pulses of magmas (ultramafic, mafic, intermediate and lamprophyric) in mesozonal magma chambers (e.g., Lisboa et al., 2019; Soares et al., 2022; Pereira et al., 2020, 2023; Oliveira et al., 2023).

The evolution of felsic plutonic systems has been studied using microgranular enclaves (e.g., Vernon, 2010; Weidendorfer et al., 2014; Kumar, 2020). The nature and sources of mafic and felsic magmas (e.g., Meng et al., 2019; Samadi et al., 2021), the degree of hybridization (e.g., Weidendorfer et al., 2014), the presence of mafic magma inflows (e.g., Fernandez and Barbarin, 1991; Adam et al., 2019), and the rise of magmas in the continental crust (Li and Zhang, 2022) can all be inferred from studies of microgranular enclaves.

Variations in temperature, pressure, and oxygen fugacity during magma evolution can be inferred from the chemistry of pyroxene, amphibole, olivine, and mica (e.g., Anderson et al., 2008; Lisboa et al., 2020, Aranda et al., 2021; Gündüz and Asan, 2022). Recent research has shown that biotite can record temperature and pressure

during hydrothermal phases (Tang et al., 2019) and metamorphic stages (Henry, 2015), as well as magmatic phases (Esfahani et al., 2017; Li and Zhang., 2019; Mbassa et al., 2020; Li and Zhang, 2022). Intensive parameters of magma crystallization (e.g., temperature and pressure) can be calculated using empirical algorithms, calibrated with experimental studies and, more recently, using machine learning.

Biotite is the ubiquitous mafic mineral in microgranular enclaves in granitoids in the Sergipano Orogenic System and the intensive parameters obtained with this mineral is very useful for petrogenetic purposes, allowing future comparisons of crystallization conditions between intrusions in this orogen. This paper presents and discusses unpublished petrographic and mineral chemistry data on biotite crystals from microgranular enclaves in the biotite-granites of the Glória Sul Stock, using classical and machine-learning thermobarometry.

2. GEOLOGICAL BACKGROUND

The Sergipano Orogenic System (SOS), situated in the south of Borborema Province (Figure 1A), has a complex evolution (Van Schmus et al., 2008), marked by a collisional event (650-500 Ma) between the Sanfranciscana plate and the Pernambuco-Alagoas Superterrane (Van Schmus et al., 1995; Oliveira et al., 2010; Brito Neves and Silva Filho, 2019; Pereira et al. 2023).

The SOS comprises distinct geological domains (Davison and Santos, 1989), occurring as NW-SE oriented (Figure 1B) and delimited by shear zones (Santos et al., 1998). These geological domains, from south to north, include: Estância, Vaza Barris, Macururé, Marancó, Poço Redondo, Canindé and Rio Cururipe. The Estância and Vaza Barris domains exhibit low-grade metamorphism, while the other domains consist of metasedimentary and metavolcanic-sedimentary rocks with metamorphism ranging from low to medium grade and varied plutonism.

The Macururé Domain (MD), housing the Glória Sul Stock (GSS), shares tectonic boundaries with the Vaza-Barris, Marancó, Poço Redondo, Canindé and Rio Cururipe domains. The MD comprises metasedimentary rocks and intrusive bodies (Figure 1B).

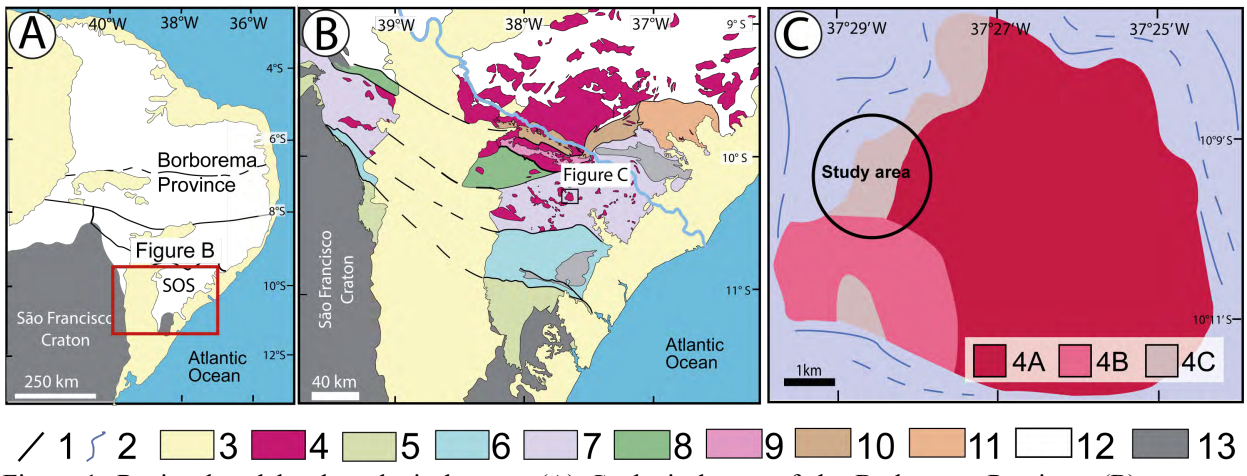


Figure 1. Regional and local geological maps. (A) Geological map of the Borborema Province. (B) Geological map of the Sergipano Orogenic System. (C) Simplified geological map of Glória Sul Stock. 1 = Shear Zone; 2= Metamorphic foliation; 3= Phanerozoic Covers; 4= Granite intrusions (Stock Sul Glória: 4A=Granite bearing biotite and muscovite; 4B= Muscovite granite; 4C= Biotite granite with diopside); 5= Estâncio Domain; 6= Vaza-Barris Domain; 7= Macururé Domain; 8= Marancó Domain; 9= Poço Redondo Domain; 10= Canindé Domain ; 11= Rio Cururipe Domain; 12= Borborema Province ; 12= São Francisco Craton.

The intrusions in the MD amount to around 60 bodies of various types (mafic, intermediate, and felsic), formed between 630-600 Ma, all of which have enclaves (Conceição et al., 2016; Lisboa et al., 2019, 2020; Fernandes et al., 2020; Oliveira et al., 2023; Pereira et al. 2019, 2023). These enclaves demonstrate the contribution of mantle magmas, contemporary with the felsic magmas. Various studies (e.g., Long et al., 2005; Oliveira et al., 2015; Conceição et al., 2016; Fernandes et al., 2020; Lisboa et al. 2020; Pereira et al. 2019, 2023) enable the grouping of MD into four suites:

- [1] Macururé Mafic Suite (636-629 Ma): Includes diorites, gabbros, monzonites with hornblendites and subordinate granites. This intermediate to basic plutonism, with high-K₂O calc-alkaline content and shoshonitic characteristics, was emplaced before and during regional deformation.
- [2] High-K₂O Calc-alkaline Granodioritic Suite (631-618 Ma): Comprises granodiorites and granites with diopside, exhibiting the geochemical signature of a volcanic arc environment.
- [3] Shoshonitic Suite (630-615 Ma): Formed by monzonites, with subordinate granitic and syenitic terms. These bodies are very rich in enclaves (diorites, lamprophyres, phlogopite-clinopyroxenites, and mafic monzonites), and geochemical data indicate shoshonitic to ultrapotassic magmatism.
- [4] High-K₂O Calc-alkaline Granitic Suite (626-600 Ma): Essentially composed of leucocratic, metaluminous granites, with more evolved peraluminous terms.

Corresponds to granites of the magnetite series, Type I and bears the geochemical signature of Cordilleran granites.

3. GLÓRIA SUL STOCK

The Glória Sul Stock (GSS), dated at 624 ± 11 Ma (Conceição, 2019), is a circular intrusion spanning 41 km^2 within the metasedimentary rocks of the MD (Figure 1B). It stands out as the largest stock within the MD, comprising fine- to medium-grained granites interspersed with xenoliths of MD rocks, surmicaceous and microgranular enclaves. Conceição et al. (2016) describe the GSS as encompassing muscovite granite, biotite- and muscovite-bearing granite, diopsidic-bearing biotite granite, and garnet-bearing granite. According to these authors, the diverse granite types within this stock result from intricate mixing between mafic shoshonitic and felsic high- K_2O calc-alkaline magmas, potentially with a contribution of pelitic rocks from the MD. The chemistry of GSS granites is identified as I type, displaying high- K_2O calc-alkaline signatures and volcanic arc.

Diopsidic-bearing biotite granites (BG) are localized in the northwest and southwest sectors of the GSS (Figure 1C). These granites exhibit a light gray in color, fine- to medium-grain size, in general isotropic, but occasionally revealing magmatic flow foliation that aligns the biotite and the numerous microgranular enclaves (Figure 2). Available chemical data from BG indicate that they represent the least differentiated types within the GSS. The saturation temperatures of apatite in both MEs and BG range from 984° to 925° C (Conceição, 2019).

4. SAMPLING AND ANALYTICAL METHODS

Thirteen representative rocks were collected during fieldwork, resulting in a total of eleven polished slides: two of biotite-granite and nine of the microgranular enclaves.

The polished slides sections underwent examination using the petrographic and electron microscopes of the Multiuser Geoscience Lab (CLGeo) at the Federal University of Sergipe (UFS). The Scanning Electron Microscope (SEM) at CLGeo-UFS, a Tescan® (Vega 3 LMU) model, is equipped with secondary and backscattered electron detectors, cathodoluminescence and an energy dispersive spectrometer (EDS).

In this study, 711 chemical analyses were conducted on biotite crystals, with their compositions determined using both energy dispersive spectrometry (EDS) and wavelength dispersive spectrometry (WDS).

EDS analysis took place using an EDS-SEM of the CLGeo-UFS, employing an acceleration potential of 20 kV, an electron beam current of 17 nA (diameter of 1 μm), 30-second analysis time. The reliability of the analysis was assessed using ASTIMEX international mineral standards and internal the laboratory standards (Table 1). Analytical uncertainties with EDS were less than 2%wt for elements with a content of more than 10%wt and errors between 4% and 19%wt for elements with a content of less than 5%wt.

WDS analyses were carried out using a JEOL JXA-8230 electronic probe from the Microanalysis Laboratory at the Federal University of Pará (LABMEV-UFPA). Analytical conditions included a constant acceleration voltage of 15kV, electron beam current of 20 nA, and electron beam diameter of 10 μm . Counting times for major and minor elements analysis were 20 and 40s, respectively. Calibration standards for WDS analysis included various minerals covering a range of elements: fluorite (F), sodalite (Na_2O), diopside (MgO), anorthite (Al_2O_3), orthoclase (SiO_2 , K_2O), wollastonite (CaO), celestine (SrO), magnetite (FeO), rhodonite (MnO), barite (BaO), rutile (TiO_2), sodalite (Cl), vanadinite (V_2O_3), Cr_2O_3 (Cr_2O_3) and NiO (NiO).

Table 1. Compares the compositions of the Astimex mineral standards and the laboratory's in-house standards, obtained though electron microprobe (EPMA) and those obtained in this study EDS. 2σ = error calculated by EDS for 2 sigmas. MD = modulus of the difference between the analysis of the standard and that obtained with the EDS-MEV in this study.

	EPMA	EDS	2σ	MD	Astimex	EDS	2σ	MD	EPMA	EDS	2σ	MD	EPMA	EDS	2σ	MD
SiO_2	37.54	38.01	0.09	0.47	38.72	38.82	0.27	0.1	39.88	39.7	0.3	0.18	40.93	41.12	0.3	0.19
TiO_2	2.88	2.77	0.17	0.11	1.77	1.75	0.1	0.19	1.06	1.1	0.2	0.04	0.67	0.62	0.1	0.05
Al_2O_3	13.41	13.46	0.18	0.05	15.13	15.53	0.19	0.4	12.88	13	0.2	0.12	12.94	13	0.2	0.06
FeO	17.85	18	0.27	0.15	10.72	9.65	0.17	1.07	13.09	13.91	0.51	0.82	13.3	13.12	0.2	0.18
MnO	0.89	0.29	0.09	0.6	0.04	0.09	0.08	0.05	0.22	0.36	0.07	0.14	0.3	0.4	0.1	0.1
MgO	13.21	13.51	0.04	0.3	19.52	19.82	0.19	0.3	17.2	17.74	0.22	0.54	17.01	17.23	0.2	0.22
CaO	0.03		0.11	0.11	0.1	0.23	0.06	0.13		0.12	0.06	0.12	0.1	0.2	0.1	0.1
Na_2O	0.01	0.57	0.06	0.56		0.01	0.08	0.01	0.01				0.09	0.1	0.09	
K_2O	9.75	9.39	0.12	0.36	9.91	10.01	0.11	0.1	10.36	9.99	0.21	0.37	10.25	10.14	0.1	0.11
Cr_2O_3	0.07		0.07	0.07		0.09	0.07	0	0.09	0.08	0.08	0.01	0.08	0.1	0.08	
Total	95.64	96			95.91	96	0.27	0	95.11	96			95.5	96		

Chemical data from the crystals were recorded in Excel® spreadsheets. The structural formula of biotite was calculated based on 22 oxygens and the iron content in valences 2 and 3 was determined following Dymek's proposition (Dymek 1983). H_2O content was calculated assuming that the $(\text{OH} + \text{F} + \text{Cl})$ site is filled. Li_2O was estimated using the empirical equation ($\text{Li}_2\text{O}=0.287*\text{SiO}_2-9.552$) from Tischendorf et al. (2004).

Temperature and pressure calculations for biotite crystallization were conducted using the classic algorithms of Henry et al. (2005) and Uchida et al. (2007), respectively. Machine learning methodology was applied using the software "Machine Learning Thermobarometry for Biotite-Bearing Magmas" by Li and Zhang. (2022) accessible at "https://lixiaoyan.shinyapps.io/Biotite_thermobarometer/por". Chemical analyses of the biotite crystals obtained are available in two files: magmatic crystals (Appendix 1) and reequilibrated magmatic crystals (Appendix 2).

5. RESULTS

5.1. Geology

The microgranular enclaves within the Glória Sul Stock are fine-grained, displaying shades of dark to light grey (Figure 2). Ranging in size varies from centimeters to decimeters, the enclaves generally possess a rounded shape (Figure 2A), with occasional elliptical forms (Figures 2A). Angular MEs are uncommon/scarce, with most showcasing a rounded contour, and the magmatic flow orients the elongated enclaves (Figure 2B).

Well-defined contacts between MEs and biotite-granite are evident (Fig. 3). Some contacts appear fine-grained at the edges and exhibit darker in color due to the higher concentration of biotite (Figure 3A). The majority of enclaves are single, occasional featuring multiple enclaves (Figure 3B). White feldspar xenocrysts (2 to 4 mm) are sporadically found within the MEs, displaying the same orientation as in the biotite-granite (Figures 3B, C, D). Small and rounded clots (< 3 cm) of green diopside and biotite are present in some of the MEs (Figures 3E, F) as well as in the biotite-granite.

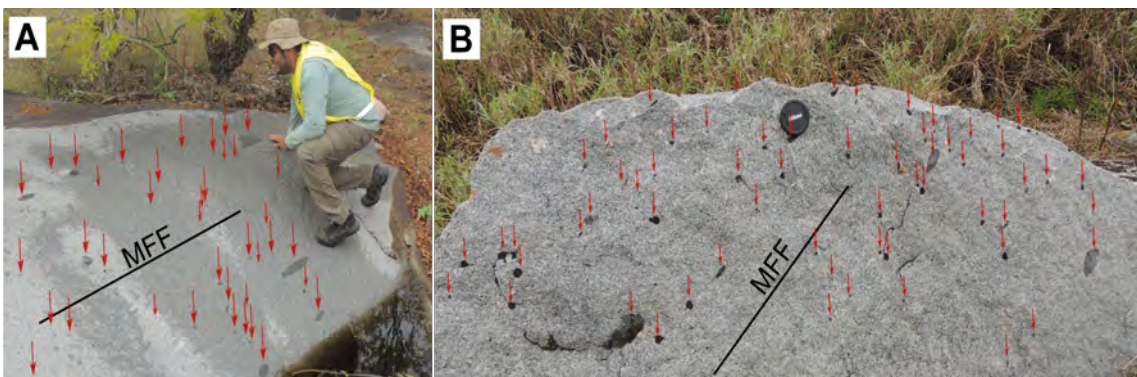


Figure 2. Photographs A and B correspond to biotite-granite outcrops where the studied enclaves occur. High abundance of microgranular enclaves characterize of these granites. The red arrows point to enclaves of varying sizes, with small enclaves predominating in these outcrops. The black circle in image B has a diameter of 6 cm. MFF = magmatic flow foliation that orients enclaves and minerals in the biotite-granite.

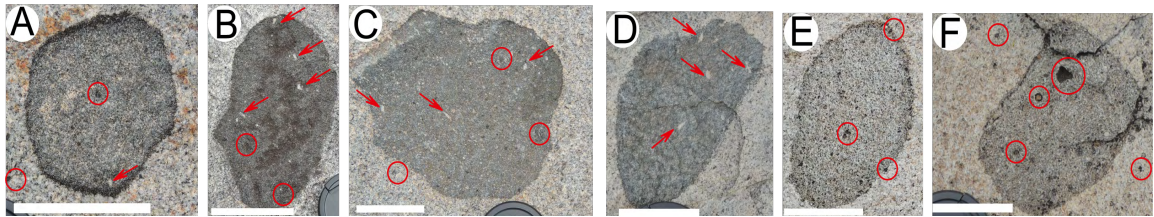


Figure 3. Images of microgranular enclaves hosted in biotite-granite from Glória Sul Stock. The white bar in the images corresponds to 6 cm. Most of the studied enclaves have an ellipsoid shape with circular (A) and ellipsoidal (B, C, D and E) sections. In the sequence of enclaves from A to F, there is a variation in color, where enclaves A and B have a dark gray color, and C, E and F have a light gray color. Biotite edges (darker in color and smaller crystals) are present in enclaves A (well-marked and continuous) and in enclaves E and F (discontinuous). Note that in several enclaves there are feldspar xenocrysts (white color and indicated in the photograph with a red arrow). In enclaves A, B, E and F, clots of biotite and diopside (black areas) are present (red circle). Biotite and diopside clots are also present in granites (C and F). Also note the fine-grain and light color of the granite in these photos.

5.2. Petrography

5.2.1. Microgranular enclaves

The studied MEs are fine-grained syenites with allotriomorphic and hypidiomorphic textures. Some enclave show rounded clots of diopside and biotite (Figure 4A). Mineral composition in the MEs includes orthoclase, microcline, plagioclase, quartz, biotite, diopside, hornblende, opaque minerals, titanite, apatite, zircon, carbonate, muscovite, and epidote (Figure 4B and C).

Oligoclase and albite crystals (0.05 - 0.6 mm) exhibit anhedral and subhedral shapes, displaying albite and albite-Carlsbad twinning. Some crystals show a thin, dark-colored rim as seen in the backscattered electron images, corresponding to albite ($An < 5\%$; Figure 4D). Amoebic contacts in oligoclase and albite suggest corrosion. Included within these crystals are acicular apatite (<0.2 mm), biotite, titanite, and zircon (Figures 4D).

Orthoclase and microcline (0.02-0.7 mm) are anhedral (Figure 4B and C), perthitic and includes subhedral crystals of biotite, apatite (Figure 4D), titanite, zircon, magnetite, and ilmenite. Quartz is anhedral (0.01 – 1.4 mm) and includes (<0.1 mm) biotite, apatite, titanite and opaque minerals. The brown biotite (0.2 – 1.8 mm) are subhedral (Figure 4F), euhedral, and with a blade texture (Figure 4D and E). These biotite crystals include of acicular apatite and zircon, titanite, diopside, opaque minerals, and are partially altered to chlorite. Locally ocellar quartz can be found, surrounded by crystals of biotite, orthoclase, diopside and titanite (Figure 4F). Green diopside (0.03 – 0.8 mm) is subhedral and anhedral (Figures 4B, C), including titanite, biotite, apatite, and zircon. Some enclaves contain rounded clots of diopside and biotite (Figure 4A).

Green amphibole (0.05 - 0.4 mm) is subhedral and anhedral, including anhedral diopside, as well as subhedral and euhedral crystals of titanite, biotite, apatite, and zircon. Apatite (<0.2 mm) is acicular (Figures 4D, G) well-distributed throughout the enclaves (Figure 4G), suggesting that phosphorus saturation in trachyte magma was very early. Zircon is euhedral (Figures 4H and I), subhedral and may have an acicular habit with gulls suggestive of corrosion (Figure 4J), including thorite and acicular apatite (Figure 4I). Titanite (0.06-0.3 mm) is euhedral, subhedral, and displays curved contacts and zonation (Figure 4L). Magnetite, ilmenite, and pyrite are the opaque minerals presents in these rocks.

5.2.2. Crystallization Sequence

The crystallization sequence in the trachytic magma (MEs) is established based on observed textures. Apatite is the first liquidus mineral, followed by zircon. Subsequently, titanite, biotite, diopside, ilmenite, magnetite, alkali feldspar, plagioclase and quartz are formed. The extended crystallization history of biotite is indicated by its presence as inclusions in magmatic minerals such as diopside, titanite, alkali feldspar, hornblende, and quartz). Hornblende crystallization results from the destabilization of diopside. The presence of the biotite-diopside clots in the enclaves and granites suggests the disintegration of early pulses of trachytic magma in the rhyolitic magma chamber (GSS). In the late-magmatic stage, albite, the exsolution of alkali feldspar, epidote, pyrite, carbonate, chlorite, titanite, and muscovite are formed.

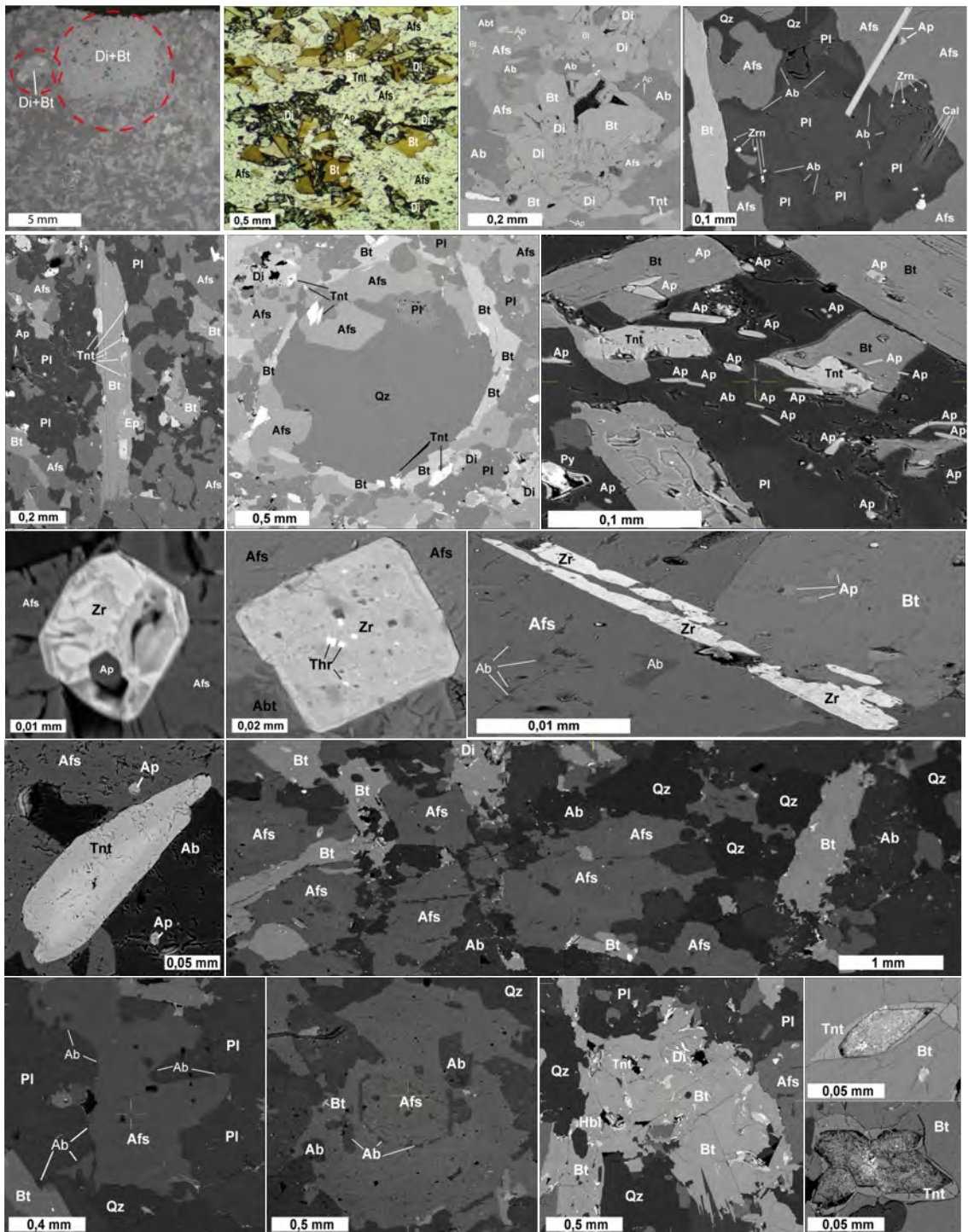


Figure 4. Textures present in the microgranular syenitic enclaves (A-L) and the host biotite-granite (M-S). Apart from image B, which was obtained using an optical microscope with transmitted and polarized light, the other images were obtained using a backscattered electron (BSE) detector in the SEM. [A] texture with millimetric clots of diopside (Di) + biotite (Bt). The clots are highlighted by dashed red circles. [B] characteristic fine-grained texture of the enclaves, with the presence of clots of diopside (light green) and biotite (brown) crystals. The transparent mineral is alkali feldspar and the dark spots in the biotite correspond to crystals of zircon (Zr) and titanite (Tnt). [C] texture in the enclave where it is possible to see the association of biotite, diopside, alkali feldspar (Afs), albite (Ab), apatite (Ap). [D] image of plagioclase crystals (Pl) with albite coronae. The contact between plagioclase and albite (darker gray region) is normally ameboid. Note the acicular apatite crystal included in both the albite and the alkali feldspar. [E] biotite crystal with inclusions of titanite and epidote (Ep). [F] ocellar quartz texture. The anhedral quartz crystal (Qz) is surrounded by biotite, alkali feldspar, plagioclase and titanite crystals. The white dots correspond to apatite crystals. [G] common texture in the studied enclaves with many

acicular apatite crystals. Some apatite crystals are included in various crystals, such as plagioclase and biotite. [H and I] euhedral zircon crystals. Note that in image I the zircon is included in alkali feldspar and has inclusions of thorite (Thr) crystals. [J] inclusion of a skeletal zircon crystal in alkali feldspar perthite. [L] zoned titanite crystal is a frequent texture in enclaves. The images M - S correspond to textures present in the biotite-granites with diopside that host the enclaves. [M] allotriomorphic texture of medium to fine-grained biotite-granites. [N] plagioclase crystals with albite coronae. [O] zoned and perthitic alkali feldspar phenocrysts. Note that the albite has the prismatic shape of alkali feldspar. [P] biotite-granite texture showing subhedral biotite crystals, with titanite inclusions, associated with diopside and hornblende. Images Q and R show the characteristic texture of the euhedral titanite crystals in these granites, with the central region altered to a porous, white material in reflected light.

5.2.3. Petrography of the host biotite-granites

The host biotite granites primarily consist of alkali feldspar, quartz, plagioclase, and biotite, with accessory minerals including diopside, titanite, epidote, zircon, apatite, hornblende, and opaque minerals. Alkali feldspar is subhedral (Figure 4M), occurring as phenocrysts (0.8 – 4.25 mm) and smaller crystals (0.05-0.7 mm), often display perthitic texture (Figures 4N, O) and zonation (Figure 4O).

Phenocrysts include inclusions of biotite, plagioclase, epidote, titanite, apatite, zircon, and opaque minerals. Plagioclase is subhedral, can occur as phenocrysts, and in the matrix the crystals range in size from 0.05 to 1.4 mm. Saussuritization is observed in some crystals. Antiperthite and zoned textures are present, including alkali feldspar, biotite, titanite, epidote, apatite, zircon, and opaque minerals.

The brown biotite crystals (<2 mm) are straight and irregular, containing inclusions of alkali feldspar, zircon, apatite, titanite, epidote and opaque minerals (Figures 4M, P).

Subhedral green diopside (<1.3 mm) makes curved contacts with alkali feldspar, quartz, and hornblende crystals. Clots of biotite and diopside (< 1.5 cm in diameter), as well as biotite aggregates, occur randomly, possibly represent xenocrysts from the disaggregation of early pluses of trachytic magmas (MEs).

Green hornblende (<2 mm) is subhedral and includes crystals of diopside, alkali feldspar, biotite, and opaque minerals. Epidote (<1 mm) is subhedral and anhedral, associated with biotite, plagioclase, and includes quartz, titanite, biotite, and opaque minerals.

Subhedral titanite (<0.8 mm) is associated with biotite, showing central part altered (Figures 4P, Q, R) to titanium oxide and hydroxides. Subhedral zircon (<0.13 mm) occurs zoned and acicular, including apatite and opaque minerals. Apatite is subhedral, euhedral, and acicular (<0.2 mm). Subhedral muscovite (<1 mm) makes straight contacts with rock minerals, except biotite which is curved and sutured.

Muscovite and chlorite likely form from biotite. Micro-fractures in the rocks are occupied by carbonate, albite, and opaque minerals.

5.3. Mineral Chemistry

In the studied biotite crystals from both ME and host biotite granite, there were no significant chemical variations observed between the center and edge analyses, but variations were noted between crystals from different rocks. The chemical compositions of the brown biotite (Table 2) in the enclaves correspond to Mg-biotite and Fe-biotite, while in the granites, Fe-biotite predominates (Figure 5).

In the studied biotite crystals, the occupation of the tetrahedral site (^{IV}T) is done by Si⁴⁺ and Al³⁺. The octahedral (^{VI}X) and dodecahedral (^{XII}Y) sites have vacancies (Table 2). In ^{VI}X and ^{XII}Y sites its occupancy varies from 0-28% (<0.6 atoms per formula unit = apfu) in the enclaves and 0-9.5% (<0.2 apfu) in the BG. Variations identified in biotite compositions indicate the existence of cationic substitutions. Good cationic correlations were observed between:

[i] ${}^{VI}R^{2+} + 2 {}^{VI}Al^{3+} = {}^{VI}\square + 2 {}^{IV}Si^{4+}$ (^{VI}□ = vacancy in the octahedral site; Figure 6A): This substitution, according to Stussi and Cuney (1996), involving aluminum (^{IV}Al) from the tetrahedral site, the sum of divalent cations (R²⁺= Fe + Mg + Mn) in the octahedral site, and silicon (^{IV}Si⁴⁺), in the tetrahedral site, generating vacancies in the octahedral site (^{VI} □). The correlation diagrams (Figure 6A) show good linear correlations ($r^2 \approx 0.9$), indicating the nature of the substitution.

[ii] ${}^{VI}R^{2+} + {}^{VI}Ti = 2 {}^{VI}Al$ (Figure 6B): This substitution occurs in the octahedral site and involves the exchange of divalent cations and Ti for octahedral aluminum. The diagram show reasonable alignment ($r^2 \approx 0.73$), suggesting the occurrence of this substitution in the biotite crystals.

Table 2. Representative chemical analyses of the biotite crystals studied. Structural formula calculated for 22 oxygens. Microgranular enclaves (EMs) and biotite-granite (BG).

	Microgranular Enclaves					Biotite Granites				
SIO ₂	38.50	38.78	38.29	38.62	38.58	37.54	36.85	38.00	36.24	36.45
TiO ₂	2.59	2.88	3.06	3.18	3.01	3.17	3.14	2.80	3.29	3.10
Al ₂ O ₃	15.74	15.46	14.01	13.69	13.74	14.69	14.06	14.60	14.51	14.37
FeO	16.13	15.36	16.96	17.00	16.78	19.58	19.57	18.84	19.79	18.95
MnO	0.10	0.29	0.27	0.22	0.25	0.29	0.30	0.28	0.10	0.00
MgO	13.34	13.25	12.77	13.09	13.08	10.46	10.01	10.08	10.02	9.85
CaO	0.00	0.00	0.07	0.01	0.09	0.00	0.30	0.11	0.00	0.00
Na ₂ O	0.00	0.00	0.18	0.14	0.06	0.58	1.89	1.48	1.04	1.74
K ₂ O	8.93	10.08	10.18	10.00	10.08	9.79	9.46	9.41	9.40	9.09
BaO	0.00	0.00	0.00	0.00	0.00	0.00	0.24	0.25	0.08	0.10
Cr ₂ O ₃	0.00	0.00	0.12	0.04	0.14	0.00	0.11	0.08	0.17	0.29
NiO	0.00	0.00	0.02	0.00	0.04	0.00	0.00	0.00	0.29	0.29
F	0.70	0.80	0.03	0.00	0.14	0.00	0.00	0.00	0.00	0.00
Cl	0.10	0.00	0.05	0.01	0.01	0.00	0.00	0.00	0.80	1.29
OH=F=Cl	-0.32	-0.34	-0.02		-0.06				-0.18	-0.29
Total	95.81	96.56	95.99	96.01	95.95	96.10	95.93	95.91	95.54	95.22
SI	5.727	5.746	5.758	5.791	5.793	5.702	5.660	5.774	5.610	5.663
Al ^{IV}	2.273	2.254	2.242	2.209	2.207	2.298	2.340	2.226	2.390	2.337
Al ^{VI}	0.488	0.445	0.241	0.210	0.225	0.332	0.206	0.389	0.257	0.295
TI	0.290	0.321	0.346	0.358	0.340	0.362	0.363	0.320	0.383	0.362
Cr	0.000	0.000	0.015	0.005	0.017	0.000	0.013	0.009	0.021	0.035
^T Fe	2.007	1.903	2.133	2.132	2.107	2.488	2.514	2.394	2.562	2.462
Mn	0.012	0.036	0.034	0.028	0.032	0.037	0.039	0.036	0.013	0.000
Mg	2.959	2.926	2.862	2.927	2.929	2.369	2.292	2.283	2.313	2.281
Ni	0.000	0.000	0.002	0.000	0.005	0.000	0.000	0.000	0.036	0.036
Ca	0.000	0.000	0.011	0.002	0.014	0.000	0.049	0.017	0.000	0.000
Na	0.000	0.000	0.053	0.042	0.017	0.170	0.563	0.436	0.311	0.523
K	1.694	1.905	1.952	1.913	1.931	1.897	1.852	1.824	1.856	1.802
Ba	0.000	0.000	0.000	0.000	0.000	0.000	0.014	0.015	0.005	0.006
Total	19.450	19.536	19.649	19.616	19.616	19.655	19.906	19.723	19.756	19.803
OH	3.645	3.625	3.973	3.997	3.931	4.000	4.000	4.000	3.790	3.660
F	0.329	0.375	0.014	0.000	0.066	0.000	0.000	0.000	0.000	0.000
Cl	0.025	0.000	0.013	0.003	0.003	0.000	0.000	0.000	0.210	0.340
Li	0.877	0.921	0.853	0.905	0.900	0.733	0.624	0.812	0.522	0.561
Fe ³⁺	0.000	0.086	0.036	0.000	0.009	0.090	0.375	0.441	0.059	0.296

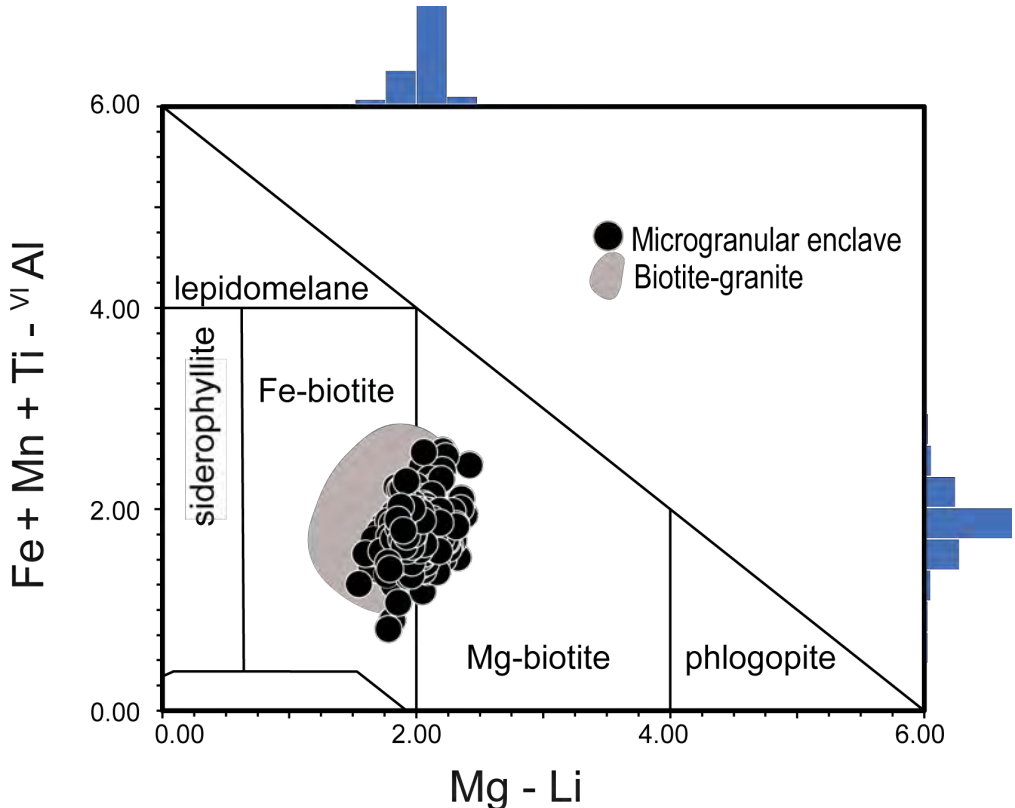


Figure 5. Mg-Li versus $\text{Fe}+\text{Mn}+\text{Ti}-\text{VII Al}$ diagram for the classification of micas from Tischendorf et al. (1997), applied to the analyzed biotite crystals. The added sidebars illustrate the distribution of the 621 analyses corresponding to biotite from the microgranular enclaves.

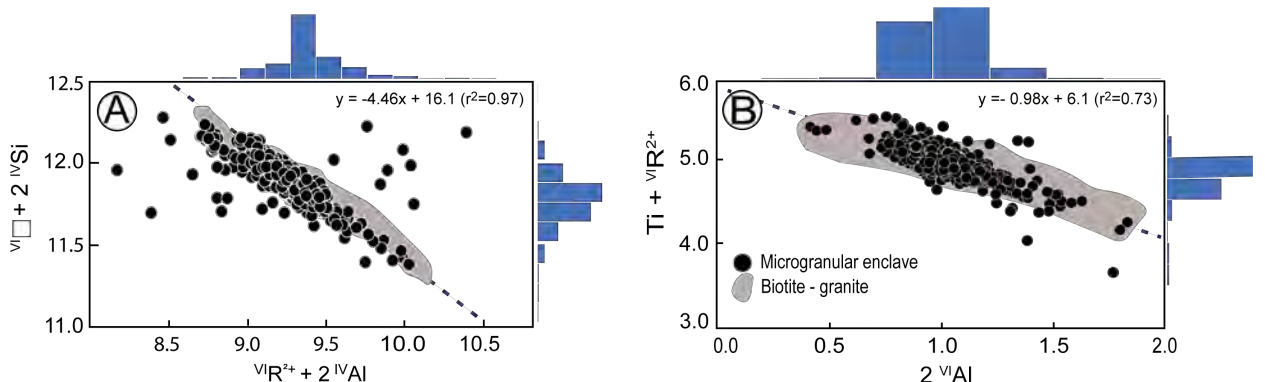


Figure 6. Cation correlation diagrams used to illustrate the chemical evolution of the studied biotite crystals. A) substitution $\text{VI} \square + 2 \text{IV} \text{Si} = \text{VI} \text{R}^{2+} + 2 \text{IV} \text{Al}$ ($\text{VI} \square =$ vacancy in the octahedral site; $\text{R}^{2+} = \text{Fe}+\text{Mg}+\text{Mn}$). B) substitution $\text{Ti} + \text{VI} \text{R}^{2+} = \text{VI} \square + 2 \text{VI} \text{Si}$. The added bars illustrate the distribution of the 621 analyzes corresponding to biotite from the microgranular enclaves. The linear correlation equations for the two diagrams are presented with their correlation coefficients (r^2).

6. DISCUSSION

The presence of microgranular enclaves in igneous rocks typically indicates mingling between magmas (e.g., Fernandez and Barbarin, 1991). Conceição et al. (2016) identified that in the BG, the least evolved rocks of the GSS, that the largest volume of MEs occurs in the BG, and they correspond to syenites. The multiple

enclaves observed in the biotite-granite suggests occurrence of pulses of trachytic magmas in the rhyolitic magma chamber of the GSS.

The MEs in the GSS are characterized by a rounded, finer-grained/fine-grained texture compared to host BG, and by abundant acicular apatite and zircon crystals, indicating rapid cooling of the enclave magma against the biotite granite magma. The rounded shape of the MEs and fine grain size / their fine-grained texture suggest the coexistence of magmas with different compositions (Conceição et al. 2016). Additionally, features such as the blade texture of biotite and by the abundance of zoned plagioclase and titanite crystals in the GSS further indicate magma mingling, consistent with findings in previous studies (e.g., Hibbard, 1991; Weidendorfer et al., 2014; Esfahani et al., 2017; Gogoi et al., 2018; Mbassa et al., 2020).

Spear (1984) considers as evidence when magmatic biotite has a grain size similar to that of other magmatic minerals in the rock. On the other hand, Nachit et al. (2005) consider that magmatic biotite is brown. Liu et al. (2020) suggest that biotite is considered as magmatic if the crystals are euhedral, subhedral and have clear contacts with other magmatic minerals. The textures presented by biotite in the MEs and in the host BG have the features that the literature reports for magmatic crystals.

The cooling history of felsic plutonic systems are complex due to late-stage percolation of hydrothermal fluids that can chemically re-equilibrate the minerals (e.g., Bonin, 1995, Cobbing 2000). In this context, Nachit et al. (2005) use the TiO₂, FeO, MnO and MgO content in biotite to deduce whether it is magmatic, reequilibrated magmatic or non-magmatic (Figure 7A). The chemistry of biotite from the MEs plots in the field of re-equilibrated magmatic biotite, with certain crystals, included in feldspars, closely bordering magmatic biotite field. The chemistry of the biotite crystals of the BG plots in the fields of magmatic biotite and re-equilibrated magmatic biotite (Figure 7A). There is significant variation in the TiO₂ content in the biotite crystals of MEs (0.6<%TiO₂ <3.2) and BG (1<%TiO₂ < 3.6). This variation maintains the MgO/(FeO+MnO) ratio relatively constant. Generally, the value of this ratio is higher in BG crystals (0.44-0.52) compared with biotite of the enclaves (0.42-0.46; Figure 7B). This behavior probably reflects the effect of the partial chemical equilibrium in biotite. The reduction of titanium in biotite and the simultaneous increase in aluminum are controlled by the substitution R²⁺ + ^{VI}Ti = 2 ^{VI}Al³⁺ (Figure 8B). However, the ratios of Mg/(Fe+Mn) do not appear to have been affected (Figure 7A). The enrichment of aluminum in biotite, as suggested by Stussi and Cuney (1996), indicates a decrease in

temperature, which is associated with the evolution of magma crystallization and the influence of hydrothermal fluids.

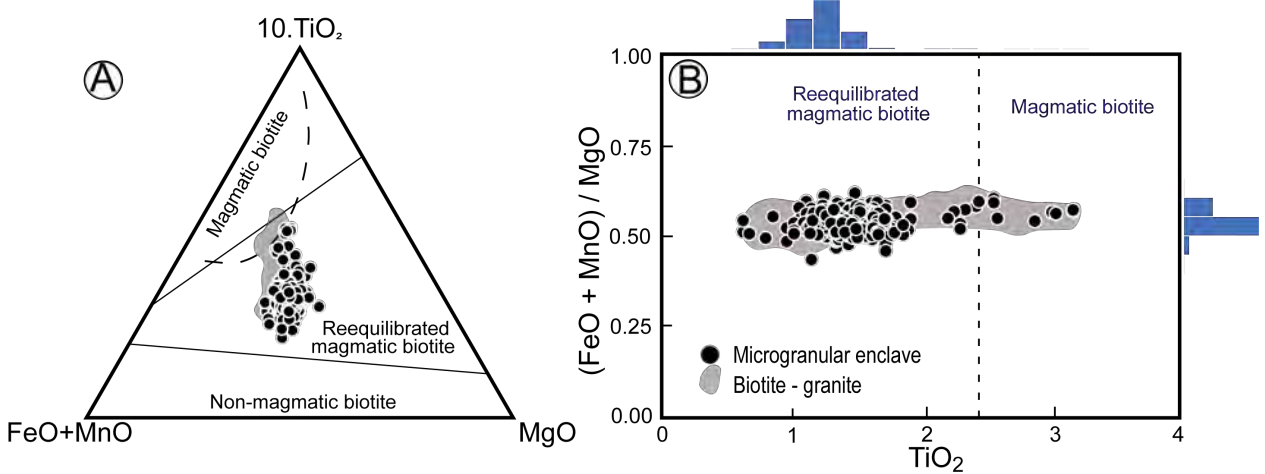


Figure 7. Discriminating chemical diagrams for biotite. (A) $\text{MgO} - (\text{FeO} + \text{MnO}) - 10\text{TiO}_2$ diagram Nachit et al. (2005) to discriminate magmatic, magmatic, re-equilibrated and non-magmatic biotite applied to the analyzed crystals. (B) $(\text{FeO} + \text{MnO} + \text{MgO}) / (\text{FeO} + \text{MnO})$ versus TiO_2 proposed to note the variation of these oxides in the analyzed crystals. The added bars illustrate the distribution of the 621 analyzes corresponding to biotite analyzes of the studied microgranular enclaves.

Biotite, a common mineral in igneous rocks, has a complex chemical composition, limiting its use in inferring intensive parameters of magmas. However, researchers have used biotite to calculate temperature (e.g., Robert, 1976; Luhr et al., 1984; Patiño Douce, 1993; Henry et al., 2005, Li and Zhang. 2022), pressure (Uchida et al., 2007; Li and Zhang. 2022) and the oxidation conditions (Wones and Eugster, 1965), as well as its magmatic affinity (e.g., Nachit et al., 1985; Abdel Ramam, 1994) and the source of the magmas (Zhou et al., 1986). In this study, biotite crystals from MEs with higher titanium contents and magmatic crystals from biotite-granite were used to estimate the pressure, temperature, and oxygen fugacity conditions of the analyzed rocks (Table 2).

In their study on Japanese granites, Uchida et al. (2007) identified a good correlation between aluminum in hornblende and biotite and proposed the use of Al contents in biotite as a geobarometer, according to the equation: $P \text{ (kbar)} = 3.03 \times \text{Al} - 6.53 (\pm 0.33)$, where P = pressure (kbar) and Al corresponds to total aluminum ($^{VI}\text{Al} + ^{IV}\text{Al}$). Biotite crystals with higher titanium (0.25-0.36 apfu) in MEs yielded calculated pressures of 1.8-0.8 kbar (6,7-3 km) and those from the host biotite-granite the pressure varies from 2.1-1.2 kbar (7,8-4 km). However, caution should be exercised when applying the barometer of Uchida et al. (2007) to granitic rocks. Li and Zhang. (2022) points out that pressures calculated using that geobarometer provide lower values than the experimental data. These authors suggest that it is more appropriate to apply a geobarometer based on machine learning, which is an algorithm that uses a dataset

based on random trees of biotite compositions for a wide range of temperatures and pressures (1325-625 °C, 48-1 kbar). Applying the algorithm of Li and Zhang. (2022) calculated biotite crystallization pressure of the studied rocks/our rocks, shows 10.7-4.3 kbar for the microgranular enclaves and 6.3-3.4 kbar for the granites (Table 1). In other words, in the MEs, biotite crystallizes earlier at depths from 39 to 16 km, while in granites it crystallizes at depths from 23 to 13 km. These results indicate that the initial crystallization of biotite in trachytic magma occurs at great depths (39 km, in the SOS is equivalent, according to the geophysical studies of Oliveira et al. (2023), to the base of the continental crust or upper mantle). The higher-pressure values for granite's biotite (23 km) may correspond to the maximum depth at which the trachytic and rhyolitic magmas mixed. On the other hand, the variation between the maximum and minimum pressure values obtained may reflect the continued crystallization of biotite or its geochemical reequilibration during the ascent of those coeval magmas towards its final emplacement at 13 km depth.

Table 3. Maximum and minimum temperature and pressure values obtained in this study. Temperature values were calculated using P saturation in whole rock (Harrison and Watson, 1984), after the data from Conceição et al. (2016). Temperature and pressure values were calculated using chemical data from biotite crystals with a high titanium content from enclaves (MEs) and magmatic biotite from biotite-granites (BG).

	Temperature (°C)						Pressure (kbar)			
	P-saturation*		Henry et al. (2005)		Li and Zhang (2022)		Uchida et al. (2007)	Li and Zhang (2022)		
MEs	984	961	993	801	900	780	1.8	0.8	10.7	4.3
BG	930	925	993	782	809	765	2.1	1.2	6.3	3.4

The titanium in biotite is sensitive to temperature variations, which is why several authors suggest that biotite can be used as a geothermometer (e.g., Robert, 1976; Luhr et al., 1984; Patiño Douce, 1993; Henry et al., 2005). The experimental work of Henry et al. (2005) proposes the use of the Ti-biotite geothermometer for metapelitic rocks, but several authors have applied this geothermometer to granitic rocks (e.g., Tang et al., 2019). The Henry et al. (2005) expression is: $T = \{[\ln(Ti) - ac(X_{Mg})^3]/b\}^{0.333}$, with an error of ± 24 °C; where T = temperature (°C), $X_{Mg} = Mg/(Mg+Fe)$ and the constants are: a = -2.3594, b = 4.6482×10^{-9} and c = -1.7283. The calibration range for this expression is $X_{Mg} = 0.275-1.000$, Ti = 0.04-0.60 apfu, T = 800-480 °C, and 6-3 kbar. Applied to biotite crystals of the MEs, temperatures range from 993-801 °C, and temperatures of BG crystals range from 993-782 °C (Table 1). The maximum values obtained in this study exceed the limits established for the geothermometer by Henry et al. (2005) and should therefore be used with caution. Some authors (e.g. Cesare et al., 2008;

Azadbakht et al., 2020; Li and Zhang., 2022) have evaluated the reliability of the thermometer of Henry et al. (2005) in igneous rocks and found that the calculated temperature usually diverges from the values obtained in experiments. In the thermometer calibrated by Li and Zhang. (2022), the temperatures obtained for the studied rocks were 900-780 °C for EMs and 809-765 °C for granites. The two temperatures sets obtained by the two different geothermometers undoubtedly represent liquidus temperatures. Although experimental studies with rhyolitic and trachytic magmas saturated in H₂O indicate that biotite can crystallize at temperatures between 950-1000 °C (e.g. Costa et al., 2020), we consider that the temperature of 900 °C is the most likely for early crystallization of biotite in the enclaves.

By correlating the P-T data for magmatic biotite crystals (Figure 8), it can be seen that: (1) the range of temperature (900-800 °C) obtained for biotite crystallization in both the microgranular enclaves and the granite are undoubtedly magmatic; (2) the evolution marked by the decrease in temperature and pressure for the two sets of biotite crystals (enclave and granite), may reflect the rise of magmas towards the mesozonal crust; (3) most pressure obtained on biotite crystals from granites concentrates between 6-3 kbar and only 4 analyses distance themselves from this set and show pressure and temperature values similar to the highest values found in the enclaves. These high-temperature and pressure biotite crystals in granites may correspond to xenocrysts assimilated from the trachytic magma during magma interaction, supporting the hypothesis of more intense assimilation and disaggregation observed in some enclaves. More intense assimilation between the magmas, observed in some enclaves and the disaggregation of clinopyroxene and biotite clots, are features present in the studied rocks that support this hypothesis.

The maximum temperature values obtained for the crystallization of biotite are lower than those found for phosphorus saturation (Figure 8). Assuming the presence of biotite xenocrysts in the granites, the interaction between the trachytic and rhyolitic magmas likely occurred at 23 km depth and temperatures around 800 °C (Figure P-T). Fernandez and Barbarin (1991) propose that to generate microgranular enclaves, the degree of crystallization of the host magma must reach 20-30%, creating a significant temperature and viscosity between contrasting magmas. Under these conditions, the temperature difference, capable of generating the thermal shock necessary to form the acicular apatite, skeletal zircon, and biotite blade textures in the studied microgranular

enclaves. On the other hand, the biotite included in alkali feldspar can be preserved from interaction with hydrothermal fluids frequent in the cooling of plutonic systems.

Wones and Eugster (1965) suggest that the molar fraction of magnesium ($X_{Mg} = [Mg/(Mg+Fe)]$) in magmas and fluids tends to increase with higher oxygen fugacity. They propose a diagram correlating Fe^{2+} - Fe^{3+} - Mg^{2+} that allows inferences about the conditions of oxygen fugacity in the magma where biotite crystallized. The biotite crystals from both MEs and the host biotite-granite are above the QFM buffer and in the NNO, indicating relatively oxidized conditions, as the values range between -19 and -16 (Table 3). The titanite-magnetite-quartz paragenesis, that characterizes high degree of oxidation according to Wones (1989) is present in the mineral composition of MEs and biotite-granite.

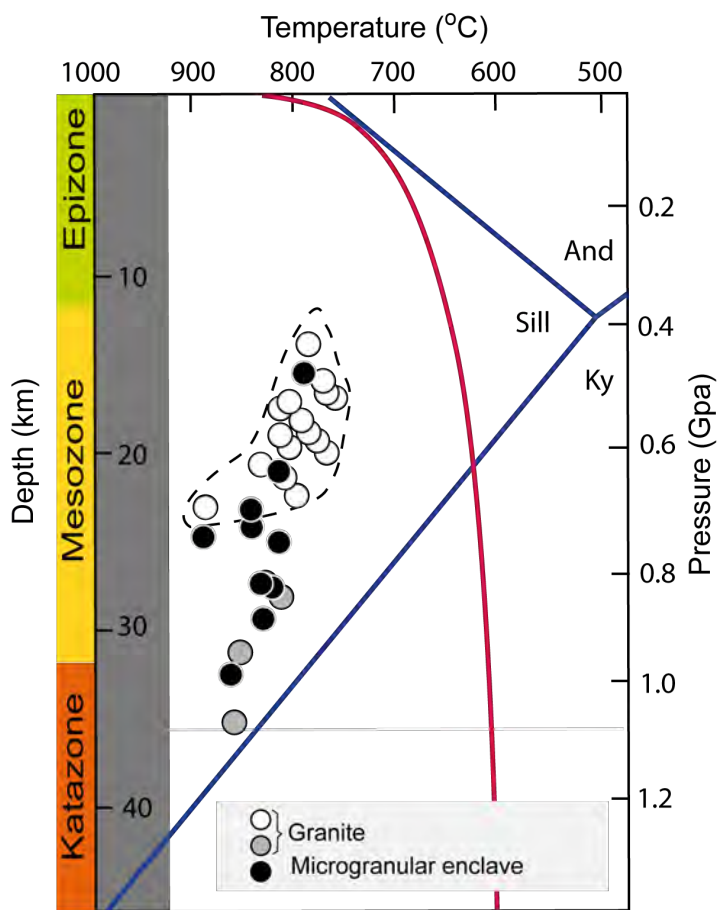


Figure 8. Temperature (°C) - Pressure (kbar) diagram with thermobarometric determinations, calculated using the Li and Zhang. (2022) algorithm, of the biotite crystals from the enclaves and studied biotite-granites. The gray rectangle corresponds to the temperature range for saturation of the trachytic magma (enclave) in phosphorus, calculated using the Harrison and Watson (1984) algorithm. Red curve = water-saturated granite solidus. Blue curves delimit the stability fields of the minerals kyanite, andalusite and sillimanite. Black circle = biotite crystals from microgranular enclaves; white circle = biotite crystals from granite, and gray circle = biotite xenocrystals from granites

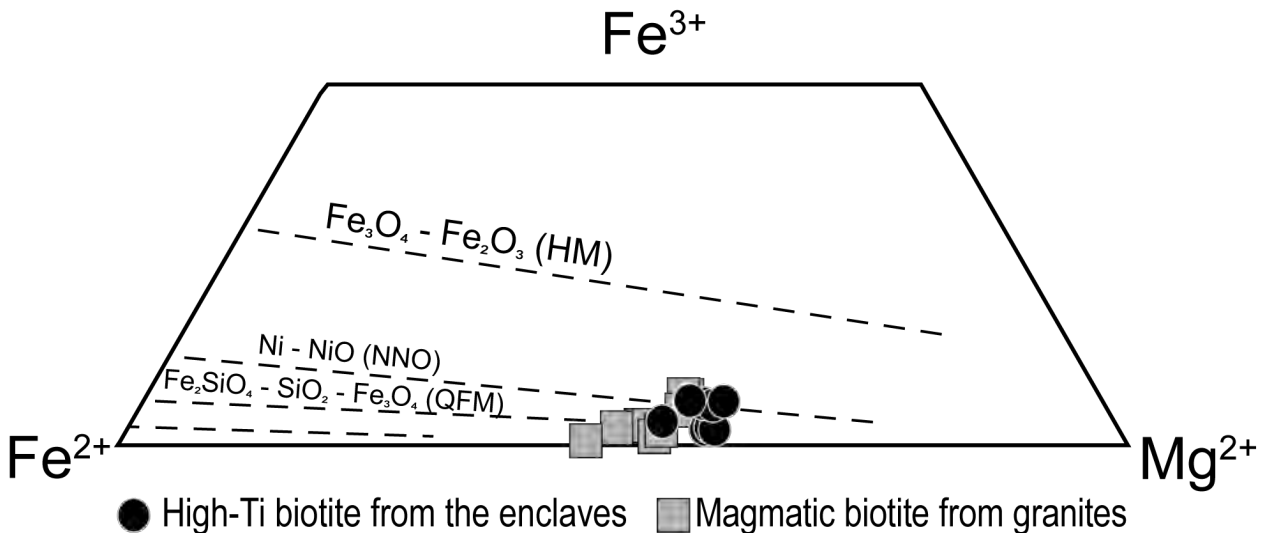


Figure 9. Fe^{2+} - Fe^{3+} - Mg^{2+} diagram of the Wones and Eugster (1965) for inferring oxygen fugacity conditions, applied to the studied biotite crystals. Quartz-fayalite-magnetite (QFM), nickel-nickel oxide (NNO) and hematite-magnetite (HM) buffers. The circles correspond to microgranular enclave biotite crystals and the biotite square to host biotite-granite.

Several studies have demonstrated the existence of relationships between the chemistry of magmatic biotite and the composition of the magma from which it was formed (e.g., Nachit et al., 1985; Abdel Ramam, 1994). The chemical data obtained in this study suggest that the GSS biotite (enclaves and granites) has crystallized from magmas of the magnetite series (Figure 10A), which reinforces the hypothesis of crystallization under high oxygen fugacity conditions, and indicates magmas generated through melting of igneous protoliths.

The analyzed biotite crystals show affinities with orogenic magmas (Figure 10B and C). The biotite from MEs shows calc-alkaline affinity and that from BG shows calc-alkaline and peraluminous affinities (Figure 10B). By correlating the cation contents of Al and Mg, the biotite analyses of the studied rocks plot in the calc-alkaline field (Figure 10C). According to Zhou et al. (1986) the MgO and $\text{Fe}^{\#}$ values discriminate the source of the magmas from which the biotite crystals were crystallized (Figure 11). The studied biotite data (enclave and granite) occupy a field of magmas formed by the mixture between crustal and mantle sources (Figure 11). These results support the hypothesis proposed by Conceição et al. (2016) that GSS rocks result from the interaction between magmas and for various other SOS intrusions (e.g., Lisboa et al., 2019, 2020; Soares et al., 2022; Sousa et al., 2022, 2022a).

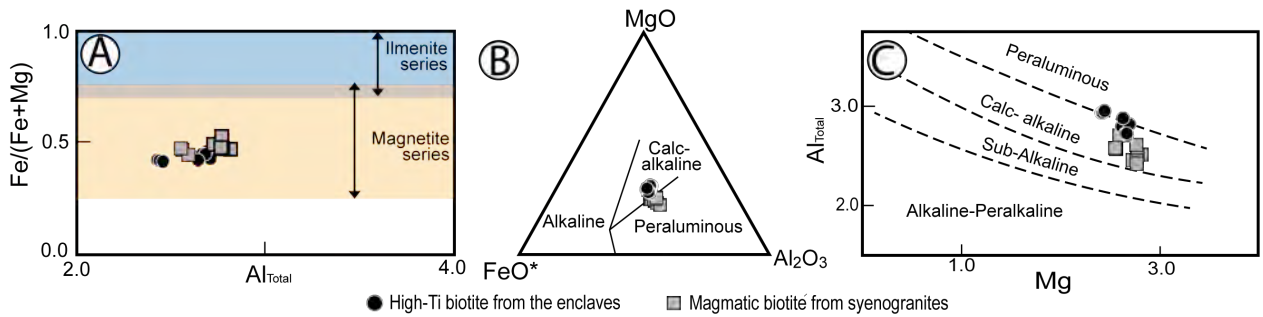


Figure 10. Diagrams for magmatic affinity inferences based on chemical data from biotite crystals applied to the analyzes of this study. (A) $\text{Fe}/(\text{Fe}+\text{Mg})$ - total Al diagram of the Anderson (2008). (B) Triangular diagram FeO^* - MgO - Al_2O_3 with fields of crystallized biotite in alkaline, calc-alkaline, and peraluminous magmas (Abdel Raman 1994). (C) Total Al - Mg diagram Nachit et al. (1985), with crystallized biotite fields in alkaline, calc-alkaline, aluminopotassic and peraluminous magmas. The circles correspond to biotite crystals from MEs and the area delimits the composition of biotite crystals from syenogranites.

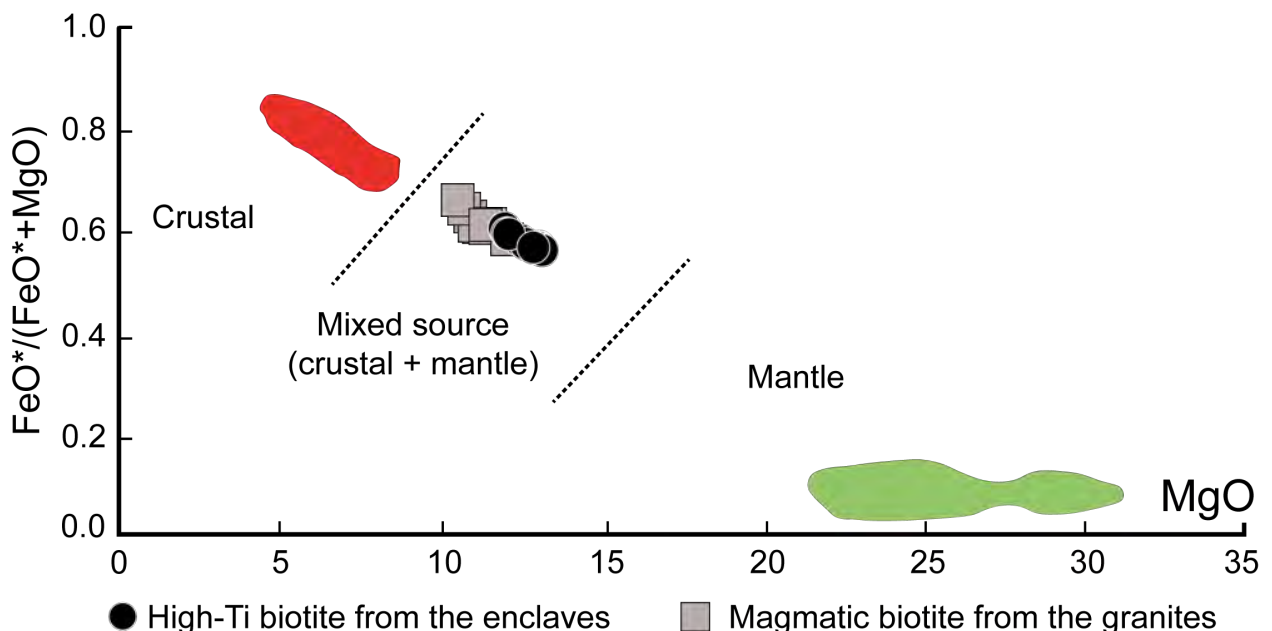


Figure 11. $\text{FeO}/(\text{FeO}+\text{MgO})$ versus MgO diagram Sousa et al. (2019) modified from Zhou (1986) for inference on the nature of the biotite-forming magma applied to the biotite crystals studied from Glória Sul Stock. The biotite fields of leucogranites (crustal source in red) and phlogopite of peridotites (mantle source in green).

7. FINAL CONSIDERATIONS

Microgranular syenitic enclaves are abundant in the dioside-bearing biotite granite from the Glória Sul Stock. These enclaves are centimetric, homogeneous and multiple, fine-grained, ranging in color from black to light grey, with well-defined contacts, rounded and ellipsoid shapes and host feldspar xenocrysts. These features indicate that two distinct magmas were present in the structuring of this Gloria Sul Stock: trachytic (enclaves) and rhyolitic (granites). Texture and mineral chemistry studies have led to the conclusion that:

- (1) The biotite crystals (magmatic and reequilibrated magmatic) present in the studied rocks are euhedral, subhedral and correspond to Fe- and Mg-biotite, with Mg-biotite dominant in the enclaves.

(2) The chemical evolution of the studied biotite crystals is controlled by two chemical substitutions (${}^{VI} R^{2+} + 2 {}^{VI} Al^{3+} = {}^{VI} \square + 2 {}^{IV} Si^{4+}$ and ${}^{VI} R^{2+} + {}^{VI} Ti = 2 {}^{VI} Al$) that control the increase in aluminum and the decrease in titanium and R^{2+} (Mg, Fe and Mn), reflecting the decrease in temperature and pressure, marking their rise.

(3) The use of geothermobarometers made it possible to determine the initial crystallization temperature of the biotite in the enclaves (900 °C) and granites (800 °C), as well as the respective pressures around 10.7 kbar (39 km) and around 6.3 kbar (23 km). The maximum depth estimated for the interaction between trachytic and rhyolitic magmas was 23 km in a magma chamber with a maximum temperature of 800 °C.

(4) The chemical data of biotite indicates that it crystallized from Type I, oxidizing, calc-alkaline (enclave) and calc-alkaline and peraluminous (granite) magmas, and that these rocks resulted from the mingling of mantle (enclave) and crustal (granite) magmas.

CRediT authorship contribution statement

Asayuki Rodrigues Menezes: Fieldwork, Writing – review & editing, Writing – original draft, Investigation, Data curation, Software, Conceptualization. **Joane Almeida da Conceição:** Fieldwork, Writing - original draft, Research, Data curation. **Maria de Lourdes da Silva Rosa:** Fieldwork, Writing – review & editing, Project administration, Methodology. **Gisele Tavares Marques:** Formal analysis, Data curation. **Claudio Nery Lamarão:** Supervision, Resources, Funding acquisition. **Herbet Conceição:** Fieldwork, Writing – review & editing, Writing – original draft, Validation, Supervision, Resources, Project administration, Methodology, Funding acquisition, Formal analysis, Conceptualization.

Declaration of competing interest

The authors declare that they have no known competing financial interests or personal relationships that could have appeared to influence the work reported in this paper.

ACKNOWLEDGMENTS

This study was carried out with the support from the Coordenação de Aperfeiçoamento de Pessoal de Nível Superior — Brazil (CAPES) — Financing Code 001. Asayuki Rodrigues Menezes thanks CAPES for the master's scholarship. Herbet Conceição (310740/2021-5), Maria de Lourdes Rosa (311023/2021-5), and Claudio Nery Lamarão (305607/2021-9) are fellows of the Brazilian National Council for Scientific and Technological Development (CNPq). The authors are grateful for the support of the Laboratory of Petrology Applied to Mineral Research at the Universidade Federal de Sergipe and the Microprobe Laboratory of the Federal University of Pará in the development of the research.

REFERENCES

- Adam, M.S.M., Kim, T., Song, Y.-S., Kim, Y.-S., 2019. Occurrence and origin of the zoned microgranular enclaves (MEs) within the Cretaceous granite in Taejongdae, SE Korea. *Lithos* 324–325, 537–550. <https://doi.org/10.1016/j.lithos.2018.11.008>
- A.-F. M. Abdel-Rahman, 1994. Nature of Biotites from Alkaline, Calc-alkaline, and Peraluminous Magmas. *Journal of Petrology* 35, 525–541. <https://doi.org/10.1093/petrology/35.2.525>
- Anderson, J.L., Barth, A.P., Wooden, J.L., Mazdab, F., 2008. Thermometers and Thermobarometers in Granitic Systems. *Reviews in Mineralogy and Geochemistry* 69, 121–142. <https://doi.org/10.2138/rmg.2008.69.4>
- Aranda, R.D.O., Horn, A.H., Medeiros Júnior, E.B.D., Venturini Junior, R., 2021. Geothermobarometry of igneous rocks from Afonso Cláudio Intrusive Complex (Espírito Santo state, Southeastern Brazil), Araçuaí-West Congo Orogen: Further evidence for deep emplacement levels. *Journal of South American Earth Sciences* 110, 103016. <https://doi.org/10.1016/j.jsames.2020.103016>
- Barbarin, B., 2005. Mafic magmatic enclaves and mafic rocks associated with some granitoids of the central Sierra Nevada batholith, California: nature, origin, and relations with the hosts. *Lithos* 80, 155–177. <https://doi.org/10.1016/j.lithos.2004.05.010>
- Brito Neves, B.B., Silva Filho, A.F.D., 2019. Superterreno Pernambuco-Alagoas (PEAL) na Província Borborema: ensaio de regionalização tectônica. *Geol. USP. Sér. Cient.* 19, 3–28. <https://doi.org/10.11606/issn.2316-9095.v19-148257>
- Clark, D.B., 1992. *Granitoid Rocks*. Chapman & Hall. London. 283p.
- Cobbing, J. 2000. The geology and mapping of granite batholiths. In: *Lecture Notes in Earth Sciences* 96. Editors S. Bhattacharji, G.M. Friedman, T.H.J. Neugebauer, A. Seilacher. Springer, Berlin. 141p.
- Conceição, H., Rosa M.L.S., Lisboa, V.A.C., Fernandes, D.M., Sousa, E.S., Cruz, J.W.S., Cruz, H.J., Oliveira, I.R., Souza, J.M.D., Oliveira, I.L., 2017. Magmatismos no Domínio Macururé, Sistema Orogênico Sergipano: Estado do conhecimento. *XXVII Simpósio de Geologia do Nordeste*. João Pessoa: SBG.
- Conceição, J.A.D., 2019. Magmatismo leucogranítico do Domínio Macururé, Sistema Orogênico Sergipano, Província Borborema, NE do Brasil (Tese). Instituto de Geociências – UFBA, Salvador.
- Conceição, J.A.D., Rosa, M.L.S., Conceição, H., 2016. Sienogranitos leucocráticos do Domínio Macururé, Sistema Orogênico Sergipano, Nordeste do Brasil: Stock Glória Sul. *Braz. J. Geol.* 46, 63–77. <https://doi.org/10.1590/2317-4889201620150044>
- Costa, S., Masotta, M., Gioncada, A., Pistolesi, M., Bosch, D., Scarlato, P., 2020. Magma evolution at La Fossa volcano (Vulcano Island, Italy) in the last 1000 years: evidence from eruptive products and temperature gradient experiments. *Contribuiton Mineral Petrology* 175, 31. <https://doi.org/10.1007/s00410-020-1669-0>

- Davison, I., Santos, R.A., 1989. Tectonic evolution of the Sergipano Fold Belt, NE Brazil, during the Brasiliano orogeny. *Precambrian Research* 45, 319–342. [https://doi.org/10.1016/0301-9268\(89\)90068-5](https://doi.org/10.1016/0301-9268(89)90068-5)
- Didier, J., Barbarin, B., 1991. Enclaves and Granite Petrology (Development in Petrology). Elsevier, Oxford (UK).
- Dymek, R.F., 1983. Titanium, aluminium, and interlayer cation substitutions in biotite from high-grade gneisses, West Greenland. *American Mineralogist* 68, 880–899.
- Faure, G. 2001. Origin of Igneous Rocks: The Isotopic Evidence. Springer, Berlin. 496p.
- Esfahani, M.M., Khalili, M., Bakhshi, M., 2017. Petrogenesis of Soheyle- Pakuh and Golshekanan granitoid based on mineral chemistry of ferromagnesian minerals (north of Nain), Iran. *Journal of African Earth Sciences* 129, 973–986. <https://doi.org/10.1016/j.jafrearsci.2017.01.033>
- Faure, G., 2001. Origin of Igneous Rocks: The Isotopic Evidence. Springer-Verlag, Berlin (DE).
- Fernandes, D.M., Lisboa, V.A.C., Rosa, M.L.S., Conceição, H., 2020. Petrologia e idade do Stock Fazenda Lagoas, Domínio Macururé, Sistema Orogênico Sergipano, NE-Brasil. *Geol. USP. Sér. Cient.* 20. <https://doi.org/10.11606/issn.2316-9095.v20-160040>
- Fernandez, A., Barbarin, B., 1991. Relative rheology of coeval mafic and felsic: nature of resulting interaction process. Shape and mineral fabrics of mafic microgranular enclaves, in: Enclaves and Granite Petrology. Elsevier, Oxford (UK), pp. 116–128.
- Gogoi, B., Saikia, A., Ahmad, M., 2018. Field evidence, mineral chemical and geochemical constraints on mafic-felsic magma interactions in a vertically zoned magma chamber from the Chotanagpur Granite Gneiss Complex of Eastern India. *Geochemistry* 78, 78–102. <https://doi.org/10.1016/j.chemer.2017.11.003>
- Gündüz, M., Asan, K., 2023. MagMin_PT: An Excel-based mineral classification and geothermobarometry program for magmatic rocks. *Mineral Magazine* 87, 1–9. <https://doi.org/10.1180/mgm.2022.113>
- Harrison, T.M., Watson, E.B., 1984. The behavior of apatite during crustal anatexis: Equilibrium and kinetic considerations. *Geochimica et Cosmochimica Acta* 48, 1467–1477. [https://doi.org/10.1016/0016-7037\(84\)90403-4](https://doi.org/10.1016/0016-7037(84)90403-4)
- Henry, D.J., Guidotti, C.V., Thomson, J.A., 2005. The Ti-saturation surface for low-to-medium pressure metapelitic biotites: Implications for geothermometry and Ti-substitution mechanisms. *American Mineralogist* 90, 316–328. <https://doi.org/10.2138/am.2005.1498>
- Hibbard, M. j., 1991. Textural Anatomy of Twelve Magma - Mixed Granitoid Systems, in: Enclaves and Granite Petrology. Elsevier, Oxford (UK), pp. 431–444.
- Kumar, S., 2020. Schedule of Mafic to Hybrid Magma Injections Into Crystallizing Felsic Magma Chambers and Resultant Geometry of Enclaves in Granites: New Field and Petrographic Observations From Ladakh Batholith, Trans-Himalaya, India. *Front. Earth Sci.* 8, 551097. <https://doi.org/10.3389/feart.2020.551097>

- Li, W., Cheng, Y., Yang, Z., 2019. Geo- f O₂: Integrated Software for Analysis of Magmatic Oxygen Fugacity. *Geochemistry Geophysics Geostatistics*. 2019GC008273. <https://doi.org/10.1029/2019GC008273>
- Li, X., Zhang, C., 2022. Machine Learning Thermobarometry for Biotite-Bearing Magmas. *JGR Solid Earth* 127, e2022JB024137. <https://doi.org/10.1029/2022JB024137>
- Lisboa, V.A.C., Conceição, H., Rosa, M.L.S., Fernandes, D.M., 2019. The onset of post-collisional magmatism in the Macururé Domain, Sergipano Orogenic System: The Glória Norte Stock. *Journal of South American Earth Sciences* 89, 173–188. <https://doi.org/10.1016/j.jsames.2018.11.005>
- Lisboa, V.A.C., Conceição, H., Rosa, M.L.S., Marques, G.T., Lamarão, C.N., Lima, A.L.R., 2020. Amphibole crystallization conditions as record of interaction between ultrapotassic enclaves and monzonitic magmas in the Glória Norte Stock, South of Borborema Province. *Braz. J. Geol.* 50, e20190101. <https://doi.org/10.1590/2317-4889202020190101>
- Liu, P., Pan, Y., Zhang, D., Wu, M., Qiu, K., Li, P., Jia, H., Wang, Z., Zhang, J., 2020. Primary magmatic biotite in granitoid intrusions associated with Late Mesozoic Jinchanggouliang-Erdaogou lode gold deposits, North China Craton: Linkage to gold mineralization. *Ore Geology Reviews* 125, 103679. <https://doi.org/10.1016/j.oregeorev.2020.103679>
- Long, L.E., 2005. Age, Origin and Cooling History of the Coronel Joao Sa Pluton, Bahia, Brazil. *Journal of Petrology* 46, 255–273. <https://doi.org/10.1093/petrology/egh070>
- Luhr, J.F., Carmichael, I.S.E., Varekamp, J.C., 1984. The 1982 eruptions of El Chichón Volcano, Chiapas, Mexico: Mineralogy and petrology of the anhydritebearing pumices. *Journal of Volcanology and Geothermal Research* 23, 69–108. [https://doi.org/10.1016/0377-0273\(84\)90057-X](https://doi.org/10.1016/0377-0273(84)90057-X)
- Mbassa, B.J., Njonfang, E., Ngwa, C.N., Grégoire, M., Itiga, Z., Kamgang, P., Ntepe, M., Viñas, J.S., Benoit, M., Dili-Rake, J., Eddy, F.M., 2020. Mineral Chemistry and Descriptive Petrology of the Pan-African High-K Granitoids and Associated Mafic Rocks from Mbengwi, NW Cameroon: Petrogenetic Constraints and Geodynamic Setting. *Journal of Geosciences and Geomatics* 8, 58–75.
- Meng, Y., Xiong, F., Xu, Z., Ma, X., 2019. Petrogenesis of Late Cretaceous mafic enclaves and their host granites in the Nyemo region of southern Tibet: Implications for the tectonic-magmatic evolution of the Central Gangdese Belt. *Journal of Asian Earth Sciences* 176, 27–41. <https://doi.org/10.1016/j.jseae.2019.01.041>
- Nachit, H., Ibhi, A., Abia, E.H., Ben Ohoud, M., 2005. Discrimination between primary magmatic biotites, reequilibrated biotites and neoformed biotites. *Comptes Rendus Geoscience* 337, 1415–1420. <https://doi.org/10.1016/j.crte.2005.09.002>
- Nachit, H., Razafimahefana, N., Stussi, J.M., Carron, J.P., 1985. Composition chimique des biotites et typologie magmatique des granitoïdes. 1. *Comptes Rendus Académie Sciences Paris*. 301, 813–918.
- Nédélec, A., Bouchez, J.-L., 2011. *Pétrologie des granites, structure, cadre écologique*. Vuibert, Société géologique de France. Paris

- Oliveira, A.C., 2014. Petrogênese do Stock Granítico Monte Alegre, Noroeste do Domínio Macururé, Faixa Sergipana (Dissertação). Programa de Pós-Graduação em Geociências e Análises de Bacias-UFS, São Cristóvão.
- Oliveira, E.P., Bueno, J.F., McNaughton, N.J., Silva Filho, A.F., Nascimento, R.S., Donatti-Filho, J.P., 2015. Age, composition, and source of continental arc- and syn-collision granites of the Neoproterozoic Sergipano Belt, Southern Borborema Province, Brazil. *Journal of South American Earth Sciences* 58, 257–280. <https://doi.org/10.1016/j.jsames.2014.08.003>
- Oliveira, R.G., Domingos, N.R.R., Medeiros, W.E., 2023. Deep crustal structure of the Sergipano Belt, NE-Brazil, revealed by integrated modeling of gravity, magnetic, and geological data. *Journal of the Geological Survey of Brazil* 6(1): 1 – 22. <https://doi.org/10.29396/jgsb.2023.v6.n1.1>
- Oliveira, I.R., Menezes, A.R.D., Rosa, M.L.S., Conceição, H., 2023. Petrologia e geocronologia dos stocks Mocambo e Frutuoso, Domínio Macururé, Sistema Orogênico Sergipano. *Geol. USP. Sér. Cient.* 22, 109–133. <https://doi.org/10.11606/issn.2316-9095.v22-196735>
- Oliveira, E.P., Windley, B.F., Araújo, M.N.C., 2010. The Neoproterozoic Sergipano orogenic belt, NE Brazil: A complete plate tectonic cycle in western Gondwana. *Precambrian Research* 181, 64–84. <https://doi.org/10.1016/j.precamres.2010.05.014>
- Patiño Douce, A.E., 1993. Titanium substitution in biotite: an empirical model with applications to thermometry, O₂ and H₂O barometries, and consequences for biotite stability. *Chemical Geology* 108, 133–162. [https://doi.org/10.1016/0009-2541\(93\)90321-9](https://doi.org/10.1016/0009-2541(93)90321-9)
- Pereira, F.D.S., Rosa, M.D.L.D.S., Conceição, H., Bertotti, A.L., 2020. Age, composition, and source of the Macururé Mafic Suite, Southern Borborema Province, Brazil. *Braz. J. Geol.* 50, e20190105. <https://doi.org/10.1590/2317-4889202020190105>
- Pereira, F.S., Conceição, H., Rosa, M.D.L.S., Marinho, M.M., Tassinari, C.C.G., Neto, J.M.M., Lafon, J.-M., 2023. Late Cryogenian–Ediacaran magmatism in southern Borborema Province, NE Brazil: Ages, sources, petrogenesis, and tectonic setting. *Geoscience Frontiers* 14, 101626. <https://doi.org/10.1016/j.gsf.2023.101626>
- Pereira, F.S., Rosa, M.D.L.D.S., Conceição, H., 2019. Condições de colocação do magmatismo mafico do Domínio Macururé, Sistema Orogênico Sergipano: Maciço Capela. *Geol. USP. Sér. Cient.* 19, 3–29. <https://doi.org/10.11606/issn.2316-9095.v19-151464>
- Perugini, D., Poli, G., 2011. Intrusion of Mafic magmas Into Felsic Magma Chambers: New Insights from Natural Outcrops and Fluid-Mechanics Experiments. *Italian Journal of Geosciences* 130, 3–15. <https://doi.org/10.3301/IJG.2010.22>
- Pinho Neto, M.A., Rosa, M.L.S., Conceição, H., 2019. Petrologia do Batólito Sítios Novos, Sistema Orogênico Sergipano, Província Borborema, NE do Brasil. *Revista do Instituto de Geociências-USP* 19, 135–150. <https://doi.org/10.11606/issn.2316-9095.v19-152469>

- Pitcher, Z.P. 1993. The Nature and Origin of Granite. Blackie Academic & Professional, London. 321p.
- Robert, J.-L., 1976. Titanium solubility in synthetic phlogopite solid solutions. *Chemical Geology* 17, 213–227. [https://doi.org/10.1016/0009-2541\(76\)90036-X](https://doi.org/10.1016/0009-2541(76)90036-X)
- Samadi, R., Torabi, G., Kawabata, H., Miller, N.R., 2021. Biotite as a petrogenetic discriminator: Chemical insights from igneous, meta-igneous and meta-sedimentary rocks in Iran. *Lithos* 386–387, 106016. <https://doi.org/10.1016/j.lithos.2021.106016>
- Santos, R.A., Martins, A.A.M., Neves, J.P., Rômulo, A.L., 1998. Geologia e Recursos Minerais do Estado de Sergipe. Texto Explicativo do Mapa Geológico do Estado de Sergipe, escala 1.250.000. Serviço Geológico do Brasil, Brasília.
- Soares, H.S., Sousa, C.S., Fernandes, D.M., Da Silva Rosa, M.D.L., Conceição, H., 2022. Evolution of amphiboles of the Serra do Catu intrusive suite: Crystallization conditions of Ediacaran shoshonitic rocks in the Sergipano Orogenic System, NE Brazil. *Journal of South American Earth Sciences* 116, 103849. <https://doi.org/10.1016/j.jsames.2022.103849>
- Sousa, C.S., Soares, H.S., Rosa, M.L.S., Conceição, H., 2019. Petrologia e geocronologia do Batólito Rio Jacaré, Domínio Poço Redondo, Sistema Orogênico Sergipano, NE do Brasil. *Geol. USP. Sér. Cient.* 19, 171–194. <https://doi.org/10.11606/issn.2316-9095.v19-152494>
- Speer, J.A., 1984. Micas in Igneous Rocks. In: Bailey, S.W. (Ed.), *Micas*. De Gruyter, pp. 299–356. <https://doi.org/10.1515/9781501508820-013>
- Streckeisen, A., 1976. To each plutonic rock its proper name. *Earth-Science Reviews* 12, 1–33. [https://doi.org/10.1016/0012-8252\(76\)90052-0](https://doi.org/10.1016/0012-8252(76)90052-0)
- Stussi, J.M., Cuney, M., 1996. Nature of Biotites from Alkaline, Calc-alkaline and Peraluminous Magmas by Abdel-Fattah M. Abdel-Rahman: A Comment. *Journal of Petrology* 5, 1025–1029. <https://doi.org/10.1093/petrology/37.5.1025>
- Tang, P., Chen, Y., Tang, J., Wang, Y., Zheng, W., Leng, Q., Lin, B., Wu, C., 2019. Advances in Research of Mineral Chemistry of Magmatic and Hydrothermal Biotites. *Acta Geologica Sinica (Eng)* 93, 1947–1966. <https://doi.org/10.1111/1755-6724.14395>
- Tischendorf, G., Gottesmann, B., Förster, H.-J., Trumbull, R.B., 1997. On Li-bearing micas: estimating Li from electron microprobe analyses and an improved diagram for graphical representation. *Mineral. mag.* 61, 809–834. <https://doi.org/10.1180/minmag.1997.061.409.05>
- Tischendorf, G., Rieder, M., Förster, H.-J., Gottesmann, B., Guidotti, Ch.V., 2004. A new graphical presentation and subdivision of potassium micas. *Mineral. mag.* 68, 649–667. <https://doi.org/10.1180/0026461046840210>
- Tulloch, A.J., Challis, G.A., 2000. Emplacement depths of Paleozoic-Mesozoic plutons from western New Zealand estimated by hornblende-Al geobarometry. *New Zealand Journal of Geology and Geophysics* 43, 555–567. <https://doi.org/10.1080/00288306.2000.9514908>

- Uchida, E., Endo, S., Makino, M., 2007. Relationship Between Solidification Depth of Granitic Rocks and Formation of Hydrothermal Ore Deposits. *Resource Geology* 57, 47–56. <https://doi.org/10.1111/j.1751-3928.2006.00004.x>
- Van Schmus, W.R., De Brito Neves, B.B., Hackspacher, P., Babinski, M., 1995. U/Pb and Sm/Nd geochronologic studies of the eastern Borborema Province, northeastern Brazil: initial conclusions. *Journal of South American Earth Sciences* 8, 267–288. [https://doi.org/10.1016/0895-9811\(95\)00013-6](https://doi.org/10.1016/0895-9811(95)00013-6)
- Van Schmus, W.R., Oliveira, E.P., Da Silva Filho, A.F., Toteu, S.F., Penaye, J., Guimarães, I.P., 2008. Proterozoic links between the Borborema Province, NE Brazil, and the Central African Fold Belt. SP 294, 69–99. <https://doi.org/10.1144/SP294.5>
- Vernon, R.H., 2010. Granites Really Are Magmatic: Using Microstructural Evidence to Refute Some Obstinate Hypotheses. *J.Virt.Ex* 35. <https://doi.org/10.3809/jvirtex.2011.00264>
- Vernon, R.H., Etheridge, M.A., Wall, V.J., 1988. Shape and microstructure of microgranitoid enclaves: Indicators of magma mingling and flow. *Lithos* 22, 1–11. [https://doi.org/10.1016/0024-4937\(88\)90024-2](https://doi.org/10.1016/0024-4937(88)90024-2)
- Warr, L.N., 2021. IMA–CNMNC approved mineral symbols. *MinMag* 85, 291–320. <https://doi.org/10.1180/mgm.2021.43>
- Weidendorfer, D., Mattsson, H.B., Ulmer, P., 2014. Dynamics of Magma Mixing in Partially Crystallized Magma Chambers: Textural and Petrological Constraints from the Basal Complex of the Austurhorn Intrusion (SE Iceland). *Journal of Petrology* 55, 1865–1903. <https://doi.org/10.1093/petrology/egu044>
- Wones, D.R., 1989. Significance of the assemblage titanite + magnetite + quartz in granitic rocks. *American Mineralogist* 74, 744–749.
- Wones, D.R., Eugster, H.P., 1965. Stability of biotite: experiment, theory, and application. *American Mineralogist* 50, 1228–1272.
- Zhou, Z., 1986. The origin of intrusive mass in Fengshandong, Hubei Province. *Acta Petrologica Sinica* 2, 56–70.

CAPÍTULO 3: Considerações Finais

3.1 CONCLUSÕES GERAIS

Os enclaves microgranulares do SGS correspondem a diopsídio biotita álcalfeldspato sienito, diopsídio biotita quartzo álcalfeldspato sienito, diopsídio biotita sienitos e diopsídio biotita quartzo-sienitos, eles ocorrem com dimensões centimétricas, granulação fina, arredondados, e exibem contatos bem definidos com os biotitasienogranitos hospedeiros. Os tamanhos diminutos e a usual orientação sugerem que o fluxo magmático desagregou, dispersou e orientou as gotas de magma máfico-intermediário responsáveis pela formação dos enclaves.

A biotita, é o mineral máfico mais abundante nos enclaves microgranulares ocorrendo com volume variando de 18-28%, é marrom, subédrica e tem tamanhos similares aos outros minerais ígneos. Os cristais têm composição de Mg-biotita e Fe-biotita, sendo que nos enclaves microgranulares domina Mg-biotita enquanto no sienogranito encaixante predomina Fe-biotita.

A maioria dos cristais de biotita das rochas estudadas são magmáticos reequilibrados, ocorrendo cristais mais preservados (alto titânio) e magmáticos, nos enclaves e sienogranito encaixante respectivamente, como inclusões em feldspatos. A evolução química dos cristais analisados foi influenciada por duas substituições principais: (1) $V^{VI}R^{2+} + 2 V^{VI}Al^{3+} = V^{VI}\square + 2 V^{IV}Si^{4+}$ e (2) $V^{VI}R^{2+} + V^{VI}Ti = 2 V^{VI}Al$, evidenciando que o aumento do conteúdo de alumínio está relacionado a diminuição do titânio e R^{2+} (Mg, Fe e Mn) que indica a diminuição de temperatura e pressão.

As estimativas termobarométricas indicam temperaturas de cristalização da biotita nos enclaves microgranulares entre 900-780 °C e de 809-765 °C para os sienogranitos, e pressões máximas para a cristalização de 10,7 kbar para os enclaves e de 6,3 kbar para os sienogranitos. A semelhança entre as temperaturas das duas rochas sugere que essas temperaturas sejam o registo da interação entre os magmas traquítico (enclaves) e riolítico (sienogranito). A pressão indica a biotita nos Sem iniciou a uma profundidade de 39 km e a interação entre os magmas ocorreu a cerca de 23 km. A paragênese presente nos enclaves (titanita + diopsídio + magnetita + quartzo) é oxidante e compatível com a inferida com os dados químicos da biotita.

A composição química da biotita estudada indica que este mineral foi cristalizado a partir de magma com elevada fugacidade de oxigênio da série magnetita (fusão de protólito ígneo), cálcio-alcalino e orogênico. Estes dados químicos também indicam evolução complexa deste magma, envolvendo mistura entre magmas mantélico e crustal na formação destas rochas. Essa hipótese é coerente com o panorama petrológico advogado para os magmas no Domínio Macururé do Sistema Orogênico Sergipano.

ANEXO:
Comprovante de Submissão do Artigo

Date: Jun 03, 2024
To: "ASAYUKI RODRIGUES MENEZES" asayuki_45@hotmail.com;asayukirm@outlook.com
From: "Journal of South American Earth Sciences" support@elsevier.com
Subject: Decision on submission to Journal of South American Earth Sciences

Manuscript Number: **SAMES-D-23-00809R1**

Chemical-memory of biotite crystals preserves the temperature and pressure conditions of the mixing process between trachytic and rhyolitic magmas in the Glória Sul Stock, Sergipano Orogenic System, Northeast Brazil

Dear Mr. MENEZES,

Thank you for submitting your manuscript to Journal of South American Earth Sciences.

I am pleased to inform you that your manuscript has been accepted for publication.

My comments, and any reviewer comments, are below.

Your accepted manuscript will now be transferred to our production department. We will create a proof which you will be asked to check, and you will also be asked to complete a number of online forms required for publication. If we need additional information from you during the production process, we will contact you directly.

Open Access: In accordance with Funding Body requirements, Elsevier does offer alternative open access publishing options. Visit <https://www.elsevier.com/journals/cretaceous-research/0195-6671/open-access-options> for full information.

We appreciate you submitting your manuscript to Journal of South American Earth Sciences and hope you will consider us again for future submissions.

We encourage authors of original research papers to share the research objects – including raw data, methods, protocols, software, hardware and other outputs – associated with their paper. More information on how our open access Research Elements journals can help you do this is available at https://www.elsevier.com/authors/tools-and-resources/research-elements-journals?dgcid=ec_em_research_elements_email.

Kind regards,
Monica da Costa Pereira Lavalle Heilbron
Section Editor

Journal of South American Earth Sciences

Editor and Reviewer comments:

APÊNDICE:
Análises Químicas dos Cristais de Biotita

Rock Sample Position	ME SOS-600I C	ME SOS-600I I	ME SOS-600I I	ME SOS-600I I	ME SOS-600I I	ME SOS-600I I	ME SOS-600I I	ME SOS-600I B	ME SOS-600I C	ME SOS-600I C
SiO ₂	39.84	39.17	39.55	40.03	38.02	40.03	38.59	39.36	39.46	39.26
TiO ₂	1.54	1.44	1.44	1.34	1.15	1.34	1.15	1.54	1.44	1.92
Al ₂ O ₃	16.61	16.70	16.90	16.51	17.18	16.51	16.70	15.26	16.42	16.99
FeO	14.50	15.55	14.78	14.88	17.18	14.88	17.76	15.26	14.78	15.26
MnO	0.10	0.19	0.19	0.10	0.10	0.10	0.10	0.10	0.19	0.10
MgO	13.34	12.77	13.25	13.06	13.34	13.15	13.15	12.86	13.15	12.58
CaO										
Na ₂ O										
K ₂ O	9.31	9.31	9.22	9.41	7.68	9.12	7.58	9.31	9.02	9.22
BaO										
Cr ₂ O ₃										
NiO										
F	0.80	0.70	0.80	0.70	1.40	0.70	0.90	1.32	1.60	1.10
Cl	0.20	0.10		0.10		0.10	0.10	0.20	0.10	0.10
*OH=F=Cl	-0.38	-0.32	-0.34	-0.32	-0.59	-0.32	-0.40	-0.60	-0.70	-0.49
TOTAL	96.23	95.94	96.13	96.13	96.06	95.94	96.04	95.22	96.16	96.53
Si	5.867	5.815	5.828	5.900	5.674	5.902	5.743	5.932	5.865	5.800
Al ^{IV}	2.133	2.185	2.172	2.100	2.326	2.098	2.257	2.068	2.135	2.200
Al ^{VI}	0.750	0.739	0.763	0.769	0.698	0.771	0.674	0.643	0.742	0.759
Ti	0.170	0.161	0.160	0.149	0.129	0.149	0.129	0.174	0.161	0.213
Cr										
^T Fe	1.785	1.931	1.822	1.834	2.145	1.835	2.210	1.924	1.838	1.886
Mn	0.012	0.024	0.024	0.012	0.012	0.012	0.012	0.012	0.024	0.012
Mg	2.929	2.826	2.910	2.869	2.969	2.890	2.918	2.890	2.915	2.769
Ni										
Ca										
Na										
K	1.749	1.763	1.732	1.769	1.462	1.715	1.440	1.790	1.711	1.736
Ba										
TOTAL	19.396	19.444	19.411	19.401	19.416	19.372	19.382	19.433	19.391	19.376
*OH	3.577	3.646	3.627	3.649	3.339	3.649	3.551	3.320	3.223	3.461
F	0.373	0.329	0.373	0.326	0.661	0.326	0.424	0.629	0.752	0.514
Cl	0.050	0.025		0.025		0.025	0.025	0.051	0.025	0.025
*Li	1.087	0.986	1.041	1.119	0.801	1.119	0.894	1.033	1.035	0.997
*Fe ³⁺	0.326	0.283	0.289	0.389		0.345		0.325	0.284	0.263
T °C (Henry <i>et al.</i> , 2005)	597	532	551	505	388	507	375	587	555	701
P kbar (Uchida <i>et al.</i> , 2007)	2.21	2.33	2.36	2.16	2.63	2.16	2.35	1.69	2.19	2.43
T °C (Li <i>et al.</i> , 2022)	834	825	847	843	824	830	794	846	829	855
P kbar (Li <i>et al.</i> , 2022)	8.72	6.78	7.18	8.4	5.21	7.21	5.34	6.98	5.72	7.76
										8.92

ME SOS-600I C	ME SOS-600I I	ME SOS-600I B	ME SOS-600I C										
39.55	40.13	39.26	38.49	39.02	38.89	38.76	38.42	38.99	38.99	38.57	39.32	38.86	38.67
1.44	1.44	1.25	1.56	1.53	1.51	1.59	1.80	1.61	1.61	1.29	1.51	1.47	1.42
16.51	16.42	16.42	15.15	15.24	15.21	15.19	16.14	16.59	16.59	16.03	15.60	15.36	15.62
14.88	14.88	15.46	17.18	16.22	16.20	16.14	15.89	15.37	15.37	15.67	15.98	16.39	16.83
0.10	0.10	0.19	0.27	0.24	0.25	0.23	0.30	0.25	0.25	0.31	0.24	0.23	0.28
13.54	13.15	13.54	13.31	13.85	13.72	13.73	13.17	13.10	13.10	13.79	13.78	13.55	13.49
			0.11	0.12			0.12	0.09	0.09	0.13	0.07	0.10	0.12
			0.15	0.05	0.15	0.05	0.22	0.25	0.25	0.18		0.13	0.13
9.31	9.50	8.64	9.72	9.59	9.50	9.58	9.74	9.46	9.46	9.45	9.36	9.76	9.33
				0.08	0.07		0.14	0.06	0.06	0.01	0.12	0.08	
				0.04	0.10	0.19		0.04	0.04	0.09	0.04		0.01
0.70	0.40	1.30			0.35	0.56		0.17		0.51		0.03	0.04
		0.20	0.07	0.01	0.06		0.05	0.05	0.08			0.04	0.03
-0.29	-0.17	-0.59	-0.02	0.00	-0.16	-0.24	-0.01	-0.08	-0.02	-0.21		-0.02	-0.02
96.03	96.02	96.25	96.01	95.99	96.01	96.02	95.99	96.02	95.88	96.02	96.02	95.99	95.97
5.836	5.900	5.828	5.760	5.796	5.800	5.792	5.712	5.764	5.764	5.743	5.813	5.787	5.759
2.164	2.100	2.172	2.240	2.204	2.200	2.208	2.288	2.236	2.236	2.257	2.187	2.213	2.241
0.707	0.744	0.701	0.432	0.463	0.473	0.466	0.540	0.655	0.655	0.556	0.531	0.483	0.500
0.160	0.159	0.139	0.176	0.171	0.169	0.179	0.202	0.179	0.179	0.144	0.168	0.165	0.159
				0.009	0.008		0.017	0.007	0.007	0.001	0.015	0.009	
1.836	1.830	1.919	2.151	2.015	2.021	2.016	1.975	1.901	1.901	1.951	1.976	2.041	2.096
0.012	0.012	0.024	0.034	0.030	0.032	0.029	0.037	0.031	0.031	0.039	0.030	0.029	0.035
2.977	2.882	2.995	2.968	3.067	3.050	3.058	2.919	2.888	2.888	3.060	3.036	3.007	2.994
				0.005	0.012	0.023		0.005	0.005	0.010	0.005		0.001
				0.017	0.020		0.018	0.014	0.014	0.021	0.011	0.015	0.020
				0.045	0.014	0.044	0.014	0.064	0.072	0.072	0.053	0.039	0.039
1.752	1.782	1.636	1.856	1.817	1.808	1.826	1.848	1.783	1.783	1.794	1.765	1.855	1.772
19.445	19.410	19.414	19.679	19.611	19.617	19.612	19.620	19.535	19.535	19.629	19.536	19.642	19.617
3.673	3.814	3.339	3.982	3.997	3.820	3.735	3.987	3.908	3.980	3.760	4.000	3.976	3.974
0.327	0.186	0.610			0.165	0.265		0.079		0.240		0.014	0.019
		0.050	0.018	0.003	0.015		0.013	0.013	0.020			0.010	0.008
1.043	1.132	1.002	0.881	0.963	0.945	0.926	0.864	0.952	0.952	0.891	1.007	0.939	0.907
0.264	0.379	0.148	0.113	0.124	0.120	0.089	0.193	0.276	0.276	0.170	0.130	0.182	0.098
556	546	464	571	578	570	606	670	607	607	485	570	548	520
2.17	2.09	2.17	1.57	1.55	1.57	1.57	2.04	2.23	2.23	1.99	1.71	1.64	1.78
869	857	805	776	799	797	844	789	799	786	829	817	789	780
9.21	9.97	4.88	4.6	6.43	4.93	7.43	5.25	6.27	6.15	6.24	7.27	5.74	5.63

ME SOS-600I B	ME SOS-600I C												
37.95	39.07	39.11	38.76	39.45	38.65	38.70	38.65	38.41	38.59	38.74	39.13	39.51	38.89
1.46	1.56	1.35	1.66	1.72	1.67	1.54	1.56	1.66	1.62	1.25	1.57	1.55	1.45
15.34	15.34	15.37	15.64	16.02	15.68	15.63	15.21	15.24	15.24	15.27	15.86	16.15	15.73
18.60	16.05	16.69	16.45	15.24	16.29	16.62	16.74	16.62	16.72	16.73	16.10	15.15	16.53
0.20	0.25	0.24	0.23	0.24	0.14	0.25	0.27	0.13	0.23	0.29	0.28	0.18	0.35
13.50	13.72	13.80	13.34	13.56	13.54	13.74	13.55	13.41	13.24	13.91	13.14	13.77	12.96
0.13	0.06	0.05	0.04	0.21	0.06	0.13	0.11	0.09	0.28	0.09	0.04	0.08	0.12
0.01	0.12	0.05	0.02	0.01		0.12			0.16	0.20	0.12		0.08
8.49	9.75	9.07	9.77	9.51	9.72	9.11	9.53	9.59	9.86	9.35	9.72	9.30	9.68
0.07	0.05	0.02	0.01	0.05	0.08	0.05	0.12			0.05	0.02	0.16	0.15
0.02					0.09	0.10		0.10		0.10		0.11	
0.15						0.22	0.22	0.01	0.01	0.01	0.03		0.06
0.09	0.02	0.24	0.07		0.09	0.03	0.06		0.24	0.03		0.05	
-0.08	0.00	-0.05	-0.02		-0.02	-0.01	-0.11	-0.09	-0.06	-0.01	-0.01	-0.01	-0.03
96.00	96.00	95.99	96.00	96.01	96.00	96.01	96.01	95.47	96.19	96.01	96.01	96.00	95.99
5.690	5.801	5.811	5.769	5.811	5.750	5.747	5.773	5.766	5.767	5.769	5.803	5.813	5.790
2.310	2.199	2.189	2.231	2.189	2.250	2.253	2.227	2.234	2.233	2.231	2.197	2.187	2.210
0.402	0.486	0.503	0.512	0.594	0.499	0.483	0.450	0.463	0.451	0.451	0.576	0.613	0.551
0.165	0.175	0.151	0.186	0.190	0.187	0.172	0.176	0.187	0.182	0.140	0.176	0.171	0.162
0.008	0.006	0.002	0.001	0.006	0.009	0.006	0.014			0.006	0.002	0.019	0.018
2.332	1.993	2.074	2.048	1.877	2.027	2.064	2.091	2.086	2.090	2.084	1.997	1.864	2.058
0.026	0.031	0.030	0.029	0.030	0.018	0.031	0.034	0.017	0.029	0.036	0.035	0.023	0.044
3.017	3.036	3.055	2.960	2.979	3.002	3.041	3.016	3.001	2.949	3.088	2.906	3.019	2.876
0.002					0.010	0.011		0.012		0.012		0.012	
0.022	0.009	0.008	0.006	0.033	0.009	0.021	0.017	0.014	0.045	0.014	0.006	0.012	0.018
0.003	0.036	0.014	0.006	0.003		0.036			0.047	0.058	0.033		0.022
1.623	1.847	1.719	1.855	1.788	1.845	1.726	1.816	1.836	1.879	1.776	1.840	1.746	1.838
19.598	19.620	19.557	19.603	19.500	19.607	19.591	19.614	19.616	19.672	19.665	19.570	19.479	19.588
3.906	3.995	3.940	3.982	4.000	3.977	3.992	3.881	3.896	3.934	3.988	3.986	3.988	3.972
0.071							0.104	0.104	0.005	0.005	0.014		0.028
0.023	0.005	0.060	0.018		0.023	0.008	0.015		0.061	0.008		0.012	
0.793	0.970	0.977	0.922	1.024	0.903	0.909	0.906	0.871	0.897	0.918	0.979	1.033	0.943
	0.174	0.058	0.139	0.239	0.109	0.036	0.078	0.083	0.208	0.079	0.238	0.193	0.228
515	593	498	615	655	625	573	582	619	598	452	583	596	526
1.69	1.61	1.63	1.78	1.90	1.80	1.76	1.58	1.64	1.60	1.59	1.87	1.95	1.84
783	789	775	797	831	804	777	806	846	788	774	816	809	811
5.59	5.74	5.04	6.66	8.26	7.7	5.5	5.72	9.14	6.77	4.09	6.81	6.96	6.1

ME SOS-600I B	ME SOS-600I C												
38.47	38.70	38.34	38.68	38.82	38.98	38.76	38.61	37.43	38.97	38.05	38.41	37.79	38.83
1.47	1.73	1.69	1.43	1.49	1.54	1.31	1.53	1.45	1.66	1.29	1.50	1.66	1.61
15.95	15.72	15.14	15.62	15.53	15.59	15.76	15.86	15.23	15.59	15.74	15.52	15.02	15.38
16.96	16.21	17.30	16.72	15.88	16.45	16.93	16.18	18.64	16.38	17.69	16.78	18.08	16.29
0.32	0.26	0.23	0.31	0.34	0.26	0.32	0.23	0.29	0.27	0.33	0.25	0.32	0.18
12.29	13.48	13.09	13.25	13.46	12.87	13.54	13.46	13.28	13.48	13.63	13.74	12.63	13.56
0.19	0.03	0.10	0.10	0.12	0.23	0.07	0.09	0.03	0.09	0.22	0.10	0.10	0.26
0.21	0.10	0.04			0.25	0.14	0.07	0.20	0.05	0.04	0.06	0.27	0.10
9.83	9.70	10.02	9.78	9.62	9.47	8.93	9.69	9.28	9.34	8.99	9.44	9.58	9.57
0.12	0.01	0.01	0.11	0.19	0.20	0.20	0.19	0.11	0.12		0.09	0.15	0.17
0.01				0.03	0.04		0.04	0.05				0.01	
0.17	0.04			0.55							0.11	0.41	
0.02	0.04	0.05	0.02		0.12	0.06	0.05	0.03	0.06	0.03	0.02	0.01	0.03
-0.08	-0.03	-0.01	0.00	-0.23	-0.03	-0.01	-0.01	-0.01	-0.01	-0.01	-0.05	-0.17	-0.01
96.01	96.00	96.01	96.01	96.02	96.00	96.02	95.98	96.01	95.99	96.01	96.01	96.02	96.00
5.759	5.753	5.749	5.766	5.791	5.802	5.758	5.742	5.644	5.783	5.684	5.728	5.713	5.774
2.241	2.247	2.251	2.234	2.209	2.198	2.242	2.258	2.356	2.217	2.316	2.272	2.287	2.226
0.573	0.508	0.425	0.510	0.522	0.537	0.517	0.522	0.350	0.510	0.456	0.457	0.390	0.469
0.165	0.193	0.191	0.160	0.167	0.172	0.146	0.171	0.164	0.185	0.145	0.168	0.189	0.180
0.015	0.001	0.001	0.012	0.023	0.024	0.024	0.023	0.013	0.014		0.010	0.018	0.020
2.124	2.016	2.169	2.085	1.981	2.048	2.104	2.012	2.351	2.033	2.210	2.093	2.286	2.026
0.040	0.033	0.029	0.039	0.042	0.033	0.040	0.029	0.037	0.034	0.041	0.032	0.041	0.023
2.742	2.987	2.927	2.944	2.993	2.857	2.997	2.984	2.982	3.036	3.054	2.847	3.006	
0.001				0.003	0.005		0.005	0.006				0.001	
0.031	0.005	0.015	0.015	0.018	0.037	0.011	0.014	0.005	0.014	0.035	0.015	0.016	0.041
0.061	0.028	0.011			0.072	0.041	0.019	0.059	0.014	0.011	0.017	0.079	0.028
1.877	1.839	1.917	1.860	1.830	1.797	1.691	1.837	1.785	1.768	1.712	1.795	1.848	1.815
19.630	19.609	19.686	19.626	19.580	19.581	19.571	19.615	19.754	19.553	19.647	19.640	19.713	19.610
3.914	3.971	3.987	3.995	3.741	3.970	3.985	3.987	3.992	3.985	3.992	3.943	3.801	3.992
0.080	0.019				0.259						0.052	0.196	
0.005	0.010	0.013	0.005		0.030	0.015	0.013	0.008	0.015	0.008	0.005	0.003	0.008
0.878	0.910	0.859	0.909	0.934	0.957	0.920	0.896	0.710	0.953	0.808	0.865	0.772	0.932
0.310	0.123	0.120	0.160	0.182	0.273	0.048	0.153		0.103		0.033	0.071	0.168
518	645	613	521	563	560	467	571	510	618	452	558	588	604
2.00	1.81	1.58	1.79	1.75	1.76	1.83	1.89	1.67	1.73	1.87	1.74	1.58	1.64
796	788	816	789	836	771	769	795	768	782	778	801	814	790
6.34	6.06	8.33	6.1	6.71	6.04	4.36	6.28	4.3	5.21	5.4	6.42	5.46	7.1

ME SOS-600I B	ME SOS-600I C	ME SOS-600I B	ME SOS-600I C	ME SOS-600I I	ME SOS-600I B	ME SOS-600J C	ME SOS-600J B	ME SOS-600J C	ME SOS-600J B	ME SOS-600J C	ME SOS-600J B	ME SOS-600J C	ME SOS-600J B
38.56	38.71	38.86	36.20	38.83	38.67	39.17	38.78	38.78	38.30	38.78	38.98	38.78	38.78
1.58	1.45	1.37	1.63	1.48	1.52	1.44	1.34	1.44	1.25	1.44	1.44	1.73	1.73
15.40	15.81	15.97	15.22	15.77	15.95	15.26	15.65	15.07	14.88	14.40	14.88	16.03	16.03
16.68	16.50	15.79	17.06	16.28	16.35	15.55	16.13	16.42	15.65	16.51	17.09	16.32	16.32
0.28	0.20	0.31	0.24	0.30	0.33	0.38	0.29	0.38	0.38	0.38	0.29	0.38	0.38
13.60	13.29	13.47	13.20	13.42	13.12	13.92	13.82	13.63	14.40	13.82	13.06	12.38	12.38
0.17	0.11	0.28	0.04	0.08					1.25				
	0.19	0.17	0.07	0.10	0.03								
9.59	9.03	9.40	10.04	9.68	9.96	9.50	9.31	9.60	8.83	9.41	9.60	9.50	9.50
0.09	0.21	0.23											
	0.48	0.12	0.23			0.70	0.30	0.70	0.30	1.20	0.60	0.90	0.50
0.05	0.04	0.04	0.04					0.10	1.00	0.10	0.10		0.10
-0.01	-0.21	-0.06	-0.11			-0.29	-0.13	-0.32	-0.35	-0.53	-0.28	-0.38	-0.23
96.00	96.02	96.02	93.97	95.93	95.92	95.93	95.63	96.13	95.86	96.05	96.03	96.04	95.74
5.748	5.768	5.765	5.592	5.772	5.759	5.837	5.783	5.809	5.764	5.847	5.851	5.804	5.804
2.252	2.232	2.235	2.408	2.228	2.241	2.163	2.217	2.191	2.236	2.153	2.149	2.196	2.196
0.453	0.545	0.558	0.363	0.536	0.559	0.518	0.534	0.470	0.404	0.405	0.484	0.632	0.632
0.178	0.162	0.153	0.190	0.165	0.170	0.161	0.151	0.162	0.141	0.163	0.163	0.194	0.194
0.010	0.025	0.027											
2.079	2.057	1.959	2.204	2.024	2.036	1.938	2.011	2.056	1.969	2.082	2.145	2.043	2.043
0.035	0.025	0.039	0.031	0.037	0.041	0.048	0.036	0.049	0.049	0.037	0.049	0.049	0.049
3.023	2.951	2.978	3.040	2.974	2.914	3.092	3.073	3.044	3.230	3.107	2.922	2.763	2.763
0.028	0.017	0.044	0.006	0.012					0.364				
	0.055	0.050	0.020	0.028	0.008								
1.823	1.717	1.778	1.979	1.835	1.893	1.806	1.771	1.834	1.695	1.809	1.838	1.814	1.814
19.628	19.555	19.586	19.832	19.612	19.622	19.565	19.576	19.615	19.804	19.615	19.589	19.495	19.495
3.987	3.764	3.934	3.877	4.000	4.000	3.670	3.859	3.643	3.602	3.402	3.690	3.574	3.738
	0.226	0.056	0.112			0.330	0.141	0.332	0.143	0.572	0.285	0.426	0.237
0.013	0.010	0.010	0.010					0.025	0.255	0.026	0.025		0.025
0.890	0.914	0.935	0.514	0.932	0.907	0.990	0.927	0.931	0.855	0.937	0.965	0.930	0.930
0.081	0.129	0.237		0.175	0.196	0.144	0.079	0.101	0.203	0.055	0.155	0.223	0.223
590	533	513	615	550	559	558	505	541	486	547	520	625	625
1.67	1.88	1.93	1.86	1.84	1.95	1.59	1.80	1.53	1.47	1.22	1.45	2.04	2.04
785	810	790	840	806	834	830	818	812	789	811	814	851	814
5.82	5.79	5.31	8.21	6.77	8.46	5.19	6.89	4.35	4.53	3.43	5.18	6.1	5.67

ME SOS-600J C	ME SOS-600J B	ME SOS-600J C											
38.88	38.88	39.65	39.26	38.98	39.17	38.78	39.55	39.55	39.55	39.65	39.26	39.46	39.65
1.63	1.63	1.44	1.44	1.54	1.54	1.63	1.44	1.44	1.44	1.54	1.54	1.54	1.44
15.55	15.94	14.98	15.74	15.26	15.74	15.46	15.94	16.03	16.03	15.84	15.55	15.07	15.84
16.80	16.22	16.13	16.61	16.99	16.61	16.70	16.42	16.22	16.22	16.03	17.28	16.80	16.51
0.29	0.29	0.29	0.29	0.38	0.19	0.38	0.29	0.29	0.29	0.19	0.19	0.19	0.19
12.96	13.15	13.92	12.48	12.96	12.86	12.58	12.67	13.06	13.06	12.77	12.67	12.58	12.96
9.41	9.31	9.41	9.50	9.22	9.60	9.50	9.31	9.31	9.31	9.41	9.50	9.22	
										0.48			
0.40	0.60	0.10	0.60	0.60			0.20		0.30			0.80	0.10
0.10	0.10	0.10	0.10	0.10					0.10		0.10		0.10
-0.19	-0.28	-0.06	-0.28	-0.28			-0.08		-0.15		-0.02	-0.34	-0.06
96.02	96.12	96.01	96.03	96.03	95.71	95.04	95.82	95.90	96.30	95.81	96.00	95.94	96.01
5.806	5.789	5.877	5.863	5.834	5.829	5.826	5.870	5.847	5.847	5.865	5.843	5.909	5.868
2.194	2.211	2.123	2.137	2.166	2.171	2.174	2.130	2.153	2.153	2.135	2.157	2.091	2.132
0.543	0.586	0.493	0.634	0.527	0.590	0.563	0.657	0.640	0.640	0.627	0.571	0.570	0.632
0.183	0.183	0.161	0.162	0.173	0.172	0.184	0.161	0.160	0.160	0.171	0.172	0.173	0.160
										0.056			
2.098	2.020	1.999	2.074	2.127	2.067	2.099	2.037	2.006	2.006	1.983	2.151	2.104	2.044
0.036	0.036	0.036	0.036	0.049	0.024	0.049	0.049	0.036	0.036	0.024	0.024	0.024	0.024
2.885	2.919	3.076	2.778	2.892	2.854	2.816	2.803	2.877	2.877	2.815	2.811	2.808	2.860
1.792	1.769	1.779	1.810	1.759	1.822	1.821	1.763	1.756	1.756	1.757	1.786	1.816	1.740
19.538	19.514	19.544	19.495	19.527	19.530	19.532	19.457	19.475	19.475	19.434	19.514	19.495	19.460
3.786	3.692	3.928	3.691	3.691	4.000	4.000	3.906	4.000	3.835	4.000	3.975	3.621	3.928
0.189	0.283	0.047	0.283	0.284			0.094		0.140			0.379	0.047
0.025	0.025	0.025	0.025	0.025					0.025		0.025		0.025
0.944	0.942	1.063	1.007	0.962	0.988	0.934	1.048	1.044	1.044	1.061	1.004	1.042	1.061
0.126	0.129	0.133	0.274	0.107	0.216	0.188	0.258	0.216	0.216	0.272	0.178	0.263	0.214
594	605	545	513	557	557	592	516	524	524	561	544	552	519
1.76	1.94	1.40	1.87	1.63	1.84	1.76	1.92	1.93	1.93	1.84	1.74	1.53	1.84
807	817	789	813	806	821	799	824	815	801	824	785	855	804
6.2	6.29	4.68	6.55	4.26	8.4	5.59	6.94	6.73	6.16	7.8	6.69	7.73	6.51

ME SOS-600J C	ME SOS-600J C	ME SOS-600J C	ME SOS-600J C	ME SOS-600J C	ME SOS-600J B								
39.65	38.78	39.07	38.98	37.92	38.08	38.76	38.95	38.44	38.82	38.02	38.43	39.03	38.71
1.44	1.25	1.06	1.54	1.35	1.46	1.33	1.44	1.38	1.47	1.24	1.38	1.60	1.51
15.84	15.74	15.46	15.65	15.43	15.77	15.79	15.33	15.74	16.16	15.35	15.38	15.54	15.76
16.51	18.53	17.57	16.13	18.42	16.73	16.60	16.80	16.76	15.69	17.91	17.43	16.31	16.72
0.19	0.38	0.19	0.19	0.33	0.41	0.34	0.22	0.37	0.33	0.41	0.24	0.49	0.31
12.96	12.10	12.96	12.77	13.02	13.43	13.01	13.22	13.32	13.45	13.05	12.91	12.85	12.88
				0.11	0.11	0.04	0.07	0.08	0.07	0.03	0.12	0.03	
					0.37	0.12	0.16	0.16	0.37	0.41	0.28	0.29	0.18
9.22	8.93	9.22	9.50	8.84	9.28	9.62	9.46	9.25	9.28	9.52	9.61	9.51	9.52
				0.10	0.19	0.14	0.20	0.25	0.20	0.19	0.15	0.17	0.32
					0.01	0.37	0.07	0.08			0.04		0.25
0.20		0.40	0.60										
0.10		0.10		0.07	0.06	0.02	0.05	0.10	0.13	0.06	0.05	0.09	0.06
-0.11		-0.19	-0.25	-0.02	-0.17	0.00	-0.01	-0.02	-0.03	-0.01	-0.01	-0.02	-0.01
96.11	95.81	96.02	95.54	96.01	96.03	95.99	96.00	96.02	96.00	96.02	96.01	96.00	96.00
5.868	5.807	5.843	5.837	5.693	5.700	5.774	5.801	5.731	5.752	5.714	5.755	5.808	5.768
2.132	2.193	2.157	2.163	2.307	2.300	2.226	2.199	2.269	2.248	2.286	2.245	2.192	2.232
0.632	0.585	0.568	0.599	0.423	0.482	0.547	0.493	0.497	0.574	0.433	0.470	0.534	0.536
0.160	0.141	0.119	0.173	0.153	0.164	0.149	0.161	0.155	0.164	0.140	0.156	0.179	0.169
	0.011		0.023	0.017	0.024	0.029	0.027	0.024	0.022	0.018	0.020	0.037	0.029
2.044	2.320	2.197	2.020	2.313	2.094	2.068	2.093	2.090	1.944	2.252	2.184	2.030	2.084
0.024	0.049	0.024	0.024	0.042	0.052	0.042	0.028	0.047	0.041	0.053	0.030	0.062	0.039
2.860	2.700	2.889	2.850	2.913	2.996	2.888	2.935	2.959	2.971	2.923	2.883	2.851	2.862
				0.001		0.008	0.009					0.005	
					0.017	0.017	0.006	0.011	0.012	0.011	0.005	0.018	0.005
					0.109	0.033	0.047	0.047	0.108	0.119	0.081	0.084	0.053
1.740	1.705	1.758	1.815	1.693	1.772	1.828	1.796	1.760	1.754	1.826	1.836	1.806	1.810
19.460	19.510	19.555	19.505	19.682	19.636	19.613	19.600	19.653	19.599	19.731	19.681	19.560	19.610
3.881	4.000	3.785	3.716	3.982	3.810	3.995	3.987	3.975	3.967	3.985	3.987	3.977	3.985
0.094		0.189		0.284		0.175							
0.025		0.025			0.018	0.015	0.005	0.013	0.025	0.033	0.015	0.013	0.015
1.061	0.931	0.977	0.963	0.789	0.814	0.923	0.953	0.870	0.928	0.806	0.872	0.966	0.914
0.214	0.097	0.151	0.245		0.040	0.212	0.166	0.129	0.217	0.073	0.181	0.220	0.200
519	396	325	566	465	539	477	523	502	554	420	487	587	545
1.84	1.89	1.73	1.84	1.74	1.90	1.87	1.63	1.85	2.02	1.71	1.70	1.73	1.86
808	793	807	860	760	793	778	777	767	775	766	773	772	769
6.56	5.16	6.24	8.9	4.04	4.3	5.05	5.38	4.66	5.28	3.57	5.69	3.54	5.37

ME SOS-600J C	ME SOS-600J B	ME SOS-600J C	ME SOS-600J C	ME SOS-600J B	ME SOS-600J C	ME SOS-600J B	ME SOS-600J C	ME SOS-600J B	ME SOS-600J C	ME SOS-600J B	ME SOS-600J C	ME SOS-600J C	ME SOS-600J B
38.72	38.53	38.68	38.84	39.02	38.65	38.82	38.95	38.77	39.09	39.49	38.03	38.62	38.76
1.60	1.56	1.52	1.70	1.54	1.61	1.63	1.63	1.61	1.22	1.57	1.35	1.36	1.44
15.49	15.80	15.29	15.64	16.08	15.50	15.56	15.77	16.09	15.71	15.99	16.89	15.88	15.36
16.59	16.45	17.05	16.27	15.87	16.51	16.58	16.17	15.82	16.00	15.80	16.13	16.48	16.69
0.30	0.33	0.35	0.24	0.31	0.39	0.23	0.35	0.35	0.35	0.37	0.24	0.37	0.26
12.81	12.97	13.03	13.23	13.26	13.06	13.03	13.03	13.19	13.56	12.25	12.98	13.17	13.21
0.04	0.05	0.03	0.07			0.06	0.03	0.15	0.03	0.16	0.08	0.12	0.05
0.17	0.26		0.14	0.28	0.23	0.02	0.13	0.23	0.04	0.50	0.48	0.09	0.13
9.76	9.53	9.59	9.57	9.47	9.76	9.71	9.65	9.53	9.67	9.32	9.43	9.80	9.46
0.20	0.16	0.11	0.15	0.10	0.16	0.19	0.12	0.16	0.18	0.08	0.05	0.05	0.12
0.16	0.03			0.02			0.08			0.10			
0.07	0.25	0.03	0.09			0.11			0.17	0.22	0.31		0.46
0.09	0.09	0.12	0.05	0.08	0.11	0.05	0.11	0.08	0.01	0.14	0.06	0.05	0.08
-0.05	-0.13	-0.04	-0.05	-0.02	-0.02	-0.06	-0.02	-0.02	-0.07	-0.12	-0.14	-0.01	-0.21
96.01	96.01	95.79	96.00	96.01	95.99	95.99	96.01	95.99	96.02	96.00	96.01	96.00	96.02
5.784	5.755	5.792	5.777	5.781	5.769	5.787	5.790	5.753	5.806	5.863	5.668	5.755	5.799
2.216	2.245	2.208	2.223	2.219	2.231	2.213	2.210	2.247	2.194	2.137	2.332	2.245	2.201
0.512	0.536	0.491	0.518	0.588	0.497	0.521	0.553	0.567	0.556	0.661	0.635	0.544	0.507
0.180	0.175	0.171	0.190	0.171	0.181	0.183	0.182	0.180	0.136	0.176	0.152	0.153	0.162
0.024	0.019	0.013	0.018	0.011	0.019	0.023	0.015	0.019	0.021	0.009	0.006	0.006	0.014
2.073	2.055	2.135	2.024	1.966	2.061	2.067	2.010	1.963	1.988	1.962	2.010	2.054	2.088
0.038	0.041	0.044	0.030	0.039	0.050	0.029	0.044	0.043	0.043	0.047	0.030	0.047	0.033
2.852	2.887	2.908	2.933	2.927	2.905	2.895	2.887	2.918	3.001	2.711	2.884	2.926	2.946
0.020	0.003			0.002			0.009			0.011			
0.006	0.008	0.005	0.011			0.009	0.005	0.024	0.005	0.026	0.012	0.020	0.008
0.050	0.075		0.042	0.080	0.067	0.006	0.039	0.066	0.011	0.144	0.139	0.025	0.039
1.860	1.816	1.832	1.816	1.788	1.859	1.845	1.829	1.804	1.831	1.765	1.792	1.863	1.804
19.615	19.616	19.597	19.582	19.573	19.639	19.577	19.573	19.585	19.593	19.512	19.660	19.638	19.600
3.944	3.859	3.955	3.945	3.980	3.972	3.936	3.972	3.980	3.918	3.861	3.839	3.987	3.762
0.033	0.118	0.014	0.042			0.052			0.080	0.103	0.146		0.218
0.023	0.023	0.030	0.013	0.020	0.028	0.013	0.028	0.020	0.003	0.035	0.015	0.013	0.020
0.918	0.887	0.913	0.934	0.960	0.906	0.933	0.951	0.921	0.974	1.039	0.801	0.900	0.927
0.218	0.193	0.122	0.172	0.222	0.189	0.179	0.210	0.231	0.210	0.440	0.235	0.209	0.159
584	571	550	629	574	593	598	603	603	442	571	493	495	527
1.74	1.90	1.65	1.78	1.98	1.74	1.75	1.84	2.00	1.80	1.95	2.46	1.92	1.68
786	795	780	789	776	772	806	777	781	805	787	798	786	803
5.24	5.62	4.76	6.11	5.16	3.91	6.65	4.62	4.82	5.51	5.35	6.36	5.2	5.51

ME SOS-600J C	ME SOS-600J C	ME SOS-600J B	ME SOS-600J C										
38.72	38.93	39.16	38.58	38.71	39.15	39.09	39.26	40.14	38.78	38.65	38.76	36.99	38.86
1.23	1.37	1.16	1.24	1.31	0.98	0.99	1.11	1.12	1.33	1.26	1.45	1.39	1.32
15.51	15.14	15.47	15.49	15.60	15.57	14.69	15.89	15.76	15.48	15.31	15.75	15.84	16.24
16.92	15.89	16.27	17.05	16.79	15.11	16.00	15.63	15.13	16.68	17.02	16.27	17.82	16.02
0.38	0.33	0.38	0.26	0.40	0.32	0.41	0.41	0.24	0.26	0.36	0.25	0.47	0.27
13.05	13.67	13.58	12.98	12.79	13.78	13.69	13.51	13.20	13.11	13.07	13.33	12.36	13.18
0.03	0.34			0.04	0.78	0.17	0.03	0.02	0.02	0.03	0.15	0.04	
	0.12	0.26	0.42	0.22	0.33	0.40	0.16	0.60	0.18	0.27	0.21	0.68	0.32
9.99	9.67	9.56	9.69	9.89	9.43	9.72	9.69	9.53	9.72	9.73	9.65	9.72	9.50
0.08	0.21		0.10	0.12	0.17	0.14	0.22	0.14	0.18	0.23	0.10	0.33	0.12
0.01	0.13	0.11	0.05	0.06		0.05	0.07		0.19	0.03		0.05	
	0.13				0.29	0.52						0.15	
0.08	0.01	0.05	0.15	0.09	0.14	0.15	0.02	0.11	0.06	0.05	0.07	0.24	0.14
-0.02	-0.06	-0.01	-0.03	-0.02	-0.15	-0.25	0.00	-0.02	-0.01	-0.01	-0.02	-0.12	-0.03
95.99	95.93	96.00	96.01	96.01	96.04	96.03	96.00	95.99	96.00	96.01	96.00	96.03	96.02
5.789	5.801	5.820	5.775	5.787	5.815	5.860	5.816	5.918	5.788	5.781	5.766	5.609	5.767
2.211	2.199	2.180	2.225	2.213	2.185	2.140	2.184	2.082	2.212	2.219	2.234	2.391	2.233
0.523	0.461	0.529	0.508	0.535	0.541	0.455	0.589	0.657	0.510	0.481	0.528	0.440	0.609
0.138	0.154	0.130	0.139	0.147	0.109	0.111	0.124	0.125	0.150	0.141	0.162	0.159	0.147
0.009	0.025		0.011	0.015	0.020	0.017	0.026	0.017	0.022	0.027	0.011	0.039	0.014
2.115	1.980	2.023	2.134	2.099	1.877	2.006	1.936	1.866	2.081	2.081	2.129	2.024	2.260
0.049	0.041	0.048	0.033	0.051	0.040	0.052	0.052	0.030	0.033	0.046	0.031	0.060	0.034
2.908	3.037	3.010	2.896	2.850	3.050	3.059	2.982	2.901	2.917	2.913	2.957	2.793	2.916
0.001	0.016	0.013	0.006	0.007		0.006	0.008		0.023	0.003			0.006
0.005	0.054			0.006	0.124	0.028	0.005	0.003	0.003	0.005	0.024	0.006	
	0.033	0.075	0.123	0.064	0.094	0.117	0.047	0.170	0.053	0.078	0.061	0.200	0.091
1.906	1.838	1.813	1.849	1.886	1.786	1.858	1.830	1.793	1.851	1.857	1.831	1.881	1.799
19.654	19.638	19.639	19.699	19.660	19.642	19.710	19.599	19.561	19.643	19.682	19.631	19.838	19.604
3.980	3.936	3.987	3.962	3.977	3.829	3.715	3.995	3.973	3.985	3.987	3.982	3.866	3.965
	0.061				0.136	0.247						0.072	
0.020	0.003	0.013	0.038	0.023	0.035	0.038	0.005	0.027	0.015	0.013	0.018	0.062	0.035
0.918	0.950	0.986	0.897	0.917	0.983	0.983	1.000	1.137	0.928	0.908	0.922	0.639	0.935
0.211	0.237	0.212	0.238	0.267	0.448	0.323	0.283	0.498	0.206	0.209	0.220	0.162	0.250
426	519	409	428	459	331	325	392	396	479	439	537	483	479
1.75	1.53	1.68	1.75	1.80	1.73	1.33	1.87	1.77	1.72	1.65	1.84	2.05	2.08
801	796	767	769	785	783	782	782	769	776	772	775	780	779
6.66	5.75	3.6	5.57	5.38	5.62	3.33	3.89	6.17	5.08	3.92	5.83	4.75	5.95

ME SOS-600J B	ME SOS-600J C	ME SOS-600J B	ME SOS-600J B	ME SOS-600J C	ME SOS-600J B								
38.62	38.98	39.29	38.87	39.03	39.15	38.99	39.37	39.37	39.21	38.49	39.08	38.63	38.90
1.36	1.15	1.15	1.26	1.25	1.19	1.32	1.14	1.18	1.21	1.32	1.38	1.16	1.07
15.51	15.64	16.03	15.18	15.27	15.34	15.71	15.66	15.41	15.32	15.79	15.74	15.71	15.78
15.58	16.64	15.54	16.41	16.27	15.99	15.96	15.60	15.90	16.21	16.82	16.23	16.58	16.24
0.36	0.37	0.37	0.36	0.34	0.24	0.37	0.30	0.40	0.30	0.33	0.19	0.36	0.36
13.58	13.15	13.51	13.36	13.55	13.86	13.48	14.24	13.78	13.77	12.91	13.32	13.24	13.75
0.37	0.01		0.08			0.05	0.02	0.18	0.08	0.10	0.03	0.10	0.02
0.89	0.12	0.36	0.16	0.40	0.20	0.16	0.08	0.05		0.38	0.15	0.35	0.32
9.50	9.69	9.61	9.87	9.72	9.83	9.70	9.43	9.61	9.51	9.60	9.51	9.75	9.35
0.05	0.06	0.12	0.33	0.08		0.11	0.11	0.11	0.25	0.18	0.16	0.04	0.15
0.03	0.07		0.09			0.11		0.01			0.09	0.06	0.04
				0.08		0.02							
0.15	0.12	0.02	0.03	0.08	0.12	0.06	0.04	0.02	0.15	0.09	0.11	0.04	0.03
-0.03	-0.03	0.00	-0.01	-0.02	-0.06	-0.01	-0.02	0.00	-0.03	-0.02	-0.02	-0.01	-0.01
96.02	96.00	96.00	95.99	95.99	96.01	95.99	95.99	96.01	96.01	96.00	96.01	96.00	96.01
5.752	5.809	5.812	5.801	5.813	5.823	5.792	5.817	5.835	5.824	5.749	5.802	5.765	5.775
2.248	2.191	2.188	2.199	2.187	2.177	2.208	2.183	2.165	2.176	2.251	2.198	2.235	2.225
0.476	0.557	0.608	0.471	0.495	0.512	0.543	0.544	0.527	0.507	0.530	0.557	0.527	0.536
0.153	0.129	0.128	0.141	0.140	0.133	0.147	0.127	0.132	0.135	0.148	0.154	0.130	0.119
0.006	0.007	0.013	0.039	0.009		0.012	0.012	0.012	0.029	0.022	0.019	0.005	0.018
1.941	2.074	1.923	2.048	2.027	1.989	1.983	1.928	1.971	2.014	2.101	2.016	2.069	2.017
0.045	0.047	0.047	0.046	0.042	0.030	0.047	0.037	0.051	0.037	0.041	0.024	0.045	0.046
3.016	2.922	2.978	2.973	3.007	3.073	2.985	3.136	3.044	3.048	2.875	2.949	2.945	3.042
0.003	0.008		0.010			0.013		0.001			0.010	0.007	0.005
0.060	0.002		0.012			0.008	0.003	0.029	0.012	0.015	0.005	0.015	0.003
0.258	0.036	0.102	0.047	0.116	0.058	0.047	0.022	0.014		0.111	0.044	0.100	0.091
1.806	1.842	1.813	1.879	1.847	1.865	1.837	1.777	1.817	1.803	1.829	1.801	1.857	1.771
19.762	19.623	19.613	19.666	19.684	19.661	19.622	19.586	19.596	19.586	19.672	19.580	19.700	19.647
3.962	3.970	3.995	3.992	3.980	3.932	3.985	3.981	3.995	3.962	3.977	3.972	3.990	3.992
0.038	0.030	0.005	0.008	0.020	0.030	0.015	0.010	0.005	0.038	0.023	0.028	0.010	0.008
0.899	0.958	1.003	0.942	0.967	0.985	0.957	1.014	1.017	0.993	0.879	0.972	0.902	0.942
0.371	0.227	0.311	0.234	0.251	0.230	0.221	0.159	0.235	0.167	0.242	0.208	0.253	0.176
518	392	412	453	453	434	486	420	428	438	465	508	400	361
1.72	1.79	1.94	1.56	1.59	1.62	1.80	1.73	1.63	1.60	1.90	1.82	1.84	1.84
768	770	779	783	766	786	776	786	784	782	775	780	775	772
5.38	4.23	4.68	4.99	3.97	5.5	4.04	5.14	4.46	5.08	5.41	6.58	4.78	4.43

ME SOS-600J C	ME SOS-600J B												
38.33	38.62	38.22	38.04	39.04	39.10	38.93	39.18	38.74	38.72	38.87	39.10	39.00	38.79
1.11	0.85	1.44	1.32	1.31	1.38	1.27	1.27	1.32	1.26	1.15	1.30	1.58	1.50
15.50	15.16	15.33	15.89	15.53	15.72	15.81	15.97	15.40	15.57	15.72	16.01	15.51	15.19
16.91	16.96	17.00	16.84	15.91	16.13	15.74	15.21	16.34	16.52	16.14	15.89	16.34	17.32
0.42	0.36	0.34	0.44	0.36	0.33	0.24	0.42	0.38	0.27	0.29	0.29	0.36	0.30
13.56	13.98	13.01	13.04	13.64	13.27	13.62	13.97	13.55	13.68	13.45	13.35	13.10	12.64
0.07	0.13	0.16	0.07	0.10	0.07	0.11		0.03	0.08	0.04	0.05	0.08	0.01
0.31	0.16	0.23	0.50	0.14	0.22	0.29	0.18	0.40	0.32	0.18	0.18	0.26	0.32
9.56	9.43	9.77	9.59	9.73	9.65	9.60	9.55	9.49	9.49	9.72	9.48	9.55	9.77
0.02	0.10		0.04	0.03	0.06		0.08	0.13		0.12	0.14	0.13	0.08
0.09	0.07	0.10	0.09	0.05		0.09		0.09	0.01	0.06		0.04	
			0.29	0.06	0.08		0.23	0.12	0.07		0.14	0.17	
0.13	0.17	0.14	0.10	0.10	0.07	0.08	0.07	0.07	0.07	0.10	0.16	0.06	0.09
-0.03	-0.04	-0.15	-0.05	-0.06	-0.02	-0.11	-0.07	-0.05	-0.02	-0.10	-0.09	-0.01	-0.02
96.01	95.99	96.03	96.00	96.02	95.99	96.00	96.02	96.02	96.01	96.02	96.02	96.00	96.00
5.736	5.775	5.747	5.699	5.805	5.807	5.787	5.794	5.775	5.765	5.792	5.799	5.800	5.809
2.264	2.225	2.253	2.301	2.195	2.193	2.213	2.206	2.225	2.235	2.208	2.201	2.200	2.191
0.471	0.446	0.464	0.506	0.527	0.560	0.558	0.578	0.480	0.498	0.552	0.598	0.519	0.490
0.125	0.096	0.163	0.148	0.146	0.154	0.142	0.141	0.149	0.141	0.129	0.145	0.177	0.169
0.002	0.011		0.005	0.003	0.007		0.009	0.016		0.014	0.017	0.016	0.009
2.116	2.121	2.138	2.110	1.978	2.003	1.958	1.881	2.037	2.057	2.011	1.971	2.032	2.169
0.054	0.045	0.043	0.056	0.045	0.041	0.030	0.053	0.048	0.034	0.036	0.036	0.046	0.038
3.024	3.116	2.916	2.912	3.023	2.937	3.019	3.079	3.010	3.037	2.987	2.952	2.905	2.822
0.010	0.008	0.012	0.010	0.006		0.010		0.010	0.001	0.007		0.005	
0.011	0.022	0.026	0.011	0.015	0.011	0.017		0.005	0.012	0.006	0.008	0.012	0.002
0.089	0.047	0.067	0.145	0.042	0.064	0.083	0.052	0.117	0.091	0.053	0.052	0.075	0.092
1.825	1.798	1.874	1.833	1.846	1.828	1.820	1.802	1.805	1.803	1.846	1.792	1.812	1.867
19.727	19.710	19.703	19.736	19.630	19.604	19.637	19.595	19.677	19.675	19.642	19.571	19.598	19.657
3.967	3.957	3.826	3.946	3.937	3.982	3.872	3.926	3.949	3.975	3.894	3.905	3.992	3.977
		0.138	0.028	0.038		0.108	0.056	0.033		0.066	0.080		
0.033	0.043	0.036	0.025	0.025	0.018	0.020	0.018	0.018	0.025	0.040	0.015	0.008	0.023
0.855	0.903	0.840	0.807	0.967	0.975	0.948	0.984	0.919	0.915	0.941	0.974	0.961	0.932
0.130	0.108	0.183	0.187	0.226	0.255	0.253	0.210	0.181	0.163	0.240	0.245	0.220	0.241
378	227	522	469	486	509	471	484	488	456	406	475	584	531
1.76	1.56	1.70	1.97	1.72	1.81	1.87	1.91	1.67	1.75	1.83	1.95	1.71	1.59
769	767	792	783	782	774	794	787	774	771	782	792	774	771
3.77	3.84	4.77	4.55	4.24	4.74	6.19	3.74	4.17	5.51	5.76	5.37	4.15	4.88

ME SOS-600J C	ME SOS-600J B												
38.65	38.37	38.78	38.78	39.18	38.67	39.01	39.08	38.95	40.13	39.22	38.88	39.40	39.00
1.55	1.53	1.21	1.26	1.27	1.32	1.24	1.02	1.12	0.80	1.08	1.15	1.19	1.18
15.43	14.74	15.24	15.96	15.74	15.77	15.58	15.71	15.50	16.09	14.98	16.07	15.79	15.74
16.90	17.42	16.61	15.76	15.87	16.27	15.75	15.57	16.00	14.23	15.59	15.24	15.83	15.42
0.30	0.32	0.30	0.17	0.23	0.37	0.42	0.38	0.33	0.25	0.37	0.31	0.26	0.36
12.85	13.07	13.48	13.64	13.64	13.46	13.54	13.80	14.21	14.84	14.29	13.88	13.53	13.99
0.07	0.10	0.01	0.14	0.12	0.08	0.12	0.21	0.02	0.11	0.11	0.18	0.19	0.26
0.06	0.20	0.37	0.44	0.28	0.11	0.24	0.29		0.13		0.14	0.03	0.25
9.72	9.92	9.79	9.76	9.60	9.76	9.70	9.34	9.65	9.28	9.70	9.72	9.72	9.46
0.23	0.16	0.16			0.10	0.05	0.14	0.05	0.07	0.09	0.10		0.11
0.09						0.07	0.07						
0.11						0.20	0.37	0.13		0.53	0.20		0.19
0.08	0.17	0.03	0.07	0.07	0.10	0.11	0.02	0.07	0.07	0.09	0.03	0.06	0.06
-0.06	-0.04	-0.01	-0.02	-0.02	-0.02	-0.11	-0.16	-0.07	-0.02	-0.24	-0.09	-0.01	-0.09
96.02	95.99	95.99	95.99	95.99	96.00	96.02	96.01	96.03	95.99	96.03	95.90	95.99	96.00
5.780	5.773	5.789	5.760	5.807	5.759	5.807	5.806	5.787	5.871	5.846	5.770	5.834	5.784
2.220	2.227	2.211	2.240	2.193	2.241	2.193	2.194	2.213	2.129	2.154	2.230	2.166	2.216
0.499	0.386	0.471	0.552	0.558	0.528	0.541	0.557	0.502	0.645	0.477	0.580	0.591	0.536
0.174	0.173	0.136	0.140	0.141	0.147	0.139	0.114	0.126	0.088	0.121	0.129	0.133	0.132
0.027	0.019	0.019			0.011	0.006	0.017	0.006	0.008	0.010	0.011		0.012
2.113	2.192	2.073	1.958	1.967	2.027	1.961	1.935	1.989	1.741	1.944	1.892	1.961	1.913
0.038	0.040	0.038	0.022	0.029	0.047	0.053	0.048	0.041	0.031	0.047	0.039	0.033	0.045
2.866	2.930	2.999	3.020	3.014	2.988	3.003	3.057	3.147	3.237	3.176	3.071	2.986	3.093
0.010						0.008	0.008						
0.011	0.015	0.002	0.023	0.018	0.012	0.018	0.034	0.003	0.017	0.017	0.029	0.030	0.041
0.017	0.059	0.108	0.127	0.080	0.030	0.069	0.083		0.038		0.041	0.008	0.072
1.853	1.903	1.864	1.849	1.815	1.855	1.841	1.770	1.828	1.732	1.844	1.839	1.835	1.789
19.608	19.719	19.711	19.692	19.623	19.646	19.640	19.623	19.641	19.536	19.635	19.631	19.576	19.632
3.928	3.957	3.992	3.982	3.982	3.975	3.878	3.821	3.921	3.983	3.727	3.899	3.985	3.896
0.052						0.094	0.174	0.061		0.250	0.094		0.089
0.020	0.043	0.008	0.018	0.018	0.025	0.028	0.005	0.018	0.017	0.023	0.008	0.015	0.015
0.907	0.866	0.928	0.923	0.986	0.907	0.963	0.973	0.951	1.126	0.998	0.938	1.021	0.957
0.177	0.153	0.228	0.298	0.265	0.186	0.269	0.268	0.116	0.292	0.187	0.267	0.294	0.246
559	552	429	466	468	482	456	347	406	238	391	427	428	441
1.71	1.39	1.60	1.93	1.80	1.86	1.75	1.80	1.70	1.88	1.44	1.99	1.82	1.81
796	778	776	791	778	781	786	785	796	794	802	798	796	785
5.41	4.98	5.03	6.6	5.77	4.73	4	4.61	5.12	5.82	4.41	5.37	6.13	4.55

ME SOS-600J C	ME SOS-600J B	ME SOS-600J C	ME SOS-600J B	ME SOS-600J C	ME SOS-600J B	ME SOS-600J C	ME SOS-600J B	ME SOS-600J C	ME SOS-600J I	ME SOS-600J I	ME SOS-600J I	ME SOS-600J I	ME SOS-600J I	ME SOS-600J I
38.69	39.41	39.00	39.52	38.86	39.14	38.86	39.41	39.11	39.02	39.36	39.59	39.20	38.92	
1.17	1.26	1.15	1.09	1.27	1.13	1.29	1.25	1.49	1.47	1.43	1.39	1.45	1.37	
15.73	13.82	15.81	15.06	16.01	15.80	15.28	15.67	15.20	15.72	15.71	15.51	15.84	15.69	
16.20	16.52	15.75	16.03	15.68	15.37	16.39	15.61	15.80	15.87	15.66	15.57	15.79	15.88	
0.36	0.40	0.36	0.24	0.36	0.36	0.36	0.30	0.39	0.33	0.27	0.33	0.24	0.31	
13.55	12.73	13.65	14.04	13.78	14.06	13.52	13.57	13.47	13.56	13.43	13.43	13.32	13.27	
	0.33	0.05	0.02	0.03	0.10	0.13	0.02	0.30	0.12	0.09		0.11	0.14	
0.29	0.95	0.18	0.10	0.11	0.40	0.39	0.12	0.26	0.13	0.26	0.13	0.26	0.30	
9.72	10.01	9.86	9.58	9.66	9.40	9.44	9.53	9.46	9.53	9.53	9.58	9.34	9.62	
							0.17	0.24	0.07	0.10	0.15	0.13	0.03	
0.22	0.35	0.12	0.06	0.05	0.15	0.12	0.14	0.12	0.12	0.16	0.18	0.15	0.26	
		0.04			0.02	0.17				0.02	0.09	0.09	0.10	
	0.15		0.18	0.18			0.07							
0.06	0.08	0.02	0.10	0.04	0.08	0.06	0.14	0.16	0.06		0.09	0.13		
-0.01	-0.08	0.00	-0.10	-0.08	-0.02	-0.01	-0.06	-0.04	-0.01		-0.02	-0.03		
95.99	96.01	95.99	96.02	96.01	96.01	96.00	96.01	96.00	96.00	95.99	95.89	96.00	96.01	
5.761	5.924	5.789	5.869	5.767	5.790	5.790	5.842	5.822	5.788	5.826	5.863	5.808	5.788	
2.239	2.076	2.211	2.131	2.233	2.210	2.210	2.158	2.178	2.212	2.174	2.137	2.192	2.212	
0.522	0.373	0.555	0.506	0.569	0.545	0.474	0.580	0.488	0.536	0.566	0.571	0.575	0.538	
0.131	0.142	0.129	0.122	0.141	0.126	0.144	0.139	0.167	0.164	0.159	0.155	0.162	0.154	
0.026	0.041	0.015	0.007	0.006	0.018	0.014	0.017	0.015	0.015	0.019	0.021	0.018	0.030	
2.018	2.077	1.956	1.991	1.946	1.901	2.042	1.935	1.967	1.969	1.938	1.929	1.957	1.975	
0.045	0.051	0.045	0.030	0.045	0.045	0.045	0.037	0.050	0.041	0.034	0.041	0.030	0.039	
3.007	2.853	3.021	3.107	3.048	3.101	3.002	3.000	2.989	2.999	2.963	2.965	2.941	2.941	
		0.005			0.002	0.021					0.002	0.010	0.011	
	0.053	0.008	0.003	0.005	0.015	0.021	0.003	0.047	0.018	0.014		0.017	0.023	
0.083	0.277	0.053	0.028	0.030	0.116	0.114	0.036	0.075	0.039	0.074	0.039	0.074	0.086	
1.847	1.920	1.867	1.815	1.828	1.773	1.793	1.803	1.795	1.804	1.800	1.810	1.766	1.825	
							0.010	0.014	0.004	0.006	0.009	0.008	0.002	
19.679	19.787	19.652	19.608	19.617	19.642	19.670	19.560	19.606	19.588	19.573	19.541	19.558	19.624	
3.985	3.908	3.995	3.890	3.905	3.980	3.985	3.932	3.960	3.985	4.000	4.000	3.977	3.967	
	0.071		0.085	0.084			0.033							
0.015	0.020	0.005	0.025	0.010	0.020	0.015	0.035	0.040	0.015			0.023	0.033	
0.910	1.038	0.958	1.044	0.935	0.978	0.939	1.024	0.979	0.962	1.014	1.053	0.989	0.947	
0.214	0.568	0.262	0.205	0.187	0.243	0.205	0.271	0.283	0.202	0.288	0.287	0.260	0.283	
416	443	414	386	474	417	468	462	563	554	538	524	542	510	
1.84	0.89	1.85	1.46	1.96	1.82	1.60	1.77	1.55	1.80	1.77	1.68	1.85	1.80	
771	790	789	788	797	774	766	779	766	776	804	793	776	772	
4.3	5.62	5.7	4.95	4.64	4.57	3.95	5.32	3.91	4.94	6.93	5.88	5.75	5.51	

ME SOS-600J I	ME SOS-600J B	ME SOS-600J	ME SOS-600J	ME SOS-600J	ME SOS-600J C	ME SOS-600J C	ME SOS-600M C	ME SOS-600M B	ME SOS-600M C	ME SOS-600M B	ME SOS-600M C	ME SOS-600M B
38.60	38.26	40.66	40.16	40.14	38.80	38.80	39.36	39.07	39.65	39.55	39.55	39.84
1.30	1.25	0.67	0.62	0.67	1.92	1.47	1.44	1.34	1.44	1.44	1.34	1.44
16.39	17.31	14.96	15.06	15.22	15.65	15.71	15.26	15.46	15.36	15.65	15.46	15.36
15.63	15.39	15.08	14.90	14.86	17.26	15.69	14.30	14.02	13.82	13.73	14.98	14.78
0.39	0.43	0.29	0.29	0.16	0.39	0.29	0.19	0.29	0.19	0.29	0.29	0.38
13.35	12.77	14.84	14.54	14.64	12.14	13.69	14.98	15.17	15.07	14.88	14.69	14.50
0.12	0.20	0.12	0.10	0.03	0.07	0.09						
0.29	0.43	0.06	0.39	0.15	0.17	0.06						
9.57	9.53	8.95	9.48	9.50	9.55	9.95	9.60	9.60	9.60	9.60	9.60	9.60
	0.14	0.05	0.12	0.17								
0.19	0.17	0.27	0.23	0.37	0.05	0.01	0.29	0.10	0.19	0.29		
0.01	0.03				0.01							
						0.70	1.00	0.70	0.60			
0.15	0.08		0.11	0.07			0.10	0.10				
-0.03	-0.02		-0.02	-0.02			-0.32	-0.44	-0.29	-0.25		
96.00	95.99	95.93	96.00	95.99	96.01	95.75	96.22	96.14	96.03	96.02	95.90	95.90
5.731	5.677	5.964	5.924	5.913	5.791	5.773	5.820	5.796	5.848	5.828	5.831	5.866
2.269	2.323	2.036	2.076	2.087	2.209	2.227	2.180	2.204	2.152	2.172	2.169	2.134
0.598	0.704	0.550	0.544	0.555	0.543	0.528	0.480	0.499	0.518	0.546	0.516	0.531
0.145	0.139	0.074	0.069	0.074	0.215	0.164	0.160	0.150	0.160	0.160	0.149	0.159
0.023	0.020	0.031	0.027	0.044	0.006	0.001	0.034	0.011	0.022	0.034		
1.940	1.910	1.850	1.838	1.831	2.154	1.952	1.769	1.739	1.705	1.692	1.846	1.820
0.049	0.054	0.036	0.036	0.020	0.050	0.036	0.024	0.036	0.024	0.036	0.036	0.048
2.955	2.824	3.246	3.199	3.215	2.702	3.036	3.301	3.354	3.314	3.268	3.228	3.182
0.001	0.003				0.001							
0.020	0.032	0.018	0.015	0.005	0.011	0.014						
0.083	0.124	0.016	0.113	0.044	0.050	0.017						
1.812	1.804	1.674	1.785	1.786	1.818	1.887	1.811	1.816	1.806	1.804	1.805	1.803
	0.008	0.003	0.007	0.010								
19.627	19.624	19.498	19.632	19.584	19.549	19.637	19.578	19.605	19.549	19.539	19.580	19.543
3.962	3.980	4.000	3.972	3.983	4.000	4.000	3.648	3.506	3.673	3.720	4.000	4.000
							0.327	0.469	0.327	0.280		
0.038	0.020		0.028	0.017			0.025	0.025				
0.893	0.836	1.214	1.140	1.136	0.931	0.928	1.013	0.970	1.058	1.041	1.042	1.087
							0.129	0.109	0.174	0.189	0.136	0.179
480	450	122	78	124	668	562	598	569	609	606	536	576
2.16	2.64	1.31	1.41	1.48	1.81	1.82	1.53	1.66	1.56	1.70	1.61	1.55
781	780	795	772	790	801	831	841	824	862	841	809	801
4.88	4.7	5.13	4.12	5.58	5.42	9.04	6.92	5.97	8.36	7.23	6.71	5.48

ME SOS-600M C	ME SOS-600M B	ME SOS-600M C	ME SOS-600M C										
39.74	39.94	38.88	40.03	39.46	39.26	40.03	39.94	39.17	40.03	39.65	39.74	39.47	
1.44	1.34	1.54	1.34	1.34	1.44	1.34	1.34	1.63	1.54	1.34	1.44	1.64	
15.46	15.07	15.07	15.46	14.98	14.88	15.17	15.17	15.17	15.36	14.69	16.32	15.74	
14.69	15.55	14.78	14.21	14.78	14.59	14.78	15.07	14.78	14.69	15.55	14.78	14.13	
0.29	0.21	0.29	0.29	0.19	0.19	0.19	0.19	0.29	0.29	0.29	0.19	0.14	
14.78	14.30	14.78	15.07	14.78	14.98	14.59	14.50	14.21	14.11	14.98	13.34	14.30	0.13
													0.11
9.50	9.60	9.41	9.50	9.60	9.70	9.89	9.70	9.70	9.60	9.50	9.89	9.49	
													0.02
													0.02
													0.78
													0.06
													-0.34
95.90	96.02	94.75	95.90	95.14	95.04	96.00	95.90	94.94	95.62	96.00	95.71	96.04	
5.844	5.890	5.804	5.869	5.861	5.841	5.891	5.886	5.839	5.902	5.857	5.859	5.833	
2.156	2.110	2.196	2.131	2.139	2.159	2.109	2.114	2.161	2.098	2.143	2.141	2.167	
0.523	0.510	0.457	0.539	0.483	0.451	0.523	0.521	0.504	0.571	0.415	0.695	0.576	
0.159	0.149	0.172	0.148	0.150	0.161	0.149	0.149	0.183	0.170	0.149	0.160	0.182	
													0.002
1.806	1.918	1.846	1.742	1.837	1.816	1.820	1.858	1.843	1.811	1.921	1.823	1.747	
0.036	0.026	0.036	0.036	0.024	0.024	0.024	0.024	0.036	0.036	0.036	0.024	0.018	
3.241	3.145	3.290	3.294	3.274	3.321	3.201	3.185	3.157	3.102	3.298	2.932	3.152	
													0.002
													0.021
													0.030
1.783	1.806	1.791	1.777	1.819	1.840	1.856	1.823	1.844	1.805	1.791	1.859	1.790	
19.548	19.554	19.593	19.536	19.587	19.613	19.572	19.559	19.567	19.496	19.610	19.493	19.522	
4.000	4.000	4.000	4.000	4.000	4.000	4.000	4.000	4.000	4.000	4.000	4.000	3.620	
													0.365
													0.015
1.070	1.104	0.944	1.113	1.034	1.004	1.118	1.104	0.990	1.120	1.059	1.073	1.030	
0.134	0.184	0.047	0.166	0.146	0.118	0.241	0.205	0.167	0.249	0.056	0.368	0.245	
583	518	629	556	546	596	537	530	653	610	532	554	666	
1.59	1.41	1.51	1.56	1.42	1.38	1.44	1.45	1.55	1.56	1.22	2.06	1.78	
811	813	806	814	821	827	841	822	809	807	802	847	846	
6.63	7.07	5.76	6.75	7.32	7.54	9.31	8.01	6.21	6.55	5.48	9.67	7.85	

ME SOS-600M B	ME SOS-600M C	ME SOS-600M B										
39.45	39.72	39.97	39.31	39.62	39.65	40.06	39.57	39.57	39.52	39.51	39.60	41.43
1.55	1.58	1.33	1.44	1.63	1.44	1.43	1.51	1.51	1.38	1.44	1.51	1.28
15.43	15.05	15.26	15.15	15.44	15.05	15.00	15.31	15.31	15.12	15.54	15.24	15.49
15.16	14.60	14.62	14.83	14.75	14.59	14.45	14.85	14.85	14.60	14.99	14.57	13.45
0.24	0.23	0.24	0.25	0.29	0.22	0.30	0.28	0.28	0.26	0.27	0.25	0.10
14.10	14.54	14.16	14.30	14.38	14.80	14.52	14.48	14.48	14.56	13.99	14.36	13.57
0.15		0.15	0.14	0.03	0.07	0.16	0.08	0.08	0.08	0.27	0.12	0.14
0.21	0.09	0.36	0.14		0.15	0.25	0.11	0.11	0.07	0.11	0.13	1.08
9.61	9.49	9.40	9.43	9.68	9.47	9.47	9.59	9.59	9.48	9.43	9.59	8.91
0.02	0.01	0.04	0.12	0.15	0.07	0.02			0.14		0.39	0.35
0.03	0.12					0.01			0.01		0.01	0.04
	0.52	0.37	0.92		0.05	0.28	0.21	0.48	0.77	0.45	0.19	0.16
0.06	0.06	0.11	0.02	0.04	0.01	0.06	0.04	0.07	0.04	0.04	0.03	
-0.01	-0.23	-0.18	-0.39	-0.01	-0.02	-0.13	-0.10	-0.22	-0.33	-0.20	-0.09	-0.07
96.00	96.03	96.02	96.06	96.00	95.57	96.01	96.02	96.32	96.03	96.03	96.00	96.00
5.827	5.874	5.901	5.845	5.835	5.859	5.904	5.842	5.842	5.860	5.847	5.844	6.034
2.173	2.126	2.099	2.155	2.165	2.141	2.096	2.158	2.158	2.140	2.153	2.156	1.966
0.513	0.497	0.557	0.500	0.514	0.481	0.511	0.506	0.506	0.503	0.557	0.496	0.694
0.172	0.176	0.148	0.161	0.181	0.160	0.159	0.167	0.167	0.154	0.160	0.167	0.140
0.002	0.001	0.004	0.014	0.018	0.008	0.002			0.017		0.046	0.040
1.873	1.806	1.805	1.844	1.816	1.803	1.781	1.834	1.834	1.811	1.854	1.799	1.638
0.030	0.029	0.030	0.031	0.036	0.028	0.037	0.035	0.035	0.033	0.034	0.031	0.012
3.105	3.206	3.116	3.171	3.157	3.261	3.191	3.186	3.186	3.219	3.085	3.159	2.947
0.003	0.015					0.001			0.001		0.001	0.004
0.024		0.024	0.023	0.005	0.011	0.026	0.012	0.012	0.012	0.043	0.018	0.022
0.060	0.025	0.102	0.042		0.044	0.071	0.030	0.030	0.019	0.030	0.038	0.304
1.811	1.791	1.770	1.788	1.818	1.784	1.779	1.806	1.806	1.792	1.779	1.805	1.655
19.593	19.545	19.556	19.574	19.545	19.580	19.558	19.577	19.577	19.561	19.543	19.562	19.456
3.985	3.742	3.800	3.562	3.990	3.974	3.855	3.892	3.758	3.629	3.779	3.904	3.926
	0.243	0.173	0.433		0.023	0.131	0.098	0.224	0.361	0.211	0.089	0.074
0.015	0.015	0.028	0.005	0.010	0.003	0.015	0.010	0.018	0.010	0.010	0.008	
1.027	1.073	1.112	1.011	1.052	1.060	1.124	1.046	1.046	1.043	1.039	1.051	1.329
0.233	0.169	0.341	0.210	0.173	0.177	0.285	0.187	0.187	0.193	0.266	0.238	0.682
605	640	529	578	650	589	580	603	603	561	565	606	507
1.61	1.42	1.52	1.51	1.59	1.41	1.37	1.54	1.54	1.48	1.68	1.51	1.53
782	816	792	827	799	805	794	806	815	831	808	806	797
4.89	4.98	4.9	5.08	5.48	5.63	4.02	4.92	4.94	5.12	5.58	5.58	6.52

ME SOS-600M C	ME SOS-600M B	ME SOS-600M C										
39.75	39.61	39.47	39.53	39.72	39.21	39.58	39.34	39.31	39.53	39.17	40.46	39.49
1.55	1.45	1.41	1.50	1.46	1.49	1.27	1.43	1.54	1.38	1.47	1.28	1.37
15.37	15.00	14.44	15.48	15.25	15.00	14.60	14.76	14.94	14.91	15.74	15.67	15.06
14.62	14.37	14.70	14.10	14.70	14.65	14.75	14.31	15.20	14.92	14.57	15.42	14.84
0.21	0.23	0.18	0.31	0.20	0.29	0.14	0.12	0.27	0.26	0.16	0.36	0.20
14.32	14.52	14.98	14.45	14.70	14.57	15.01	15.11	14.54	14.58	13.97	13.22	14.31
0.20	0.20	0.32	0.14	0.12	0.15	0.05	0.46	0.13	0.10	0.21	0.26	0.14
0.06	0.12	0.07					0.12	0.06	0.01	0.08	0.09	0.12
9.55	9.53	9.60	9.73	9.64	9.62	9.46	9.59	9.66	9.62	9.63	8.28	9.66
0.22	0.30	0.35	0.35	0.20	0.33	0.39	0.24	0.28	0.39	0.45	0.88	0.36
0.09	0.02				0.03	0.07	0.12	0.02	0.02	0.03	0.03	
0.04	0.64	0.40	0.42	0.02	0.64	0.71	0.36		0.28	0.46		0.45
0.02	0.02	0.12	0.01		0.04	0.01	0.06	0.06		0.09	0.05	0.01
-0.02	-0.27	-0.20	-0.18	-0.01	-0.28	-0.30	-0.17	-0.01	-0.12	-0.21	-0.01	-0.19
96.00	96.03	96.02	96.03	96.00	96.02	96.04	96.05	96.00	96.00	96.03	95.99	96.03
5.852	5.865	5.855	5.835	5.845	5.824	5.871	5.822	5.817	5.850	5.802	5.928	5.853
2.148	2.135	2.145	2.165	2.155	2.176	2.129	2.178	2.183	2.150	2.198	2.072	2.147
0.518	0.484	0.380	0.529	0.492	0.451	0.424	0.398	0.423	0.451	0.550	0.634	0.483
0.171	0.161	0.157	0.166	0.162	0.166	0.141	0.159	0.171	0.154	0.164	0.141	0.153
0.026	0.035	0.041	0.040	0.023	0.038	0.046	0.028	0.033	0.046	0.053	0.102	0.042
1.800	1.780	1.824	1.741	1.809	1.820	1.829	1.772	1.881	1.846	1.805	1.889	1.839
0.026	0.029	0.023	0.038	0.025	0.036	0.018	0.016	0.034	0.032	0.020	0.044	0.025
3.143	3.206	3.312	3.179	3.225	3.227	3.320	3.334	3.208	3.217	3.084	2.887	3.162
0.010	0.002				0.003	0.008	0.015	0.002	0.002	0.003	0.003	
0.032	0.032	0.050	0.023	0.018	0.024	0.008	0.073	0.021	0.015	0.034	0.041	0.023
0.016	0.036	0.019					0.036	0.017	0.003	0.022	0.025	0.036
1.793	1.800	1.817	1.833	1.809	1.823	1.789	1.810	1.823	1.816	1.819	1.548	1.825
19.536	19.565	19.623	19.548	19.563	19.589	19.583	19.640	19.612	19.582	19.555	19.314	19.589
3.976	3.695	3.782	3.801	3.991	3.689	3.664	3.816	3.985	3.869	3.762	3.988	3.787
0.019	0.300	0.188	0.196	0.009	0.301	0.333	0.168		0.131	0.215		0.211
0.005	0.005	0.030	0.003		0.010	0.003	0.015	0.015		0.023	0.012	0.003
1.073	1.056	1.034	1.040	1.066	0.993	1.053	1.011	1.006	1.042	0.984	1.182	1.038
0.241	0.253	0.190	0.251	0.184	0.165	0.130	0.215	0.139	0.175	0.279	0.284	0.254
618	593	580	614	590	605	516	597	611	554	585	464	547
1.55	1.40	1.12	1.63	1.49	1.43	1.20	1.27	1.36	1.35	1.80	1.67	1.44
813	830	822	833	835	829	850	835	796	833	825	755	828
6.79	5.96	6.08	6.5	7.98	5.43	6.99	6.7	4.79	6.84	7.78	4.33	6.5

ME SOS-600M B	ME SOS-600M C	ME SOS-600M B										
39.77	39.72	40.15	39.29	39.21	39.69	39.00	39.29	38.85	39.37	39.46	39.40	39.56
1.34	1.48	1.33	1.50	1.34	1.45	1.43	1.44	1.36	1.41	1.39	1.49	1.40
15.23	15.00	14.81	15.56	15.04	15.39	15.27	15.75	17.16	15.47	15.42	15.56	15.11
14.45	14.48	14.27	14.56	15.13	14.44	14.69	14.75	14.76	14.21	14.43	14.25	14.63
0.23	0.17	0.33	0.13	0.17	0.23	0.34	0.26	0.28	0.16	0.26	0.21	0.22
14.71	14.65	14.49	14.39	14.56	14.23	14.38	14.31	13.37	14.56	14.25	14.84	14.90
0.12	0.09	0.29	0.09	0.16	0.08	0.32	0.12	0.30	0.14	0.18	0.10	0.01
		0.20	0.02	0.05	0.12	0.25		0.14	0.01	0.05	0.08	0.08
9.62	9.64	9.61	9.59	9.68	9.39	9.38	9.60	9.37	9.70	9.38	9.44	9.65
0.26	0.46	0.51	0.35	0.25	0.38	0.47	0.27	0.39	0.43	0.39	0.37	0.20
0.19				0.19		0.15	0.01			0.03		
	0.29		0.50	0.21	0.60	0.31	0.20		0.56	0.76	0.27	0.22
0.09	0.03	0.02	0.04		0.04	0.02	0.02	0.02	0.01	0.04	0.04	0.03
-0.02	-0.13	0.00	-0.22	-0.09	-0.26	-0.14	-0.09	0.00	-0.24	-0.33	-0.12	-0.10
96.00	96.00	96.00	96.02	96.00	96.03	96.01	96.02	96.00	96.03	96.03	96.04	96.01
5.856	5.862	5.907	5.812	5.813	5.865	5.782	5.799	5.717	5.821	5.845	5.801	5.839
2.144	2.138	2.093	2.188	2.187	2.135	2.218	2.201	2.283	2.179	2.155	2.199	2.161
0.499	0.472	0.476	0.525	0.442	0.545	0.450	0.540	0.693	0.516	0.537	0.502	0.468
0.149	0.164	0.148	0.167	0.150	0.161	0.159	0.160	0.151	0.157	0.155	0.165	0.156
0.030	0.054	0.059	0.040	0.029	0.045	0.055	0.031	0.046	0.051	0.046	0.044	0.024
1.779	1.787	1.755	1.802	1.876	1.784	1.821	1.820	1.816	1.757	1.788	1.754	1.806
0.029	0.022	0.041	0.017	0.022	0.029	0.042	0.032	0.035	0.020	0.033	0.026	0.028
3.228	3.223	3.177	3.173	3.219	3.134	3.178	3.149	2.934	3.210	3.146	3.258	3.278
0.023				0.023		0.018	0.001			0.003		
0.018	0.014	0.045	0.014	0.026	0.012	0.050	0.018	0.047	0.023	0.029	0.015	0.002
		0.058	0.006	0.014	0.033	0.072		0.041	0.003	0.014	0.022	0.022
1.807	1.814	1.803	1.809	1.830	1.770	1.773	1.807	1.759	1.829	1.772	1.772	1.816
19.562	19.550	19.562	19.552	19.630	19.513	19.619	19.559	19.521	19.565	19.524	19.559	19.598
3.978	3.857	3.995	3.756	3.902	3.710	3.850	3.902	3.995	3.736	3.634	3.864	3.890
	0.135		0.234	0.098	0.280	0.145	0.093		0.262	0.356	0.126	0.103
0.022	0.008	0.005	0.010		0.010	0.005	0.005	0.005	0.003	0.010	0.010	0.008
1.076	1.069	1.136	1.003	0.991	1.066	0.958	1.001	0.926	1.015	1.031	1.016	1.044
0.205	0.205	0.350	0.196	0.162	0.251	0.209	0.191	0.312	0.236	0.244	0.154	0.154
546	603	541	605	534	584	576	575	521	580	562	614	573
1.48	1.38	1.25	1.69	1.44	1.59	1.56	1.77	2.49	1.64	1.63	1.65	1.44
808	835	784	848	840	819	794	817	789	855	828	824	816
6.01	6.96	4.33	8.18	8.17	5.22	4.19	6.92	6.29	8.56	5.32	6.22	5.67

ME SOS-600M C	ME SOS-600M B	ME SOS-600M C	ME SOS-600M B	ME SOS-600N C	ME SOS-600N B	ME SOS-600N C	ME SOS-600N B	ME SOS-600N C	ME SOS-600N B	ME SOS-600N C	ME SOS-600N B	ME SOS-600N C
39.10	39.26	39.72	39.60	39.22	39.91	39.41	39.61	39.64	39.17	39.42	39.71	39.32
1.56	1.22	1.49	1.02	1.65	1.74	1.68	1.56	1.67	1.70	1.49	1.45	1.53
16.11	15.59	15.41	15.72	15.12	15.43	14.89	15.24	15.29	14.77	15.40	15.64	15.24
14.15	14.97	14.74	14.79	15.12	14.98	15.31	15.38	15.00	16.54	15.45	14.62	15.31
0.33	0.23	0.22	0.36	0.39	0.30	0.35	0.33	0.25	0.28	0.41	0.28	0.23
14.75	15.04	14.12	14.28	14.13	14.02	14.33	13.87	14.11	13.53	13.68	14.40	13.92
0.20	0.18	0.15	0.30	0.16	0.28	0.08	0.44	0.13	0.02	0.13	0.05	0.21
0.11		0.06	0.04	0.11	0.27	0.07	0.13	0.12		0.09	0.16	0.25
9.34	8.94	9.61	9.23	9.44	8.86	9.43	9.30	9.60	9.87	9.73	9.39	9.54
0.13	0.26	0.20	0.31	0.22	0.15	0.19	0.06	0.12	0.05	0.14	0.05	0.14
		0.20	0.11	0.01	0.07		0.02	0.05			0.02	
0.17	0.33	0.08	0.24	0.44		0.27				0.01	0.23	0.24
0.03		0.01	0.04	0.03	0.01	0.02	0.06	0.01	0.07	0.05	0.02	0.07
-0.08	-0.14	-0.04	-0.11	-0.19	0.00	-0.12	-0.01	0.00	-0.02	-0.02	-0.10	-0.12
95.98	96.02	96.00	96.03	96.04	96.00	96.02	95.99	95.99	95.99	96.00	96.01	96.00
5.752	5.787	5.855	5.840	5.819	5.860	5.837	5.851	5.846	5.837	5.837	5.845	5.831
2.248	2.213	2.145	2.160	2.181	2.140	2.163	2.149	2.154	2.163	2.163	2.155	2.169
0.544	0.495	0.533	0.572	0.464	0.530	0.437	0.504	0.504	0.433	0.525	0.559	0.494
0.173	0.135	0.165	0.113	0.184	0.192	0.187	0.173	0.185	0.190	0.166	0.160	0.170
0.016	0.030	0.023	0.036	0.026	0.018	0.022	0.007	0.013	0.006	0.017	0.006	0.017
1.741	1.845	1.817	1.825	1.876	1.839	1.897	1.900	1.849	2.062	1.913	1.800	1.899
0.041	0.029	0.028	0.046	0.049	0.037	0.043	0.041	0.031	0.035	0.052	0.035	0.029
3.233	3.305	3.104	3.140	3.126	3.068	3.165	3.055	3.102	3.005	3.020	3.160	3.077
		0.024	0.013	0.001	0.008		0.002	0.006			0.002	
0.032	0.029	0.024	0.047	0.026	0.044	0.012	0.070	0.021	0.003	0.021	0.008	0.034
0.030		0.016	0.011	0.030	0.077	0.019	0.038	0.036		0.025	0.047	0.072
1.753	1.680	1.807	1.735	1.786	1.660	1.781	1.753	1.806	1.876	1.839	1.763	1.805
19.562	19.549	19.541	19.537	19.569	19.472	19.565	19.542	19.554	19.610	19.577	19.539	19.597
3.913	3.846	3.960	3.878	3.786	3.998	3.868	3.985	3.998	3.982	3.983	3.888	3.870
0.079	0.154	0.037	0.112	0.206		0.126				0.005	0.107	0.113
0.007		0.002	0.010	0.008	0.002	0.005	0.015	0.002	0.018	0.013	0.005	0.018
0.966	0.995	1.068	1.050	0.993	1.095	1.023	1.053	1.056	0.990	1.024	1.065	1.010
0.141	0.045	0.254	0.257	0.159	0.207	0.109	0.261	0.221	0.141	0.254	0.210	0.255
643	485	590	366	649	673	659	601	654	632	571	582	594
1.93	1.68	1.58	1.75	1.48	1.56	1.35	1.51	1.52	1.33	1.61	1.69	1.54
806	830	814	790	804	777	805	775	796	792	783	801	794
5.29	6.89	6.89	5.06	3.77	4.73	3.9	4.19	6.06	5.56	4.2	5.49	5.04

ME SOS-600N B	ME SOS-600N C	ME SOS-600N B										
39.49	39.52	40.61	38.97	38.73	39.29	37.88	39.55	39.71	39.24	39.24	39.12	39.48
1.50	1.54	1.62	1.52	1.65	1.55	1.61	1.58	1.62	1.70	1.70	1.51	1.44
15.12	15.12	16.68	15.08	14.81	15.14	14.93	15.09	15.67	15.15	15.15	15.17	15.39
15.22	15.35	13.59	15.95	16.74	15.34	17.48	15.72	14.64	15.42	15.42	15.83	15.40
0.36	0.32	0.12	0.36	0.37	0.35	0.35	0.33	0.25	0.40	0.40	0.27	0.36
14.04	13.90	14.27	13.48	13.21	13.92	12.81	13.88	13.98	13.98	13.98	13.85	13.77
	0.10	0.12	0.21	0.02		0.15	0.14	0.20	0.20	0.20	0.23	0.07
0.02	0.12	0.06	0.22	0.01	0.31	0.21	0.15	0.02	0.08	0.08	0.16	0.06
9.69	9.35	8.67	9.61	10.20	9.55	10.40	9.47	9.48	9.61	9.61	9.66	9.78
0.12	0.09	0.09	0.04	0.14	0.17	0.12	0.06	0.07	0.07	0.07		0.12
0.13		0.06	0.04	0.03	0.03			0.04				0.09
0.29	0.60	0.08	0.52		0.30			0.26	0.14	0.37	0.19	
0.04	0.02	0.05	0.03	0.08	0.08	0.05	0.03	0.08		0.03	0.03	0.05
-0.13	-0.26	-0.04	-0.23	-0.02	-0.14	-0.01	-0.01	-0.13	-0.06	-0.16	-0.09	-0.01
96.02	96.02	96.01	96.02	95.99	96.02	95.99	96.00	96.01	95.99	96.25	96.02	96.00
5.855	5.867	5.887	5.821	5.801	5.834	5.719	5.852	5.853	5.818	5.818	5.815	5.845
2.145	2.133	2.113	2.179	2.199	2.166	2.281	2.148	2.147	2.182	2.182	2.185	2.155
0.498	0.512	0.739	0.477	0.417	0.484	0.375	0.484	0.576	0.465	0.465	0.472	0.530
0.167	0.171	0.177	0.170	0.186	0.173	0.183	0.176	0.180	0.189	0.189	0.168	0.160
0.015	0.010	0.010	0.005	0.017	0.020	0.015	0.007	0.008	0.008	0.008		0.013
1.887	1.906	1.648	1.992	2.098	1.905	2.207	1.945	1.805	1.912	1.912	1.968	1.906
0.045	0.040	0.014	0.046	0.048	0.043	0.044	0.041	0.031	0.051	0.051	0.034	0.046
3.104	3.076	3.083	3.002	2.950	3.081	2.882	3.062	3.072	3.089	3.089	3.070	3.038
0.016		0.007	0.005	0.003	0.003			0.005				0.010
	0.015	0.018	0.034	0.003		0.025	0.023	0.032	0.032	0.032	0.037	0.011
0.006	0.036	0.016	0.064	0.003	0.088	0.062	0.044	0.005	0.022	0.022	0.047	0.017
1.832	1.770	1.603	1.831	1.948	1.809	2.002	1.786	1.783	1.817	1.817	1.831	1.847
19.568	19.537	19.315	19.626	19.672	19.607	19.795	19.568	19.496	19.585	19.585	19.627	19.578
3.854	3.713	3.951	3.747	3.980	3.839	3.987	3.992	3.859	3.934	3.819	3.903	3.987
0.136	0.282	0.037	0.246		0.141			0.121	0.066	0.173	0.089	
0.010	0.005	0.012	0.008	0.020	0.020	0.013	0.008	0.020		0.008	0.008	0.013
1.038	1.044	1.193	0.959	0.922	1.007	0.787	1.045	1.067	0.997	0.997	0.979	1.035
0.184	0.202	0.260	0.237	0.172	0.211	0.198	0.196	0.258	0.174	0.174	0.213	0.244
587	597	658	575	609	602	581	607	640	657	657	577	553
1.48	1.49	2.11	1.52	1.39	1.50	1.52	1.44	1.72	1.49	1.49	1.52	1.61
798	811	818	801	806	786	801	775	816	811	805	795	787
4.19	4.32	6.31	4.24	7.06	3.46	7.57	4.01	6.63	4.99	4.15	5.35	4.51

ME SOS-600N C	ME SOS-600N B	ME SOS-600O C										
39.72	39.73	39.74	39.40	39.21	39.35	38.88	39.30	39.48	39.19	39.00	39.13	38.98
1.51	1.41	1.56	1.56	1.62	1.62	1.45	1.59	1.37	1.44	1.56	1.49	1.63
15.24	15.36	14.78	15.48	15.27	14.91	15.05	15.17	15.40	15.35	14.72	14.91	14.69
15.31	14.76	15.47	15.43	15.62	15.74	16.08	15.32	15.66	15.11	16.42	16.69	16.13
0.41	0.20	0.43	0.30	0.33	0.23	0.41	0.36	0.30	0.40	0.41	0.29	0.29
14.11	14.37	14.07	13.89	13.75	13.94	13.53	13.80	13.55	13.64	13.43	13.32	13.82
0.03	0.19	0.17	0.15	0.13	0.11	0.11	0.28	0.12	0.32	0.54	0.18	
0.22	0.56	0.03	0.05	0.11	0.09	0.16	0.19	0.07	0.23	0.18	0.11	
9.40	9.24	9.72	9.50	9.51	9.69	9.64	9.59	9.50	9.47	9.21	9.59	9.60
0.04	0.14	0.05	0.09	0.03	0.10	0.65	0.19	0.39	0.17	0.04	0.06	0.12
95.98	96.00	96.00	96.00	96.01	95.99	96.03	96.01	96.03	96.01	96.04	95.98	95.92
5.860	5.847	5.881	5.825	5.825	5.841	5.821	5.829	5.859	5.837	5.831	5.835	5.826
2.140	2.153	2.119	2.175	2.175	2.159	2.179	2.171	2.141	2.163	2.169	2.165	2.174
0.510	0.512	0.460	0.523	0.500	0.450	0.478	0.481	0.553	0.531	0.424	0.455	0.414
0.167	0.156	0.174	0.173	0.181	0.181	0.163	0.178	0.153	0.161	0.175	0.167	0.183
0.017			0.012		0.017		0.021		0.020	0.005	0.007	0.014
1.890	1.817	1.914	1.907	1.941	1.954	2.014	1.901	1.943	1.882	2.052	2.082	2.016
0.052	0.025	0.054	0.037	0.041	0.029	0.052	0.046	0.037	0.051	0.052	0.036	0.036
3.104	3.153	3.104	3.061	3.045	3.084	3.019	3.050	2.996	3.029	2.993	2.962	3.080
0.005			0.006	0.010	0.003		0.001		0.010		0.009	
0.005	0.030	0.027	0.024	0.021	0.017	0.017	0.044	0.018	0.051	0.086	0.029	
0.063	0.159	0.008	0.014	0.030	0.025	0.047	0.055	0.019	0.067	0.053	0.031	
1.769	1.734	1.835	1.792	1.803	1.834	1.841	1.814	1.799	1.798	1.756	1.824	1.830
19.564	19.602	19.577	19.550	19.573	19.595	19.631	19.591	19.540	19.585	19.598	19.609	19.595
4.000	3.993	3.997	3.977	3.839	3.943	3.674	3.906	3.812	3.662	3.759	3.980	3.764
				0.146	0.047	0.308	0.089	0.183	0.325	0.236		0.236
	0.007	0.003	0.023	0.015	0.010	0.018	0.005	0.005	0.013	0.005	0.020	
1.069	1.069	1.077	1.020	0.993	1.016	0.947	1.007	1.037	0.992	0.966	0.984	0.961
0.189	0.293	0.214	0.192	0.180	0.179	0.198	0.258	0.256	0.302	0.217	0.194	0.093
587	562	608	601	622	623	548	617	518	560	581	547	622
1.50	1.54	1.28	1.65	1.57	1.37	1.52	1.50	1.63	1.64	1.33	1.41	1.31
789	781	793	785	795	799	805	790	807	807	795	770	827
3.74	4.88	4.37	5.15	4.32	4.91	3.53	3.99	5.59	4.07	3.89	4.29	5.94

ME SOS-6000 I	ME SOS-6000 B	ME SOS-6000 C	ME SOS-6000 B										
38.88	38.98	39.26	39.46	39.17	39.55	39.55	39.07	39.17	40.03	39.17	39.55	39.94	
1.73	1.73	1.54	1.34	1.54	1.63	1.25	1.54	1.15	1.63	2.21	2.30	2.30	
15.26	14.98	14.88	14.59	15.55	15.55	15.46	15.55	14.59	15.46	15.65	14.59	14.78	
16.03	15.84	15.46	15.46	15.17	15.07	15.55	15.55	16.22	15.17	15.17	15.74	14.98	
0.38	0.19	0.19	0.38	0.38	0.38	0.38	0.38	0.29	0.29	0.48	0.19	0.48	
13.63	13.63	13.92	14.30	14.11	13.82	13.82	13.63	14.40	13.92	12.86	13.92	14.30	
9.60	9.60	9.60	9.50	9.50	9.89	9.60	9.70	9.41	9.41	9.50	9.41	9.02	
0.38	0.29	0.58	0.77		0.10	0.29	0.10		0.19				
		0.50		0.50		0.10				1.00	0.40	0.20	
0.10				0.10					0.10	0.10	0.10	0.10	
-0.02		-0.21		-0.23		-0.04			-0.02	-0.44	-0.19	-0.11	
96.00	95.23	95.92	95.81	96.02	96.00	96.00	95.52	95.23	96.20	96.14	96.21	96.11	
5.780	5.824	5.845	5.854	5.812	5.839	5.851	5.812	5.856	5.881	5.836	5.862	5.877	
2.220	2.176	2.155	2.146	2.188	2.161	2.149	2.188	2.144	2.119	2.164	2.138	2.123	
0.455	0.462	0.456	0.406	0.533	0.546	0.546	0.539	0.428	0.557	0.584	0.411	0.442	
0.193	0.194	0.172	0.150	0.171	0.181	0.139	0.172	0.130	0.180	0.247	0.257	0.255	
0.045	0.034	0.068	0.090		0.011	0.034	0.011		0.022				
1.993	1.980	1.924	1.918	1.882	1.861	1.924	1.935	2.029	1.864	1.890	1.951	1.843	
0.048	0.024	0.024	0.048	0.048	0.048	0.048	0.048	0.036	0.036	0.061	0.024	0.060	
3.021	3.037	3.089	3.164	3.122	3.042	3.049	3.023	3.209	3.048	2.857	3.075	3.138	
1.820	1.830	1.823	1.799	1.799	1.862	1.812	1.840	1.794	1.763	1.806	1.778	1.694	
19.577	19.561	19.555	19.574	19.556	19.552	19.551	19.567	19.626	19.471	19.446	19.496	19.432	
3.975	4.000	3.765	4.000	3.740	4.000	3.953	4.000	4.000	3.975	3.504	3.787	3.882	
		0.235		0.235		0.047				0.471	0.187	0.093	
0.025				0.025					0.025	0.025	0.025	0.025	
0.940	0.961	1.004	1.033	0.986	1.043	1.045	0.972	0.993	1.116	0.990	1.047	1.102	
0.090	0.134	0.171	0.133	0.129	0.231	0.217	0.180	0.070	0.200	0.202	0.045	0.012	
651	657	597	523	605	634	466	589	425	631	798	831	848	
1.57	1.46	1.38	1.20	1.71	1.67	1.64	1.73	1.26	1.58	1.80	1.19	1.24	
779	811	839	789	806	815	802	801	793	781	846	833	796	
3.99	7.6	7.66	4.27	4.72	6.75	5.5	5.4	5	5.42	4.77	5.17	3.34	

ME SOS-6000 C	ME SOS-6000 B												
39.10	39.62	39.03	39.01	39.09	39.43	39.49	39.24	39.36	39.29	39.27	39.02	39.35	
1.63	1.90	1.55	1.70	1.72	1.79	1.54	1.50	1.69	1.37	1.77	1.52	1.49	
15.11	16.06	15.37	15.74	15.34	15.35	15.26	15.51	15.64	15.62	15.62	15.91	15.84	
15.06	14.17	15.46	14.58	15.43	14.91	15.54	15.32	14.97	15.08	14.83	15.19	14.80	
0.29	0.17	0.22	0.43	0.26	0.35	0.12	0.25	0.29	0.32	0.29	0.18	0.33	
14.02	13.42	13.85	14.09	13.82	13.73	14.06	14.08	13.85	14.05	13.86	13.88	14.07	
0.07	0.14	0.09	0.20	0.10	0.18	0.14	0.14	0.21	0.11	0.31	0.30	0.30	
0.28	0.57	0.29	0.19	0.43	0.49	0.23	0.20	0.33	0.25	0.40	0.36	0.21	
9.67	9.49	9.43	9.47	9.69	9.64	9.57	9.48	9.62	9.41	9.40	9.27	9.53	
0.12	0.05		0.02		0.06	0.01	0.08	0.05	0.10	0.17	0.14	0.08	
0.07	0.05	0.04	0.18		0.07	0.01			0.02	0.02	0.07		
0.61	0.35	0.65					0.15		0.39		0.05		
	0.02	0.07	0.02	0.13	0.03	0.01	0.06	0.01	0.02	0.06	0.10		
-0.26	-0.15	-0.29	0.00	-0.03	-0.01	0.00	-0.08	0.00	-0.17	-0.01	-0.04		
96.01	96.01	96.04	95.65	96.01	96.01	96.00	96.02	96.01	96.03	96.00	96.00	96.00	
5.820	5.836	5.812	5.776	5.798	5.828	5.837	5.807	5.809	5.818	5.796	5.769	5.799	
2.180	2.164	2.188	2.224	2.202	2.172	2.163	2.193	2.191	2.182	2.204	2.231	2.201	
0.471	0.625	0.510	0.523	0.480	0.502	0.496	0.513	0.530	0.544	0.513	0.541	0.551	
0.183	0.211	0.173	0.189	0.192	0.198	0.171	0.167	0.188	0.153	0.196	0.169	0.165	
0.014	0.006		0.002		0.007	0.001	0.009	0.006	0.011	0.020	0.017	0.009	
1.875	1.746	1.925	1.806	1.914	1.843	1.921	1.896	1.847	1.868	1.831	1.878	1.825	
0.036	0.022	0.028	0.054	0.033	0.043	0.016	0.031	0.036	0.040	0.036	0.023	0.041	
3.110	2.947	3.075	3.110	3.057	3.025	3.099	3.107	3.048	3.102	3.050	3.059	3.092	
0.008	0.006	0.005	0.022		0.008	0.001			0.002	0.002	0.008		
0.011	0.023	0.014	0.032	0.015	0.029	0.023	0.023	0.033	0.017	0.049	0.047	0.047	
0.080	0.162	0.083	0.055	0.124	0.140	0.066	0.058	0.093	0.072	0.115	0.105	0.060	
1.835	1.784	1.791	1.787	1.833	1.817	1.804	1.788	1.811	1.777	1.769	1.749	1.792	
19.623	19.529	19.603	19.581	19.647	19.612	19.597	19.592	19.592	19.585	19.581	19.595	19.582	
3.713	3.832	3.676	3.995	3.967	3.992	3.997	3.915	3.997	3.812	3.985	3.952	4.000	
0.287	0.163	0.306					0.070		0.183		0.023		
	0.005	0.018	0.005	0.033	0.008	0.003	0.015	0.003	0.005	0.015	0.025		
0.978	1.052	0.967	0.958	0.973	1.024	1.035	0.995	1.012	1.004	0.998	0.958	1.009	
0.216	0.407	0.200	0.187	0.238	0.313	0.223	0.198	0.282	0.228	0.278	0.245	0.273	
642	732	600	674	661	689	594	584	657	537	686	590	588	
1.50	1.92	1.64	1.79	1.60	1.57	1.53	1.67	1.71	1.73	1.70	1.87	1.81	
834	819	819	786	774	777	802	791	793	801	778	789	808	
6.07	7.4	5.18	3.8	5	4.07	7.17	5.07	6.01	4.89	5.05	6.49	6.15	

ME SOS-6000 C	ME SOS-6000 B	ME SOS-6000 C										
38.94	39.32	39.29	39.40	39.68	39.07	39.40	38.91	38.52	39.25	39.26	39.34	39.08
1.56	1.53	1.55	1.37	1.25	1.55	1.37	1.51	1.24	1.17	1.59	1.51	1.58
15.22	15.25	15.40	15.09	15.00	15.16	15.52	15.23	15.63	16.14	15.32	15.50	15.36
15.01	15.23	15.27	15.15	15.30	15.34	15.24	15.32	15.23	14.52	15.38	15.18	15.50
0.33	0.27	0.29	0.28	0.33	0.37	0.32	0.31	0.39	0.37	0.30	0.26	0.33
13.99	14.11	14.21	14.23	14.40	14.17	13.94	14.17	14.07	14.28	14.12	14.12	13.80
0.19	0.20	0.15	0.22	0.16	0.14	0.06	0.13	0.13	0.34	0.12	0.08	0.24
0.51	0.14	0.21	0.17	0.14		0.23	0.36	0.39	0.36	0.32	0.24	0.38
9.51	9.75	9.48	9.50	9.53	9.72	9.47	9.73	9.59	9.39	9.53	9.43	9.52
0.05	0.15	0.07	0.13	0.18	0.08	0.24	0.06	0.12	0.05	0.04	0.08	0.09
0.01		0.08	0.05		0.07	0.17	0.07	0.01				0.07
0.69			0.35		0.31	0.06	0.14		0.13		0.28	
0.02	0.05		0.07	0.02	0.04		0.08	0.05		0.02		0.05
-0.30	-0.01		-0.16	0.00	-0.14	-0.03	-0.08	-0.01	-0.05	0.00	-0.12	-0.01
96.03	96.01	95.99	96.02	95.99	96.01	96.01	96.01	95.38	96.00	96.00	96.01	96.00
5.802	5.819	5.806	5.844	5.863	5.807	5.823	5.783	5.751	5.784	5.808	5.819	5.795
2.198	2.181	2.194	2.156	2.137	2.193	2.177	2.217	2.249	2.216	2.192	2.181	2.205
0.474	0.480	0.488	0.482	0.474	0.462	0.528	0.450	0.501	0.587	0.479	0.522	0.479
0.175	0.170	0.172	0.153	0.139	0.173	0.153	0.168	0.139	0.130	0.177	0.168	0.177
0.006	0.018	0.008	0.016	0.021	0.009	0.028	0.007	0.014	0.006	0.004	0.009	0.010
1.871	1.884	1.887	1.879	1.891	1.907	1.883	1.905	1.901	1.790	1.902	1.877	1.923
0.041	0.034	0.036	0.035	0.041	0.047	0.040	0.039	0.050	0.047	0.037	0.032	0.041
3.107	3.113	3.130	3.146	3.172	3.139	3.071	3.139	3.132	3.136	3.114	3.114	3.049
0.001		0.009	0.006		0.008	0.021	0.008	0.001				0.008
0.031	0.032	0.024	0.035	0.026	0.023	0.009	0.021	0.021	0.053	0.018	0.012	0.038
0.147	0.041	0.061	0.050	0.041		0.066	0.102	0.114	0.101	0.091	0.069	0.110
1.808	1.841	1.786	1.798	1.797	1.842	1.785	1.845	1.826	1.765	1.799	1.779	1.801
19.661	19.613	19.601	19.600	19.601	19.609	19.583	19.685	19.698	19.615	19.622	19.581	19.637
3.670	3.987	4.000	3.818	3.995	3.844	3.972	3.914	3.987	3.939	3.995	3.869	3.987
0.325			0.164		0.146	0.028	0.066		0.061		0.131	
0.005	0.013		0.018	0.005	0.010		0.020	0.013		0.005		0.013
0.952	1.008	1.002	1.023	1.064	0.971	1.019	0.945	0.885	0.993	0.998	1.011	0.971
0.266	0.235	0.176	0.232	0.221	0.148	0.222	0.206	0.222	0.312	0.194	0.198	0.243
618	598	606	540	482	607	531	592	478	455	621	591	610
1.57	1.53	1.60	1.46	1.38	1.52	1.66	1.55	1.80	1.96	1.56	1.66	1.60
817	789	802	798	780	808	804	795	776	809	779	819	774
4.63	5.05	5.75	4.44	4.21	4.62	5.73	4.6	4.32	5.09	4.83	6.2	4.5

ME SOS-6000 B	ME SOS-6000 C	ME SOS-6000 B										
38.98	39.26	38.31	39.23	38.97	39.33	38.44	39.28	39.35	39.18	39.72	39.23	37.49
1.66	1.58	1.56	1.53	1.62	1.64	1.29	1.67	1.72	1.40	1.12	1.67	1.76
15.25	15.28	17.67	16.12	15.49	14.73	17.04	15.24	15.10	15.97	15.21	15.29	15.01
15.04	15.35	14.29	15.17	15.83	15.58	14.48	15.18	15.28	15.21	15.03	14.48	17.33
0.30	0.17	0.21	0.26	0.22	0.27	0.23	0.24	0.36	0.28	0.24	0.36	0.35
14.21	14.04	12.95	13.57	13.80	14.05	13.90	13.62	13.68	13.71	14.13	14.43	12.88
0.21	0.18	0.20	0.17	0.17		0.57	0.02	0.36		0.18	0.05	0.16
0.23	0.32	0.72	0.09	0.15	0.14	0.85	0.22	0.12	0.36	0.36	0.36	0.26
9.43	9.69	9.33	9.72	9.36	9.49	9.02	9.67	9.45	9.71	9.53	9.76	10.10
0.22	0.11	0.12	0.06	0.09	0.07	0.09	0.24	0.23	0.10	0.11	0.06	0.16
0.11		0.25	0.04		0.12		0.15		0.08		0.04	
0.33		0.34		0.28	0.58	0.06	0.49	0.31	0.01	0.33	0.30	0.42
0.04	0.02	0.05	0.06		0.03	0.02		0.05		0.05		0.09
-0.15	0.00	-0.15	-0.01	-0.12	-0.25	-0.03	-0.21	-0.14	0.00	-0.15	-0.13	-0.20
96.01	96.01	96.01	96.01	95.99	96.03	95.98	96.02	96.02	95.99	96.01	96.01	96.01
5.784	5.811	5.663	5.793	5.785	5.857	5.666	5.838	5.838	5.792	5.880	5.806	5.679
2.216	2.189	2.337	2.207	2.215	2.143	2.334	2.162	2.162	2.208	2.120	2.194	2.321
0.453	0.477	0.741	0.599	0.497	0.441	0.626	0.507	0.479	0.576	0.534	0.474	0.361
0.185	0.176	0.173	0.170	0.181	0.184	0.143	0.187	0.192	0.156	0.125	0.186	0.200
0.026	0.012	0.013	0.007	0.010	0.008	0.010	0.028	0.027	0.011	0.012	0.007	0.020
1.867	1.900	1.767	1.874	1.966	1.940	1.785	1.887	1.896	1.880	1.862	1.792	2.196
0.037	0.022	0.026	0.032	0.028	0.034	0.029	0.030	0.046	0.035	0.030	0.045	0.044
3.143	3.098	2.853	2.989	3.055	3.120	3.054	3.018	3.026	3.021	3.119	3.183	2.910
0.013		0.030	0.005		0.014		0.018		0.009		0.005	
0.034	0.029	0.032	0.027	0.027		0.089	0.003	0.058		0.029	0.008	0.026
0.066	0.091	0.206	0.025	0.044	0.042	0.244	0.064	0.036	0.102	0.102	0.102	0.076
1.785	1.828	1.759	1.832	1.773	1.803	1.697	1.833	1.788	1.830	1.800	1.843	1.952
19.609	19.634	19.601	19.559	19.581	19.586	19.677	19.575	19.548	19.621	19.613	19.644	19.784
3.835	3.995	3.829	3.985	3.869	3.719	3.967	3.770	3.842	3.995	3.833	3.860	3.776
0.155		0.159		0.131	0.273	0.028	0.230	0.145	0.005	0.155	0.140	0.201
0.010	0.005	0.013	0.015		0.008	0.005		0.013		0.013		0.023
0.954	0.999	0.842	0.990	0.953	1.016	0.860	1.006	1.015	0.984	1.073	0.993	0.723
0.162	0.247	0.399	0.278	0.147	0.135	0.375	0.247	0.254	0.278	0.344	0.220	0.126
655	617	602	587	619	637	504	645	660	539	420	673	638
1.56	1.55	2.80	1.97	1.69	1.30	2.44	1.56	1.47	1.90	1.51	1.55	1.59
803	790	794	795	823	814	788	832	795	804	794	819	824
4.35	6.27	6.36	6.11	6.96	4.03	6.57	6.85	4.19	7.16	5.08	5.48	6.77

ME SOS-6000 C	ME SOS-6000 B	ME SOS-6000 B	ME SOS-6000 C										
38.86	38.62	38.66	38.51	38.59	39.13	39.57	39.10	39.06	39.32	39.32	39.05	39.29	
1.42	1.31	1.70	1.67	1.63	1.33	1.51	1.50	1.66	1.57	1.42	1.50	1.49	
15.63	16.50	15.56	15.06	15.30	15.03	15.48	15.03	15.25	15.44	15.31	15.89	15.34	
15.80	16.30	16.59	17.05	16.25	15.50	15.13	15.10	15.36	14.91	15.34	14.75	15.19	
0.35	0.22	0.19	0.38	0.27	0.27	0.16	0.39	0.24	0.41	0.30	0.27	0.31	
13.89	13.33	13.65	13.54	13.90	13.83	13.70	14.39	13.99	14.45	14.11	14.62	14.24	
0.07	0.24	0.16	0.10	0.09	0.23	0.07	0.25	0.13	0.11	0.24	0.12	0.24	
0.24	0.47	0.16	0.14	0.26	0.32	0.35	0.21	0.35	0.11	0.23	0.12		
9.65	8.76	9.22	9.33	9.51	9.56	9.67	9.36	9.65	9.54	9.64	9.47	9.70	
0.03	0.08	0.12	0.11	0.08	0.27	0.29	0.22	0.13	0.14	0.04	0.22		
0.03	0.11		0.01		0.01			0.04		0.04	0.04	0.01	
0.43	0.06		0.07		0.47	0.05	0.41	0.15			0.08		
0.04	0.02		0.05	0.12	0.05	0.04	0.04		0.02	0.04		0.06	
-0.19	-0.03		-0.04	-0.03	-0.21	-0.03	-0.18	-0.06	0.00	-0.01	-0.03	-0.01	
96.43	96.02	96.01	96.01	96.00	96.01	96.01	96.01	96.02	96.02	95.99	96.00	95.98	
5.768	5.719	5.742	5.753	5.747	5.831	5.846	5.806	5.794	5.801	5.820	5.756	5.813	
2.232	2.281	2.258	2.247	2.253	2.169	2.154	2.194	2.206	2.199	2.180	2.244	2.187	
0.502	0.600	0.466	0.406	0.433	0.471	0.543	0.438	0.461	0.485	0.491	0.516	0.489	
0.159	0.145	0.190	0.188	0.183	0.150	0.167	0.167	0.185	0.175	0.158	0.166	0.166	
0.003	0.009	0.014	0.012	0.009	0.032	0.034	0.026	0.016	0.017	0.004	0.026		
1.961	2.019	2.061	2.130	2.024	1.932	1.869	1.875	1.905	1.839	1.899	1.818	1.879	
0.043	0.028	0.024	0.049	0.034	0.034	0.020	0.050	0.030	0.052	0.037	0.034	0.038	
3.074	2.944	3.022	3.015	3.086	3.073	3.017	3.185	3.093	3.177	3.114	3.212	3.140	
0.003	0.013		0.001		0.001			0.005			0.005	0.001	
0.011	0.038	0.026	0.015	0.014	0.037	0.011	0.040	0.021	0.017	0.038	0.020	0.038	
0.069	0.135	0.047	0.042	0.075	0.092	0.099	0.061	0.099	0.030	0.066		0.036	
1.827	1.656	1.746	1.778	1.807	1.817	1.822	1.773	1.825	1.796	1.820	1.779	1.830	
19.652	19.586	19.596	19.637	19.664	19.638	19.582	19.615	19.642	19.587	19.627	19.575	19.616	
3.788	3.967	4.000	3.954	3.970	3.766	3.967	3.797	3.930	3.995	3.990	3.963	3.985	
0.202	0.028		0.033		0.221	0.023	0.193	0.070			0.037		
0.010	0.005		0.013	0.030	0.013	0.010	0.010		0.005	0.010		0.015	
0.935	0.894	0.903	0.883	0.894	0.983	1.047	0.975	0.968	1.005	1.008	0.960	1.003	
0.171	0.175	0.060	0.020	0.088	0.282	0.325	0.164	0.213	0.145	0.247	0.104	0.217	
542	471	632	616	619	512	583	597	645	627	553	604	586	
1.75	2.20	1.72	1.51	1.61	1.47	1.64	1.44	1.55	1.60	1.56	1.83	1.58	
800	780	807	774	771	800	791	794	815	786	778	839	784	
4.63	5.44	7.26	3.32	4.61	4.8	6.46	3.13	6.54	3.87	4.6	7.56	4.8	

ME SOS-600O B	ME SOS-600O C	ME SOS-600P C										
39.11	39.37	39.22	39.28	39.38	39.61	39.54	39.38	39.14	39.26	38.74	38.58	40.05
1.46	1.19	1.30	1.64	1.35	1.48	1.32	1.47	1.29	1.26	1.67	1.37	1.46
15.23	15.11	15.00	14.95	14.95	15.70	15.28	15.34	15.27	15.26	15.16	15.91	15.59
15.60	15.24	15.29	15.48	15.09	14.60	14.57	15.11	15.33	15.06	15.75	15.51	13.87
0.15	0.30	0.39	0.23	0.31	0.27	0.30	0.19	0.22	0.31	0.36	0.31	0.34
13.87	14.56	14.47	14.48	14.55	14.04	14.47	14.11	14.49	14.06	14.22	13.58	14.83
0.10	0.10	0.18	0.01	0.19	0.14	0.11	0.10	0.11	0.16	0.19	0.15	0.12
0.09	0.01	0.08	0.28	0.38	0.34	0.20	0.26	0.33	0.22	0.36	0.49	0.34
9.49	9.56	9.42	9.50	9.56	9.51	9.53	9.62	9.64	9.49	9.45	9.34	9.29
												0.01
0.28	0.04	0.09	0.09	0.14	0.23	0.19	0.12	0.07	0.12	0.08	0.20	0.04
0.12			0.05		0.03	0.03	0.09				0.10	0.04
0.47	0.51	0.54			0.48	0.16	0.08	0.76			0.38	
0.05	0.04	0.08	0.01	0.09	0.05		0.06	0.07	0.05	0.03	0.07	0.01
-0.21	-0.22	-0.25	0.00	-0.02	-0.01	-0.20	-0.08	-0.05	-0.33	-0.01	-0.18	0.00
96.02	96.02	96.04	95.99	96.00	96.00	96.02	96.01	96.03	96.03	95.99	96.00	95.98
5.819	5.844	5.831	5.813	5.828	5.832	5.849	5.829	5.799	5.844	5.753	5.745	5.862
2.181	2.156	2.169	2.187	2.172	2.168	2.151	2.171	2.201	2.156	2.247	2.255	2.138
0.489	0.488	0.459	0.421	0.436	0.556	0.514	0.505	0.467	0.521	0.407	0.537	0.551
0.163	0.133	0.145	0.183	0.151	0.164	0.146	0.164	0.143	0.141	0.187	0.154	0.161
0.033	0.005	0.010	0.010	0.017	0.027	0.022	0.015	0.008	0.015	0.009	0.024	0.004
1.941	1.891	1.902	1.915	1.868	1.798	1.803	1.870	1.900	1.875	1.957	1.932	1.698
0.019	0.037	0.050	0.029	0.039	0.034	0.037	0.024	0.028	0.039	0.045	0.039	0.042
3.077	3.223	3.207	3.194	3.211	3.083	3.190	3.114	3.200	3.120	3.148	3.015	3.236
0.015			0.006		0.003	0.003	0.010				0.011	0.005
0.015	0.015	0.029	0.002	0.030	0.023	0.017	0.015	0.017	0.026	0.031	0.025	0.018
0.025	0.003	0.022	0.080	0.110	0.096	0.058	0.074	0.094	0.064	0.102	0.141	0.095
1.802	1.810	1.786	1.794	1.805	1.787	1.799	1.816	1.822	1.802	1.790	1.774	1.735
												0.001
19.580	19.605	19.609	19.632	19.666	19.570	19.589	19.608	19.677	19.603	19.675	19.651	19.546
3.766	3.751	3.726	3.997	3.977	3.988	3.775	3.910	3.945	3.630	3.992	3.803	3.998
0.221	0.239	0.254				0.225	0.075	0.037	0.358			0.179
0.013	0.010	0.020	0.003	0.023	0.012		0.015	0.018	0.013	0.008	0.018	0.002
0.979	1.019	0.995	1.002	1.018	1.050	1.044	1.018	0.979	1.004	0.916	0.893	1.115
0.178	0.161	0.149	0.108	0.230	0.306	0.246	0.241	0.199	0.266	0.110	0.241	0.255
563	461	509	644	538	587	529	577	502	488	646	523	606
1.56	1.48	1.43	1.37	1.37	1.72	1.54	1.58	1.55	1.58	1.51	1.93	1.62
823	817	806	784	778	781	822	798	795	810	775	793	788
6.83	5.23	3.8	4.84	3.79	5.93	5.77	5.64	4.8	4.33	3.8	5.55	5.11

| ME
SOS-600P
I |
|---------------------|---------------------|---------------------|---------------------|---------------------|---------------------|---------------------|---------------------|---------------------|---------------------|---------------------|---------------------|---------------------|
| 39.81 | 39.35 | 39.71 | 39.27 | 39.53 | 38.85 | 39.55 | 38.62 | 39.54 | 39.88 | 39.56 | 39.58 | 39.74 |
| 1.34 | 1.55 | 1.53 | 1.52 | 1.39 | 1.56 | 1.35 | 1.25 | 1.36 | 1.35 | 1.45 | 1.55 | 1.48 |
| 15.48 | 14.94 | 15.17 | 15.53 | 15.35 | 15.58 | 15.19 | 15.30 | 15.99 | 14.90 | 15.59 | 15.23 | 15.40 |
| 14.52 | 15.41 | 15.00 | 15.02 | 15.23 | 14.52 | 15.22 | 16.90 | 14.07 | 14.70 | 14.47 | 14.69 | 15.04 |
| 0.23 | 0.34 | 0.30 | 0.32 | 0.43 | 0.41 | 0.38 | 0.36 | 0.23 | 0.39 | 0.18 | 0.44 | 0.33 |
| 14.44 | 13.95 | 14.48 | 14.42 | 14.52 | 14.63 | 14.76 | 14.94 | 14.88 | 14.37 | 14.37 | 14.32 | 14.27 |
| 0.05 | 0.24 | 0.27 | 0.12 | 0.22 | 0.44 | 0.24 | 0.28 | 0.23 | 0.11 | 0.18 | 0.17 | 0.11 |
| 0.23 | 0.34 | 0.30 | 0.32 | 0.43 | 0.41 | 0.38 | 0.36 | 0.23 | 0.39 | 0.18 | 0.44 | 0.33 |
| 9.62 | 9.67 | 9.15 | 9.48 | 9.17 | 9.00 | 8.97 | 8.00 | 9.03 | 9.60 | 9.34 | 9.46 | 9.28 |
| 0.08 | | | | | | | 0.14 | | | 0.06 | | 0.14 |
| | 0.09 | 0.03 | 0.08 | | | 0.04 | | 0.03 | 0.08 | 0.02 | 0.18 | 0.07 |
| | | 0.12 | | | 0.05 | 0.01 | 0.10 | 0.10 | 0.09 | | 0.04 | |
| | | 0.20 | | | 0.63 | | | 0.27 | | 0.42 | | 0.01 |
| 0.06 | 0.06 | 0.04 | 0.03 | 0.05 | 0.07 | 0.07 | | 0.02 | 0.04 | 0.05 | 0.02 | 0.05 |
| -0.01 | -0.10 | -0.01 | -0.01 | -0.01 | -0.28 | -0.02 | | -0.12 | -0.01 | -0.19 | -0.01 | -0.01 |
| 95.86 | 96.12 | 96.08 | 96.11 | 96.33 | 96.15 | 96.16 | 96.23 | 95.99 | 95.95 | 95.82 | 96.13 | 96.23 |
| 5.866 | 5.839 | 5.845 | 5.791 | 5.815 | 5.754 | 5.823 | 5.712 | 5.803 | 5.889 | 5.845 | 5.832 | 5.847 |
| 2.134 | 2.161 | 2.155 | 2.209 | 2.185 | 2.246 | 2.177 | 2.288 | 2.197 | 2.111 | 2.155 | 2.168 | 2.153 |
| 0.554 | 0.452 | 0.477 | 0.491 | 0.477 | 0.474 | 0.458 | 0.380 | 0.570 | 0.482 | 0.560 | 0.476 | 0.517 |
| 0.149 | 0.172 | 0.169 | 0.168 | 0.154 | 0.173 | 0.150 | 0.139 | 0.150 | 0.150 | 0.161 | 0.171 | 0.164 |
| 0.010 | 0.003 | 0.009 | | | | 0.004 | | 0.003 | 0.009 | 0.002 | 0.021 | 0.008 |
| 1.790 | 1.912 | 1.846 | 1.853 | 1.873 | 1.799 | 1.873 | 2.090 | 1.727 | 1.815 | 1.788 | 1.810 | 1.851 |
| 0.029 | 0.042 | 0.037 | 0.040 | 0.054 | 0.052 | 0.048 | 0.044 | 0.029 | 0.049 | 0.023 | 0.055 | 0.041 |
| 3.171 | 3.086 | 3.177 | 3.170 | 3.185 | 3.230 | 3.238 | 3.293 | 3.255 | 3.163 | 3.165 | 3.146 | 3.128 |
| | | 0.015 | | | 0.006 | 0.001 | 0.011 | 0.011 | 0.010 | | 0.005 | |
| 0.008 | 0.038 | 0.042 | 0.020 | 0.035 | 0.070 | 0.038 | 0.044 | 0.036 | 0.017 | 0.029 | 0.027 | 0.017 |
| 0.066 | 0.097 | 0.085 | 0.091 | 0.123 | 0.119 | 0.110 | 0.102 | 0.066 | 0.113 | 0.052 | 0.126 | 0.093 |
| 1.808 | 1.830 | 1.718 | 1.782 | 1.720 | 1.699 | 1.684 | 1.509 | 1.691 | 1.808 | 1.760 | 1.777 | 1.742 |
| 0.004 | | | | | | | 0.008 | | 0.003 | | 0.008 | |
| 19.578 | 19.640 | 19.570 | 19.623 | 19.621 | 19.622 | 19.604 | 19.621 | 19.540 | 19.620 | 19.541 | 19.615 | 19.568 |
| 3.985 | 3.891 | 3.990 | 3.993 | 3.988 | 3.687 | 3.983 | 4.000 | 3.870 | 3.990 | 3.791 | 3.990 | 3.988 |
| | 0.094 | | | | 0.295 | | | 0.125 | | 0.196 | | 0.005 |
| 0.015 | 0.015 | 0.010 | 0.007 | 0.012 | 0.018 | 0.017 | | 0.005 | 0.010 | 0.013 | 0.005 | 0.012 |
| 1.083 | 1.015 | 1.065 | 0.997 | 1.036 | 0.932 | 1.040 | 0.893 | 1.036 | 1.096 | 1.046 | 1.046 | 1.071 |
| 0.283 | 0.272 | 0.191 | 0.182 | 0.184 | 0.166 | 0.138 | | 0.184 | 0.304 | 0.249 | 0.257 | 0.229 |
| 540 | 601 | 607 | 602 | 548 | 634 | 536 | 465 | 564 | 541 | 586 | 617 | 582 |
| 1.61 | 1.39 | 1.44 | 1.65 | 1.53 | 1.71 | 1.46 | 1.55 | 1.85 | 1.33 | 1.70 | 1.48 | 1.56 |
| 785 | 788 | 773 | 780 | 771 | 801 | 770 | 774 | 809 | 774 | 810 | 779 | 773 |
| 5.4 | 3.76 | 3.92 | 4.88 | 3.43 | 4.19 | 3.11 | 3.96 | 6 | 3.3 | 6.41 | 3.47 | 4.19 |

ME SOS-600P B	ME SOS-600P C	ME SOS-600P I	ME SOS-600P B	ME SOS-600P C	ME SOS-600P I							
39.39	39.78	39.53	39.44	39.65	39.26	39.43	39.88	39.75	39.91	39.72	39.21	39.53
1.42	1.33	1.42	1.66	1.47	1.52	1.59	1.38	1.57	1.39	1.46	1.39	1.45
16.54	15.58	15.61	15.93	15.54	15.57	15.23	15.96	15.80	15.73	15.89	15.73	15.52
13.77	14.61	14.40	14.41	14.57	14.77	14.63	14.28	14.29	14.57	14.51	15.01	15.10
0.28	0.35	0.28	0.36	0.27	0.20	0.34	0.25	0.26	0.25	0.39	0.25	0.41
14.40	14.15	14.31	14.20	14.31	14.15	14.26	14.33	14.49	14.17	14.29	14.10	14.07
0.19	0.08	0.05	0.03	0.08	0.03	0.04	0.12	0.03				0.01
0.28	0.35	0.22	0.36	0.27	0.20	0.34	0.25	0.26	0.25	0.39	0.25	0.41
9.00	9.56	9.37	9.36	9.56	9.51	9.62	9.35	9.72	9.58	9.28	9.77	9.44
									0.10			
0.04		0.21	0.19	0.13		0.09	0.01		0.15	0.08	0.09	0.04
0.13		0.11				0.06	0.03			0.10	0.10	0.09
0.43	0.48	0.45	0.36	0.02	0.93	0.54	0.11	0.04			0.08	
0.08	0.08	0.05	0.07	0.05	0.02	0.03	0.11	0.03	0.03	0.03		0.04
-0.20	-0.22	-0.20	-0.17	-0.02	-0.40	-0.23	-0.07	-0.02	-0.01	-0.04		-0.01
95.94	96.35	96.01	96.37	95.93	96.17	96.18	96.07	96.24	96.14	96.22	95.90	96.12
5.787	5.864	5.837	5.798	5.841	5.827	5.837	5.851	5.828	5.860	5.826	5.798	5.829
2.213	2.136	2.163	2.202	2.159	2.173	2.163	2.149	2.172	2.140	2.174	2.202	2.171
0.651	0.572	0.554	0.558	0.540	0.550	0.494	0.612	0.559	0.583	0.574	0.540	0.528
0.157	0.148	0.158	0.184	0.163	0.169	0.177	0.153	0.174	0.154	0.161	0.155	0.161
0.004		0.025	0.022	0.016		0.010	0.001		0.018	0.009	0.010	0.004
1.692	1.801	1.778	1.772	1.795	1.834	1.812	1.753	1.753	1.790	1.780	1.857	1.862
0.035	0.043	0.035	0.045	0.034	0.025	0.042	0.031	0.032	0.031	0.049	0.031	0.052
3.154	3.110	3.151	3.112	3.143	3.130	3.146	3.135	3.166	3.102	3.126	3.109	3.094
0.016		0.013				0.007	0.003			0.011	0.011	0.010
0.030	0.012	0.008	0.005	0.012	0.005	0.006	0.018	0.005				0.002
0.079	0.099	0.063	0.104	0.077	0.058	0.096	0.071	0.074	0.071	0.112	0.072	0.118
1.686	1.798	1.765	1.755	1.797	1.801	1.817	1.750	1.817	1.794	1.737	1.843	1.775
									0.006			
19.504	19.582	19.548	19.557	19.576	19.572	19.608	19.526	19.578	19.548	19.559	19.629	19.605
3.780	3.756	3.777	3.815	3.978	3.559	3.740	3.922	3.974	3.993	3.955	4.000	3.990
0.200	0.224	0.210	0.167	0.009	0.436	0.253	0.051	0.019			0.037	
0.020	0.020	0.013	0.017	0.012	0.005	0.008	0.027	0.007	0.007	0.007		0.010
1.012	1.079	1.040	1.020	1.057	1.001	1.026	1.089	1.069	1.095	1.063	0.989	1.039
0.240	0.318	0.232	0.220	0.262	0.218	0.239	0.286	0.256	0.301	0.231	0.235	0.230
586	528	574	662	589	605	638	557	637	552	584	547	567
2.15	1.67	1.70	1.83	1.65	1.72	1.52	1.84	1.74	1.72	1.79	1.78	1.65
793	797	802	804	783	839	814	795	801	781	781	804	769
5.31	4.87	5.2	4.83	5.25	6.97	4.38	5.97	6.3	6.38	4.32	7.46	3.76

ME SOS-600P I	ME SOS-600P I	ME SOS-600P I	ME SOS-600P I	ME SOS-600P I	ME SOS-600P B	ME SOS-600P B	ME SOS-600P C	ME SOS-600P B	ME SOS-600P C	ME SOS-600P B	ME SOS-600P C	ME SOS-600P B
39.57	39.56	39.24	39.49	39.37	39.30	38.39	39.58	39.05	39.40	39.37	39.32	38.29
1.57	1.47	1.48	1.34	1.39	1.40	1.43	1.50	1.53	1.49	1.48	1.56	1.17
15.47	15.47	15.52	15.56	15.65	15.97	15.67	15.72	16.24	15.21	15.00	15.92	16.10
15.22	15.26	14.84	15.34	15.14	15.20	16.17	15.20	15.35	15.50	15.21	14.67	17.64
0.36	0.40	0.30	0.40	0.30	0.29	0.24	0.28	0.42	0.40	0.33	0.30	0.33
14.03	13.97	14.04	13.90	14.38	13.86	13.86	14.01	13.42	13.82	13.96	14.24	13.94
0.01		0.10	0.05	0.01		0.23		0.03	0.09	0.22		0.02
0.36	0.40	0.30	0.40	0.30	0.29	0.24	0.28	0.42	0.40	0.33	0.30	0.33
9.51	9.48	9.51	9.59	9.48	9.74	8.93	9.48	9.42	9.72	9.48	9.48	7.91
			0.03	0.01	0.06				0.09			0.04
0.01	0.07	0.07		0.11	0.11	0.16		0.08	0.04	0.08	0.12	0.02
			0.04			0.01		0.01			0.11	0.08
	0.23	0.50			0.68			0.03		0.39	0.25	
0.07		0.10	0.10	0.06	0.02	0.03	0.07	0.10	0.06	0.06	0.03	0.09
-0.02	-0.10	-0.23	-0.02	-0.01	0.00	-0.29	-0.02	-0.04	-0.01	-0.18	-0.11	-0.02
96.17	96.32	96.00	96.25	96.19	96.24	96.04	96.11	96.10	96.22	95.90	96.28	95.96
5.834	5.836	5.823	5.831	5.800	5.795	5.730	5.830	5.771	5.833	5.853	5.789	5.688
2.166	2.164	2.177	2.169	2.200	2.205	2.270	2.170	2.229	2.167	2.147	2.211	2.312
0.522	0.526	0.537	0.539	0.518	0.571	0.486	0.560	0.601	0.486	0.482	0.552	0.507
0.175	0.163	0.165	0.149	0.154	0.155	0.161	0.166	0.170	0.166	0.165	0.172	0.131
0.001	0.008	0.008		0.012	0.012	0.019		0.009	0.004	0.009	0.013	0.002
1.876	1.883	1.842	1.894	1.865	1.874	2.018	1.872	1.897	1.920	1.891	1.806	2.192
0.044	0.050	0.037	0.050	0.037	0.036	0.030	0.035	0.053	0.051	0.041	0.037	0.041
3.082	3.072	3.104	3.059	3.158	3.047	3.084	3.076	2.957	3.051	3.093	3.125	3.087
			0.005			0.001		0.001			0.013	0.009
0.002		0.015	0.008	0.002		0.037		0.005	0.014	0.035		0.003
0.102	0.115	0.086	0.115	0.085	0.082	0.069	0.080	0.121	0.116	0.094	0.085	0.094
1.789	1.785	1.800	1.806	1.782	1.832	1.700	1.780	1.775	1.836	1.799	1.781	1.499
			0.002	0.001	0.003			0.005				0.002
19.592	19.602	19.594	19.627	19.614	19.613	19.606	19.569	19.588	19.649	19.609	19.584	19.567
3.983	3.893	3.740	3.975	3.985	3.995	3.671	3.983	3.961	3.985	3.802	3.876	3.977
	0.107	0.235				0.321		0.014		0.183	0.116	
0.017		0.025	0.025	0.015	0.005	0.008	0.017	0.025	0.015	0.015	0.007	0.023
1.045	1.044	0.998	1.034	1.011	1.001	0.863	1.046	0.963	1.021	1.020	1.003	0.843
0.224	0.241	0.253	0.276	0.180	0.267	0.070	0.224	0.256	0.279	0.274	0.197	
613	570	586	515	547	541	543	582	581	572	579	619	400
1.61	1.62	1.70	1.68	1.70	1.88	1.82	1.74	2.04	1.51	1.44	1.84	2.01
769	800	797	773	771	785	809	770	784	772	792	798	760
4.11	5.03	5.08	4.23	4.97	6.08	5.33	5.47	4.29	3.7	4.05	5.52	3.79

ME SOS-600P C	ME SOS-600P B	ME SOS-600P C	ME SOS-600Q B	ME SOS-600Q C	ME SOS-600Q I								
39.40	39.72	39.40	39.26	39.12	39.07	38.25	39.24	38.23	39.41	39.72	39.46	39.46	
1.61	1.37	1.56	1.40	1.58	1.63	1.44	1.34	1.53	1.34	1.48	1.44	1.44	1.34
15.95	15.79	15.51	15.55	15.25	15.44	15.58	16.11	15.16	15.50	15.55	15.74	16.03	
14.74	14.36	15.03	15.17	15.51	16.04	15.65	14.39	16.94	15.46	14.72	13.34	14.30	
0.28	0.36	0.32	0.33	0.29	0.33	0.36	0.40	0.34	0.36	0.44	0.19	0.10	
14.02	14.68	14.17	14.04	14.07	14.05	14.14	14.26	13.23	13.84	14.07	14.88	13.92	
	0.02	0.09	0.19	0.04	0.01	0.06	0.22	0.40	0.12	0.14			
0.28	0.36	0.32	0.33	0.29	0.33	0.36	0.40	0.34	0.36	0.44			
9.51	9.31	9.58	9.49	9.75	9.22	8.74	9.24	9.27	9.63	9.42	9.41	9.22	
0.19			0.25			1.36							
0.03	0.13	0.10	0.18	0.02	0.06	0.16	0.17	0.20			0.05		
		0.05		0.05		0.16	0.02						
0.09				0.03		0.01	0.35	0.42	0.15		1.60	1.52	
				0.01		0.01	0.08	0.07	0.02	0.11		0.10	
-0.04	0.00			-0.02		-0.01	-0.17	-0.19	-0.07	-0.02	-0.67	-0.66	
96.00	96.21	96.13	96.20	96.05	96.17	96.27	96.23	96.13	96.21	96.14	96.06	95.99	
5.805	5.822	5.809	5.800	5.800	5.776	5.704	5.780	5.735	5.828	5.847	5.849	5.867	
2.195	2.178	2.191	2.200	2.200	2.224	2.296	2.220	2.265	2.172	2.153	2.151	2.133	
0.574	0.550	0.505	0.508	0.465	0.467	0.443	0.577	0.416	0.531	0.545	0.599	0.677	
0.179	0.151	0.174	0.156	0.177	0.181	0.162	0.149	0.172	0.149	0.164	0.161	0.150	
0.003	0.016	0.011	0.021	0.002	0.007	0.019	0.020	0.024					
1.816	1.760	1.854	1.874	1.924	1.983	1.952	1.773	2.126	1.912	1.812	1.654	1.779	
0.035	0.045	0.040	0.041	0.036	0.041	0.045	0.050	0.043	0.046	0.055	0.024	0.012	
3.078	3.207	3.114	3.093	3.110	3.097	3.144	3.131	2.959	3.052	3.089	3.288	3.086	
			0.006	0.006		0.020	0.002			0.006			
	0.003	0.014	0.030	0.006	0.002	0.009	0.035	0.065	0.020	0.023			
0.080	0.104	0.091	0.093	0.083	0.094	0.103	0.115	0.098	0.105	0.126			
1.788	1.741	1.802	1.789	1.844	1.738	1.662	1.737	1.775	1.816	1.768	1.779	1.748	
0.011			0.014			0.080							
19.564	19.577	19.610	19.621	19.653	19.609	19.638	19.589	19.677	19.631	19.587	19.505	19.452	
4.000	3.958	3.998	4.000	3.976	4.000	3.993	3.817	3.783	3.925	3.973	3.250	3.260	
	0.042			0.014		0.005	0.163	0.199	0.070		0.750	0.715	
		0.002		0.010		0.003	0.020	0.018	0.005	0.027		0.025	
1.016	1.064	1.017	0.997	0.977	0.966	0.838	0.990	0.840	1.022	1.067	1.032	1.035	
0.243	0.213	0.220	0.270	0.185	0.075	0.098	0.266	0.158	0.286	0.296	0.202	0.261	
636	557	615	546	615	622	561	539	560	512	585	619	539	
1.86	1.74	1.64	1.68	1.55	1.62	1.77	1.95	1.59	1.66	1.65	1.80	1.98	
806	801	791	801	786	790	773	790	791	788	773	886	852	
6.73	5.25	5.44	5.76	4.6	5.01	3.97	4.51	4.47	4.71	3.91	8.15	7.27	

ME SOS-600Q I	ME SOS-600Q B	ME SOS-600Q C	ME SOS-600Q I	ME SOS-600Q I	ME SOS-600Q B	ME SOS-600Q C	ME SOS-600Q I	ME SOS-600Q C	ME SOS-600Q B	ME SOS-600Q C	ME SOS-600Q B	ME SOS-600Q C
39.84	40.13	39.17	39.55	39.46	39.26	39.46	39.26	39.10	39.27	39.30	38.93	38.71
1.73	1.73	1.44	1.44	1.44	1.44	1.34	1.34	1.59	1.59	1.14	1.28	1.16
15.94	17.76	15.46	15.84	15.84	15.65	15.74	15.36	15.53	16.31	15.81	16.06	15.82
13.34	11.71	14.78	14.40	14.40	14.21	15.36	14.98	14.52	14.05	15.20	15.31	16.17
0.19	0.10	0.10	0.10	0.19	0.19	0.10	0.29	0.10	0.16	0.24	0.24	0.24
14.78	13.92	14.30	14.50	14.11	14.11	14.02	14.02	14.41	14.19	13.89	13.20	13.82
								0.15	0.10	0.01	0.07	0.05
								0.26	0.43	0.12	0.33	0.17
9.60	9.50	9.50	9.60	9.60	9.70	9.60	9.70	9.93	9.27	9.67	9.96	9.68
								0.09	0.06			0.11
								0.02	0.09	0.04	0.04	
0.80	1.10	1.30	0.50	1.00	1.60	0.50	1.10	0.28	0.49	0.53	0.60	
	0.10	0.10				0.10		0.03	0.01	0.09	0.03	0.07
-0.34	-0.49	-0.57	-0.21	-0.42	-0.67	-0.23	-0.46	-0.12	-0.21	-0.24	-0.26	-0.02
96.22	96.05	96.15	95.92	96.04	96.16	96.22	96.04	96.01	96.03	96.04	96.04	95.99
5.846	5.849	5.836	5.835	5.847	5.851	5.837	5.854	5.787	5.783	5.833	5.801	5.755
2.154	2.151	2.164	2.165	2.153	2.149	2.163	2.146	2.213	2.217	2.167	2.199	2.245
0.602	0.900	0.550	0.589	0.614	0.600	0.582	0.554	0.497	0.614	0.599	0.622	0.527
0.191	0.189	0.161	0.160	0.160	0.161	0.150	0.151	0.177	0.176	0.128	0.143	0.130
								0.010	0.007			0.012
1.637	1.428	1.842	1.777	1.785	1.771	1.900	1.867	1.798	1.731	1.886	1.908	2.010
0.024	0.012	0.012	0.012	0.024	0.024	0.012	0.036	0.012	0.020	0.030	0.030	0.030
3.234	3.024	3.177	3.188	3.118	3.135	3.091	3.115	3.179	3.115	3.073	2.932	3.064
								0.002	0.010	0.005	0.005	
								0.024	0.015	0.002	0.011	0.008
								0.074	0.123	0.036	0.094	0.050
1.797	1.767	1.806	1.806	1.815	1.843	1.811	1.844	1.874	1.742	1.830	1.894	1.835
19.484	19.320	19.549	19.532	19.516	19.534	19.547	19.567	19.649	19.554	19.589	19.640	19.666
3.629	3.468	3.362	3.767	3.531	3.246	3.741	3.481	3.861	3.769	3.729	3.710	3.982
0.371	0.507	0.613	0.233	0.469	0.754	0.234	0.519	0.131	0.228	0.249	0.283	
	0.025	0.025				0.025		0.008	0.002	0.023	0.008	0.018
1.083	1.122	0.990	1.042	1.031	1.006	1.030	1.006	0.972	0.995	1.008	0.950	0.912
0.218	0.458	0.172	0.206	0.247	0.263	0.206	0.225	0.261	0.268	0.270	0.385	0.173
719	737	580	585	580	587	518	530	643	645	423	476	416
1.82	2.71	1.69	1.82	1.85	1.80	1.79	1.65	1.68	2.05	1.85	2.02	1.87
882	863	861	871	868	880	841	843	841	828	805	835	782
9.37	9.73	8.12	10.42	8.57	8.69	8.44	6.67	9.14	6.5	6.13	7.95	5.81

ME SOS-600Q B	ME SOS-600Q C	ME SOS-600Q B										
39.54	38.83	39.14	39.30	39.21	39.51	38.58	38.86	38.47	39.24	38.97	38.76	39.47
1.23	1.27	1.31	1.51	1.53	1.48	1.32	1.42	1.66	1.42	1.37	1.66	1.57
16.21	15.53	15.81	15.33	15.09	15.89	16.12	14.61	14.66	14.98	14.96	15.39	15.72
15.72	16.26	15.33	15.30	15.29	14.07	17.50	16.39	16.11	15.40	15.28	15.18	14.07
0.42	0.36	0.30	0.31	0.36	0.18	0.22	0.34	0.22	0.15	0.30	0.36	0.29
12.32	13.31	13.57	14.19	14.30	14.56	13.20	14.08	13.86	14.26	14.47	13.88	14.38
0.10		0.02	0.04	0.13	0.06	0.10	0.13	0.28		0.05	0.28	0.05
0.33	0.45	0.13	0.14	0.14	0.27	0.34	0.19	0.26	0.17	0.16	0.32	0.12
9.48	9.69	10.03	9.72	9.59	9.20	8.32	9.82	9.60	9.77	9.33	9.84	10.01
0.07		0.14		0.05		0.10	0.14	0.20	0.05	0.11	0.20	0.02
	0.01		0.02		0.08					0.07	0.11	
0.58	0.24	0.23	0.36	0.27	0.66	0.14		0.71	0.55	0.91		0.27
0.02	0.04		0.09	0.05	0.06	0.07	0.02	0.02	0.02	0.06	0.05	0.04
-0.25	-0.11	-0.10	-0.17	-0.12	-0.29	-0.07	0.00	-0.30	-0.24	-0.40	-0.01	-0.12
96.01	95.99	96.02	96.31	96.01	96.02	96.01	96.01	96.05	96.01	96.03	96.02	96.02
5.877	5.796	5.809	5.819	5.818	5.825	5.735	5.799	5.773	5.841	5.817	5.757	5.822
2.123	2.204	2.191	2.181	2.182	2.175	2.265	2.201	2.227	2.159	2.183	2.243	2.178
0.718	0.528	0.575	0.495	0.457	0.586	0.559	0.368	0.367	0.468	0.448	0.451	0.556
0.137	0.142	0.146	0.168	0.170	0.164	0.148	0.159	0.187	0.159	0.154	0.186	0.175
0.008		0.017		0.006		0.011	0.017	0.024	0.006	0.012	0.024	0.002
1.955	2.030	1.903	1.895	1.898	1.735	2.176	2.045	2.022	1.917	1.908	1.885	1.736
0.053	0.046	0.037	0.039	0.045	0.023	0.028	0.042	0.028	0.019	0.038	0.045	0.036
2.729	2.960	3.003	3.132	3.164	3.201	2.925	3.133	3.101	3.163	3.219	3.073	3.162
	0.001		0.002		0.009					0.008	0.013	
0.015		0.003	0.006	0.021	0.009	0.015	0.021	0.045		0.008	0.044	0.008
0.094	0.131	0.039	0.041	0.041	0.077	0.097	0.056	0.075	0.050	0.047	0.091	0.036
1.796	1.844	1.899	1.835	1.815	1.729	1.578	1.869	1.838	1.855	1.777	1.864	1.884
19.506	19.683	19.623	19.613	19.618	19.533	19.537	19.711	19.687	19.636	19.619	19.676	19.595
3.722	3.877	3.892	3.809	3.861	3.677	3.917	3.995	3.658	3.736	3.555	3.987	3.864
0.273	0.113	0.108	0.169	0.127	0.308	0.066		0.337	0.259	0.430		0.126
0.005	0.010		0.023	0.013	0.015	0.018	0.005	0.005	0.005	0.015	0.013	0.010
1.049	0.936	0.981	1.005	0.992	1.036	0.891	0.940	0.880	1.001	0.958	0.920	1.028
0.466	0.267	0.308	0.182	0.161	0.211	0.009	0.136	0.149	0.196	0.105	0.247	0.281
426	458	494	591	602	609	462	539	636	558	546	647	643
2.08	1.75	1.85	1.58	1.47	1.84	2.03	1.26	1.33	1.43	1.44	1.63	1.75
805	785	841	801	793	821	768	781	835	830	809	782	838
4.57	4.53	9.53	4.57	3.94	5.77	4.57	4.43	5.5	6.68	3.51	4.92	8.23

ME SOS-600Q C	ME SOS-600Q B	ME SOS-600Q C										
38.94	39.18	39.61	39.40	37.41	38.87	39.43	38.55	39.64	39.28	39.14	39.27	39.30
1.48	1.65	1.55	1.47	1.37	1.43	1.62	1.52	1.14	1.62	1.34	1.63	1.44
15.02	15.13	15.31	15.39	14.27	14.95	15.51	14.84	14.84	15.20	14.97	15.48	15.11
15.94	15.26	14.98	15.32	15.35	15.32	14.82	16.09	14.95	14.35	15.00	15.08	14.79
0.35	0.36	0.27	0.26	0.30	0.33	0.29	0.20	0.39	0.36	0.37	0.22	0.36
13.88	13.85	14.24	14.09	13.52	14.24	14.04	13.56	14.99	14.59	14.70	14.03	14.27
0.10		0.02	0.12	2.00	0.07	0.03	0.35			0.06	0.16	0.10
0.20		0.08	0.02	0.14	0.78	0.07	0.13	0.20	0.17	0.38	0.20	0.11
9.87		9.82	9.50	9.70	9.86	9.75	9.95	10.25	9.87	9.65	9.42	9.93
										0.04	0.06	
				0.05	0.13	0.02		0.02			0.03	
0.06		0.13	0.10	0.03	0.17	0.06		0.16				
0.16	0.56	0.35		0.61	0.89	0.16	0.21		0.54	0.77		0.96
0.03	0.01	0.08	0.03	0.23	0.05	0.03	0.06		0.05			0.03
-0.07	-0.24	-0.17	-0.01	-0.31	-0.39	-0.07	-0.10		-0.24	-0.32		-0.41
96.02	96.03	96.02	95.99	96.00	96.04	96.02	96.01	95.99	96.02	96.01	96.00	96.04
5.802	5.831	5.856	5.826	5.682	5.814	5.829	5.779	5.858	5.821	5.824	5.807	5.854
2.198	2.169	2.144	2.174	2.318	2.186	2.171	2.221	2.142	2.179	2.176	2.193	2.146
0.441	0.486	0.524	0.508	0.236	0.450	0.533	0.401	0.443	0.476	0.449	0.506	0.507
0.166	0.185	0.172	0.163	0.157	0.161	0.180	0.171	0.127	0.181	0.150	0.181	0.161
0.007	0.016	0.011	0.003	0.021	0.007		0.019			0.005	0.007	
1.986	1.900	1.852	1.895	1.950	1.917	1.833	2.017	1.847	1.779	1.867	1.865	1.843
0.044	0.045	0.034	0.032	0.038	0.041	0.036	0.026	0.049	0.045	0.047	0.028	0.045
3.084	3.074	3.138	3.107	3.060	3.175	3.095	3.029	3.301	3.223	3.260	3.091	3.167
				0.006	0.016	0.002		0.002			0.003	
0.015		0.003	0.018	0.325	0.011	0.005	0.056			0.009	0.026	0.015
0.058	0.022	0.006	0.041	0.229	0.019	0.039	0.059	0.050	0.110	0.058	0.030	
1.876	1.865	1.792	1.829	1.910	1.861	1.876	1.960	1.860	1.824	1.787	1.872	1.840
19.676	19.592	19.531	19.603	19.943	19.644	19.596	19.739	19.678	19.638	19.634	19.610	19.579
3.917	3.734	3.816	3.992	3.648	3.566	3.918	3.885	4.000	3.734	3.638	4.000	3.540
0.075	0.264	0.164		0.293	0.421	0.075	0.100		0.253	0.362		0.452
0.008	0.003	0.020	0.008	0.059	0.013	0.008	0.015		0.013			0.008
0.952	0.990	1.054	1.020	0.712	0.944	1.024	0.894	1.058	1.003	0.984	0.999	1.011
0.192	0.196	0.175	0.218	0.645	0.155	0.254	0.293	0.188	0.207	0.127	0.245	0.207
566	642	612	573	536	567	640	576	447	662	541	638	578
1.47	1.51	1.55	1.60	1.21	1.46	1.66	1.41	1.30	1.51	1.42	1.65	1.51
795	826	816	786	804	825	820	831	797	804	823	830	827
4.97	5.5	5.43	5.13	5.74	4.72	7.15	9.08	5.55	3.92	4.02	9.23	4.79

ME SOS-600Q B	ME SOS-600Q C	ME SOS-600Q B										
39.10	39.11	39.57	39.36	39.24	39.21	38.72	39.10	39.57	39.48	38.96	39.02	39.77
1.39	1.66	1.20	1.47	1.51	1.68	1.72	1.77	1.86	1.67	1.80	1.52	1.51
15.00	14.54	15.00	14.91	15.26	15.46	14.85	15.53	14.97	15.20	15.24	15.15	15.22
15.95	15.15	14.58	16.29	14.75	14.84	16.53	14.61	14.42	14.65	14.64	14.71	14.13
0.38	0.19	0.49	0.28	0.19	0.36	0.14	0.23	0.12	0.23	0.21	0.21	0.25
14.17	14.71	14.89	14.47	15.06	14.57	13.80	14.71	14.34	14.62	14.30	14.69	14.64
	0.06	0.02	0.05	0.13	0.03	0.27	0.09	0.26	0.03	0.19	0.40	0.07
0.06	0.10	0.07	0.07	0.23	0.04	0.06	0.01	0.15	0.11	0.16	0.44	0.17
9.85	9.72	9.67	9.01	9.49	9.72	9.65	9.72	9.54	9.72	9.82	9.78	9.41
	0.02		0.05	0.01	0.07	0.13		0.03		0.04		0.04
		0.07			0.11		0.12	0.01				0.02
	0.75	0.46		0.09		0.23	0.26	0.24	0.65			0.79
0.09	0.02	0.01	0.06	0.03	0.03	0.03	0.07	0.06	0.01	0.07	0.01	
-0.02	-0.32	-0.20	-0.01	-0.04	-0.01	-0.01	-0.10	-0.13	-0.11	-0.28	-0.02	-0.33
95.98	96.02	96.03	96.01	96.00	96.00	96.01	96.00	95.72	96.02	96.02	95.99	96.02
5.815	5.831	5.859	5.826	5.790	5.787	5.773	5.775	5.859	5.832	5.792	5.778	5.878
2.185	2.169	2.141	2.174	2.210	2.213	2.227	2.225	2.141	2.168	2.208	2.222	2.122
0.444	0.387	0.478	0.427	0.444	0.476	0.383	0.479	0.471	0.478	0.462	0.422	0.528
0.156	0.186	0.134	0.163	0.167	0.186	0.193	0.196	0.207	0.186	0.201	0.169	0.168
	0.002		0.006	0.001	0.008	0.016		0.003		0.005		0.004
1.983	1.889	1.806	2.017	1.819	1.832	2.061	1.805	1.785	1.810	1.820	1.821	1.747
0.048	0.024	0.061	0.035	0.024	0.046	0.018	0.029	0.016	0.029	0.027	0.026	0.031
3.141	3.269	3.286	3.192	3.312	3.206	3.068	3.238	3.166	3.219	3.170	3.242	3.225
	0.008				0.013		0.014	0.001				0.002
	0.009	0.003	0.008	0.021	0.005	0.043	0.014	0.041	0.005	0.031	0.064	0.011
0.017	0.028	0.019	0.019	0.066	0.011	0.017	0.003	0.044	0.030	0.047	0.127	0.050
1.868	1.848	1.826	1.702	1.787	1.829	1.835	1.832	1.802	1.832	1.862	1.847	1.773
19.657	19.641	19.621	19.568	19.642	19.598	19.647	19.595	19.549	19.590	19.625	19.718	19.539
3.977	3.641	3.782	3.985	3.951	3.992	3.992	3.893	3.861	3.873	3.692	3.982	3.628
	0.354	0.215		0.042			0.107	0.122	0.112	0.306		0.369
0.023	0.005	0.003	0.015	0.008	0.008	0.008		0.018	0.015	0.003	0.018	0.003
0.977	0.981	1.049	1.014	0.992	0.987	0.916	0.970	1.049	1.033	0.953	0.960	1.080
0.129	0.102	0.168		0.116	0.107	0.099	0.103	0.234	0.163	0.205	0.269	0.227
534	666	483	563	617	670	645	707	737	672	712	616	622
1.43	1.21	1.40	1.35	1.51	1.62	1.38	1.66	1.38	1.49	1.56	1.48	1.50
789	850	805	778	812	794	799	854	828	820	866	792	835
4.41	6.3	4.13	3.54	5.92	4.61	6.82	8.16	6.49	5.03	7.37	5.59	5.59

ME SOS-600Q C	ME SOS-600Q B	ME SOS-600R C	ME SOS-600R B	ME SOS-600R C	ME SOS-600R B	ME SOS-600R C	ME SOS-600R B	ME SOS-600R C	ME SOS-600R C	ME SOS-600R B	ME SOS-600R C
39.40	38.65	39.74	39.46	38.78	39.46	38.78	39.17	39.17	39.94	38.30	39.07
1.41	1.50	1.34	1.25	1.25	1.34	1.44	1.25	1.25	1.34	1.44	1.44
15.24	15.40	16.99	16.22	15.65	16.13	16.32	16.32	16.32	16.32	15.36	16.03
14.91	15.87	14.11	14.88	15.84	15.26	15.65	15.26	15.26	14.78	16.70	14.78
0.27	0.25	0.29	0.19	0.19	0.29	0.29	0.19	0.29	0.19	0.29	0.19
14.55	14.91	14.30	14.11	13.63	14.11	13.34	13.92	13.82	13.92	13.73	14.11
0.09	0.08										
0.38	0.26										
9.63	8.78	9.31	9.70	9.60	9.41	10.08	9.89	9.89	9.50	10.08	9.70
0.05	0.04										
0.08	0.08										
0.11	0.50	0.20	0.30	0.80	1.30	0.80	1.50	0.90	1.00	0.60	0.70
0.09	0.09								0.10		
-0.02	-0.07	-0.21	-0.08	-0.13	-0.34	-0.55	-0.34	-0.63	-0.38	-0.44	-0.25
96.01	96.01	96.60	96.01	95.24	96.80	97.20	96.80	97.50	96.90	97.00	95.93
5.821	5.725	5.796	5.814	5.806	5.806	5.756	5.781	5.784	5.854	5.731	5.792
2.179	2.275	2.204	2.186	2.194	2.194	2.244	2.219	2.216	2.146	2.269	2.208
0.474	0.413	0.717	0.632	0.567	0.604	0.611	0.620	0.624	0.674	0.440	0.594
0.157	0.167	0.147	0.138	0.141	0.149	0.161	0.139	0.139	0.148	0.162	0.161
0.006	0.004										
1.842	1.966	1.721	1.834	1.983	1.879	1.942	1.884	1.885	1.812	2.090	1.833
0.034	0.031	0.036	0.024	0.024	0.036	0.036	0.024	0.036	0.024	0.037	0.024
3.205	3.292	3.110	3.100	3.042	3.096	2.952	3.063	3.043	3.042	3.062	3.119
0.009											
0.014	0.012										
0.110	0.074										
1.815	1.660	1.732	1.822	1.833	1.766	1.908	1.862	1.862	1.777	1.924	1.833
19.655	19.629	19.462	19.550	19.590	19.529	19.610	19.591	19.589	19.477	19.714	19.563
3.977	3.926	3.769	3.907	3.858	3.628	3.390	3.627	3.300	3.583	3.501	3.719
0.052	0.231	0.093	0.142	0.372	0.610	0.373	0.700	0.417	0.473	0.281	0.329
0.023	0.023									0.025	
1.019	0.899	1.062	1.026	0.931	1.024	0.923	0.980	0.981	1.098	0.851	0.969
0.225	0.219	0.239	0.184	0.158	0.245	0.235	0.241	0.272	0.085	0.196	0.246
565	591	539	482	465	518	542	472	470	521	537	573
1.51	1.62	2.32	2.01	1.84	1.95	2.12	2.07	2.08	2.01	1.68	1.96
781	787	827	839	833	843	881	869	862	857	850	857
4.63	3.93	6.81	8.32	9.05	6.7	9.75	9.47	7.97	8.47	8.13	8.69
											7.49

ME SOS-600R B	ME SOS-600R C	ME SOS-600R B										
38.88	38.11	38.69	39.46	39.46	41.47	40.70	39.55	39.07	39.07	39.55	38.98	39.07
1.44	1.54	1.44	1.44	1.34	1.15	1.34	1.54	1.44	1.34	1.34	1.34	0.96
16.03	15.65	15.74	15.65	16.13	17.47	17.28	16.03	16.03	15.65	16.42	16.03	16.51
15.74	16.13	15.17	15.26	15.26	11.33	12.67	15.36	15.74	16.03	14.78	15.84	15.65
0.29	0.29	0.19	0.19	0.29	0.19	0.19	0.19	0.19	0.29	0.19	0.29	0.29
13.73	13.44	13.73	14.30	13.82	14.98	14.69	14.02	14.11	13.63	14.11	13.63	14.59
9.89	10.08	9.79	9.70	9.70	8.74	9.02	9.60	9.50	9.98	9.60	9.89	8.93
0.60	0.60	1.30	0.60	0.10	0.70	1.30	0.50	1.30	0.40	0.90	0.70	0.90
-0.25	-0.25	-0.55	-0.25	-0.04	-0.29	-0.57	-0.21	-0.55	-0.17	-0.38	-0.29	-0.38
96.60	95.83	96.05	96.60	96.10	96.03	97.30	96.60	97.40	96.40	96.90	96.70	96.90
5.762	5.727	5.793	5.819	5.816	5.959	5.876	5.816	5.766	5.801	5.807	5.777	5.747
2.238	2.273	2.207	2.181	2.184	2.041	2.124	2.184	2.234	2.199	2.193	2.223	2.253
0.562	0.499	0.571	0.539	0.618	0.919	0.817	0.594	0.554	0.540	0.648	0.577	0.610
0.160	0.174	0.162	0.160	0.149	0.124	0.146	0.170	0.160	0.150	0.148	0.150	0.106
1.951	2.027	1.899	1.883	1.882	1.361	1.530	1.889	1.943	1.991	1.815	1.963	1.925
0.036	0.037	0.024	0.024	0.036	0.023	0.023	0.023	0.024	0.036	0.024	0.036	0.036
3.033	3.011	3.064	3.145	3.038	3.208	3.161	3.072	3.104	3.017	3.089	3.012	3.200
1.869	1.932	1.870	1.824	1.823	1.601	1.662	1.800	1.789	1.891	1.798	1.869	1.675
19.612	19.679	19.591	19.573	19.545	19.237	19.339	19.525	19.575	19.625	19.523	19.608	19.552
3.719	3.715	3.384	3.720	3.953	3.682	3.382	3.767	3.393	3.812	3.582	3.672	3.581
0.281	0.285	0.616	0.280	0.047	0.318	0.594	0.233	0.607	0.188	0.418	0.328	0.419
0.937	0.822	0.915	1.026	1.026	1.318	1.203	1.039	0.965	0.970	1.038	0.953	0.962
0.173	0.142	0.209	0.162	0.230	0.426	0.316	0.188	0.098	0.207	0.226	0.200	0.030
547	582	564	564	513	520	574	594	552	501	526	503	320
1.96	1.87	1.89	1.71	1.96	2.44	2.38	1.89	1.92	1.77	2.08	1.96	2.14
857	873	877	859	824	832	824	870	879	849	860	861	809
8.5	10.07	9.17	8.66	6.91	6.59	6.57	10.68	8.55	9.42	8.35	8.27	5.16

ME SOS-600R C	ME SOS-600R B	ME SOS-600R C											
39.46	39.07	37.66	38.75	38.48	37.90	37.07	38.39	38.62	38.37	38.57	38.75	38.58	
1.34	1.34	1.54	1.51	1.42	1.73	1.49	1.71	1.30	1.23	1.63	1.39	1.54	
16.32	16.42	15.19	15.47	15.96	15.29	14.87	15.00	15.54	16.06	15.19	15.60	15.70	
15.55	14.78	17.84	16.45	16.60	17.76	19.66	17.22	17.07	16.59	17.22	16.54	16.51	
0.38	0.19	0.31	0.25	0.29	0.31	0.36	0.25	0.19	0.19	0.24	0.23	0.24	
12.86	13.63	12.80	13.04	12.58	12.85	12.36	12.87	13.55	13.21	12.74	13.67	13.09	
		0.03	0.06	0.06	0.05	0.12	0.03	0.02	0.06	0.03	0.04	0.06	
		0.02	0.01	0.03	0.05	0.15	0.10	0.08	0.10	0.08	0.09	0.09	
9.98	9.60	10.26	10.06	10.15	9.78	9.65	10.16	9.59	9.90	10.04	9.67	9.99	
		0.19	0.11	0.11	0.24	0.12	0.08		0.02		0.06	0.05	
		0.01			0.01	0.12	0.02	0.04	0.09	0.24		0.12	
0.10	1.00	0.19	0.31			0.15			0.17				
			0.01			0.03	0.03		0.03	0.03	0.06	0.02	
-0.04	-0.42	-0.08	-0.13			-0.01	-0.07		-0.08	-0.01	-0.01	0.00	
96.00	96.04	96.02	96.01	95.65	95.97	95.99	96.01	95.99	96.01	96.01	96.00	95.99	
5.839	5.802	5.692	5.794	5.764	5.698	5.643	5.769	5.759	5.732	5.783	5.765	5.757	
2.161	2.198	2.308	2.206	2.236	2.302	2.357	2.231	2.241	2.268	2.217	2.235	2.243	
0.686	0.675	0.398	0.520	0.581	0.407	0.312	0.427	0.490	0.560	0.466	0.501	0.518	
0.150	0.150	0.175	0.170	0.160	0.195	0.170	0.193	0.145	0.138	0.184	0.156	0.172	
		0.023	0.012	0.013	0.029	0.014	0.009		0.002		0.007	0.006	
1.925	1.836	2.255	2.058	2.080	2.233	2.503	2.165	2.129	2.072	2.159	2.058	2.061	
0.048	0.024	0.039	0.032	0.037	0.039	0.046	0.032	0.024	0.024	0.030	0.029	0.030	
2.838	3.017	2.883	2.906	2.808	2.881	2.804	2.884	3.011	2.942	2.847	3.032	2.913	
				0.001	0.015	0.002	0.005	0.010	0.029		0.015		
		0.005	0.009	0.009	0.008	0.020	0.005	0.003	0.009	0.005	0.006	0.009	
		0.006	0.003	0.008	0.014	0.045	0.028	0.022	0.028	0.022		0.025	
1.885	1.818	1.978	1.919	1.939	1.876	1.874	1.947	1.824	1.886	1.920	1.835	1.902	
19.530	19.521	19.761	19.628	19.635	19.683	19.804	19.692	19.653	19.672	19.663	19.625	19.651	
3.953	3.530	3.909	3.851	4.000	4.000	3.992	3.921	4.000	3.912	3.992	3.985	3.995	
0.047	0.470	0.091	0.147				0.071		0.080				
			0.003			0.008	0.008		0.008	0.008	0.015	0.005	
1.030	0.971	0.751	0.923	0.880	0.787	0.655	0.869	0.900	0.860	0.897	0.919	0.894	
0.364	0.263	0.095	0.238	0.288	0.035		0.170	0.091	0.203	0.180	0.108	0.203	
491	523	547	554	509	617	503	618	463	434	586	515	565	
2.10	2.18	1.67	1.73	2.01	1.68	1.56	1.52	1.75	2.04	1.60	1.76	1.83	
842	862	850	852	850	806	762	831	810	828	813	793	815	
7.84	8.55	9.8	10.25	10.08	6.42	4.24	8.74	8.23	8.18	8.36	6.53	9.04	

| ME
SOS-600R
C |
|---------------------|---------------------|---------------------|---------------------|---------------------|---------------------|---------------------|---------------------|---------------------|---------------------|---------------------|---------------------|---------------------|---------------------|
| 38.23 | 38.25 | 38.58 | 38.58 | 37.63 | 38.93 | 38.62 | 39.54 | 38.26 | 39.19 | 38.31 | 38.39 | 38.89 | |
| 1.69 | 1.54 | 1.41 | 1.41 | 1.60 | 1.44 | 1.65 | 1.45 | 1.34 | 1.35 | 1.41 | 1.40 | 1.46 | |
| 15.28 | 15.50 | 15.53 | 15.53 | 15.35 | 15.94 | 15.09 | 15.49 | 15.45 | 16.04 | 15.70 | 15.21 | 16.35 | |
| 17.34 | 16.97 | 16.93 | 16.93 | 17.65 | 15.91 | 17.19 | 15.48 | 16.92 | 15.91 | 17.20 | 17.33 | 15.25 | |
| 0.25 | 0.18 | 0.32 | 0.32 | 0.30 | 0.35 | 0.19 | 0.22 | 0.31 | 0.30 | 0.29 | 0.31 | 0.19 | |
| 12.91 | 13.46 | 12.94 | 12.94 | 12.54 | 13.06 | 13.11 | 13.66 | 13.17 | 13.27 | 12.60 | 12.85 | 13.66 | |
| | | 0.11 | 0.11 | 0.11 | 0.02 | 0.01 | 0.02 | 0.05 | 0.12 | 0.10 | 0.12 | 0.12 | 0.04 |
| 0.12 | 0.03 | 0.07 | 0.07 | 0.24 | 0.07 | 0.10 | 0.18 | 0.15 | 0.03 | 0.15 | | 0.54 | |
| 10.00 | 9.81 | 9.99 | 9.99 | 10.50 | 9.62 | 10.01 | 9.79 | 10.00 | 9.57 | 9.96 | 10.26 | 9.51 | 0.07 |
| 0.02 | 0.12 | 0.05 | 0.05 | 0.05 | 0.05 | 0.01 | 0.09 | | 0.01 | 0.18 | 0.08 | 0.03 | |
| 0.14 | | 0.07 | 0.07 | 0.11 | 0.05 | | 0.05 | | | 0.05 | 0.04 | | |
| | | 0.02 | | | 0.62 | | | 0.27 | 0.20 | | | | |
| 0.02 | 0.03 | | | | 0.02 | | | | 0.01 | 0.04 | | | |
| 0.00 | -0.02 | | | | -0.27 | | | -0.11 | -0.09 | -0.01 | | | |
| 96.01 | 96.01 | 96.00 | 96.00 | 95.99 | 96.04 | 96.00 | 96.00 | 96.00 | 95.97 | 96.01 | 95.99 | 95.99 | |
| 5.736 | 5.718 | 5.769 | 5.769 | 5.686 | 5.804 | 5.780 | 5.848 | 5.743 | 5.811 | 5.742 | 5.766 | 5.748 | |
| 2.264 | 2.282 | 2.231 | 2.231 | 2.314 | 2.196 | 2.220 | 2.152 | 2.257 | 2.189 | 2.258 | 2.234 | 2.252 | |
| 0.439 | 0.450 | 0.506 | 0.506 | 0.419 | 0.604 | 0.442 | 0.548 | 0.476 | 0.615 | 0.515 | 0.457 | 0.596 | |
| 0.191 | 0.173 | 0.159 | 0.159 | 0.182 | 0.161 | 0.186 | 0.161 | 0.152 | 0.151 | 0.159 | 0.158 | 0.162 | |
| 0.002 | 0.014 | 0.006 | 0.006 | 0.006 | 0.006 | 0.001 | 0.010 | | 0.001 | 0.022 | 0.009 | 0.003 | |
| 2.176 | 2.122 | 2.118 | 2.118 | 2.231 | 1.983 | 2.152 | 1.914 | 2.125 | 1.973 | 2.156 | 2.176 | 1.886 | |
| 0.032 | 0.023 | 0.040 | 0.040 | 0.038 | 0.044 | 0.024 | 0.028 | 0.039 | 0.037 | 0.037 | 0.039 | 0.024 | |
| 2.888 | 2.999 | 2.884 | 2.884 | 2.824 | 2.902 | 2.925 | 3.011 | 2.947 | 2.933 | 2.814 | 2.878 | 3.010 | |
| 0.017 | | 0.008 | 0.008 | 0.013 | 0.006 | | 0.006 | | | 0.006 | 0.005 | | |
| | | 0.017 | 0.017 | 0.017 | 0.003 | 0.002 | 0.003 | 0.008 | 0.020 | 0.015 | 0.018 | 0.020 | 0.006 |
| 0.036 | 0.008 | 0.019 | 0.019 | 0.070 | 0.019 | 0.028 | 0.052 | 0.045 | 0.008 | 0.045 | | 0.154 | |
| 1.915 | 1.871 | 1.906 | 1.906 | 2.024 | 1.829 | 1.911 | 1.847 | 1.915 | 1.810 | 1.905 | 1.966 | 1.793 | 0.004 |
| 19.696 | 19.677 | 19.663 | 19.663 | 19.810 | 19.556 | 19.673 | 19.585 | 19.719 | 19.545 | 19.676 | 19.709 | 19.638 | |
| 3.995 | 3.983 | 4.000 | 4.000 | 4.000 | 3.703 | 4.000 | 4.000 | 3.872 | 3.904 | 3.990 | 4.000 | 4.000 | |
| | 0.009 | | | | 0.292 | | | 0.128 | 0.094 | | | | |
| 0.005 | 0.008 | | | | 0.005 | | | | 0.003 | 0.010 | | | |
| 0.840 | 0.840 | 0.896 | 0.896 | 0.746 | 0.951 | 0.903 | 1.043 | 0.845 | 0.988 | 0.854 | 0.868 | 0.936 | |
| 0.116 | 0.084 | 0.215 | 0.215 | 0.189 | 0.237 | 0.150 | 0.286 | 0.196 | 0.247 | 0.237 | 0.213 | 0.280 | |
| 609 | 566 | 506 | 506 | 570 | 535 | 600 | 553 | 484 | 499 | 497 | 497 | 561 | |
| 1.66 | 1.75 | 1.76 | 1.76 | 1.75 | 1.96 | 1.54 | 1.65 | 1.75 | 1.97 | 1.87 | 1.63 | 2.10 | |
| 806 | 810 | 827 | 827 | 832 | 821 | 832 | 809 | 838 | 817 | 794 | 836 | 816 | |
| 8.53 | 7.8 | 8.7 | 8.7 | 9.71 | 5.42 | 10.45 | 7.54 | 9.21 | 6.18 | 7.63 | 9.63 | 7.62 | |

ME SOS-600R B	ME SOS-600R C	ME SOS-600R B										
38.68	39.03	38.87	38.58	40.24	38.97	39.04	38.71	41.44	38.19	38.86	39.00	38.63
1.37	1.33	1.37	1.45	1.32	1.46	1.12	1.45	1.23	1.43	1.44	1.29	1.42
15.74	16.17	15.96	15.35	15.51	16.08	16.27	16.24	16.44	15.00	16.03	15.53	15.38
16.29	15.83	16.28	16.72	15.92	15.25	16.13	15.76	13.93	17.44	15.95	15.72	16.92
0.16	0.30	0.20	0.36	0.29	0.28	0.24	0.23	0.25	0.31	0.30	0.26	0.21
13.10	13.01	13.02	12.77	11.67	13.56	13.67	13.39	12.12	12.78	12.82	13.62	13.06
				0.15	0.11	0.15	0.05	0.05	0.03	0.13	0.04	0.15
0.74	0.27	0.19	0.08	0.78	0.41	0.21	0.42	0.22	0.37	0.39	0.13	0.28
9.68	9.74	9.76	9.38	9.85	9.64	9.00	9.63	10.25	10.06	9.57	9.81	9.74
0.16	0.18	0.10	1.13	0.10	0.12		0.06	0.06	0.05	0.32	0.29	
0.04		0.18	0.08	0.15	0.12	0.07		0.01	0.12	0.13	0.22	0.09
	0.08	0.06	0.03			0.04	0.01		0.09		0.07	0.09
									0.06			
									0.07			
									-0.04			
95.97	95.94	95.99	95.92	95.99	95.98	95.94	95.95	95.99	96.00	95.94	95.99	95.96
5.767	5.797	5.781	5.797	5.971	5.769	5.771	5.743	6.056	5.755	5.783	5.800	5.774
2.233	2.203	2.219	2.203	2.029	2.231	2.229	2.257	1.944	2.245	2.217	2.200	2.226
0.534	0.626	0.578	0.516	0.684	0.575	0.606	0.583	0.887	0.419	0.595	0.523	0.483
0.154	0.149	0.154	0.164	0.148	0.162	0.125	0.162	0.135	0.162	0.161	0.144	0.160
0.005		0.021	0.009	0.018	0.013	0.008		0.001	0.015	0.016	0.026	0.010
2.031	1.966	2.025	2.101	1.975	1.889	1.994	1.956	1.702	2.198	1.984	1.956	2.114
0.021	0.037	0.025	0.045	0.036	0.035	0.030	0.029	0.031	0.039	0.038	0.033	0.027
2.913	2.880	2.886	2.860	2.582	2.992	3.012	2.962	2.639	2.870	2.843	3.020	2.909
	0.009	0.007	0.003			0.005	0.001		0.010		0.008	0.010
0.214	0.077	0.055	0.022	0.224	0.119	0.061	0.122	0.063	0.109	0.114	0.039	0.081
1.840	1.846	1.852	1.798	1.864	1.820	1.696	1.822	1.911	1.934	1.817	1.861	1.858
0.010	0.011	0.006	0.067	0.006	0.007		0.003	0.003	0.003	0.018	0.017	
19.720	19.601	19.610	19.585	19.560	19.628	19.561	19.647	19.380	19.765	19.607	19.631	19.676
4.000	4.000	4.000	4.000	4.000	4.000	4.000	4.000	4.000	3.954	4.000	4.000	4.000
									0.029			
									0.018			
0.910	0.964	0.939	0.900	1.161	0.950	0.962	0.910	1.335	0.837	0.938	0.961	0.904
0.337	0.327	0.267	0.246	0.724	0.306	0.171	0.260	0.827	0.221	0.360	0.263	0.227
501	487	498	525	454	560	390	545	444	508	528	480	512
1.85	2.04	1.95	1.71	1.69	1.97	2.06	2.08	2.05	1.54	1.99	1.72	1.68
800	808	815	793	794	811	810	816	838	800	811	808	805
7.19	6.57	7.82	5.14	7.36	7.13	6.26	7.6	10.76	6.66	6.78	7.39	7.3

ME SOS-600R C	ME SOS-600R B	ME SOS-600R B	ME SOS-600R C	ME FDS-58 C	ME FDS-58 I	ME FDS-58 I								
38.79	38.37	38.32	38.99	38.42	38.02	38.14	38.87	38.08	38.05	38.63	39.17	38.98	39.46	
1.49	1.36	1.54	1.36	1.45	1.37	1.10	1.32	1.46	1.11	1.30	1.44	1.54	1.34	
15.41	15.86	15.75	15.75	15.45	14.85	15.38	15.94	15.70	15.15	15.41	15.36	15.17	14.78	
16.16	16.22	15.63	15.47	16.88	17.31	16.42	16.53	17.04	19.07	16.44	15.17	16.03	14.78	
0.15	0.27	0.31	0.32	0.20	0.36	0.31	0.34	0.27	0.21	0.28	0.10	0.10	0.29	
13.44	13.25	13.44	13.57	13.24	12.82	13.48	13.53	13.03	13.10	12.97	14.50	13.73	14.40	
0.11	0.09		0.19	0.32	0.18	0.46	0.24	0.43	0.12	0.18				
0.05	0.15	0.24	0.27	0.31	0.27	1.12		0.20	0.17	0.57				
9.68	9.59	9.29	9.63	9.46	10.20	9.33	9.08	9.63	8.52	9.72	9.50	9.89	9.70	
0.09	0.18	1.10	0.22	0.03	0.39			0.05	0.24	0.31				
0.26	0.13	0.18	0.19	0.24	0.13	0.18	0.14	0.09	0.12	0.13				
0.12	0.02	0.12	0.03		0.08	0.04	0.01		0.02					
0.23	0.49										0.80	0.60	1.30	
0.05	0.03													
-0.11	-0.21										-0.34	-0.25	-0.55	
96.01	96.02	95.93	95.99	95.98	95.97	95.96	96.00	95.97	95.89	95.93	96.03	96.02	96.05	
5.786	5.743	5.732	5.785	5.738	5.745	5.708	5.762	5.702	5.726	5.782	5.818	5.820	5.892	
2.214	2.257	2.268	2.215	2.262	2.255	2.292	2.238	2.298	2.274	2.218	2.182	2.180	2.108	
0.494	0.541	0.510	0.541	0.457	0.391	0.421	0.547	0.472	0.413	0.500	0.508	0.489	0.494	
0.167	0.153	0.173	0.152	0.163	0.156	0.124	0.148	0.164	0.126	0.146	0.161	0.172	0.151	
0.031	0.016	0.022	0.023	0.028	0.016	0.022	0.017	0.010	0.015	0.016				
2.015	2.031	1.955	1.919	2.108	2.188	2.055	2.049	2.134	2.399	2.057	1.884	2.002	1.846	
0.019	0.034	0.039	0.040	0.026	0.045	0.039	0.042	0.034	0.027	0.035	0.012	0.012	0.036	
2.988	2.956	2.997	3.003	2.947	2.887	3.007	2.989	2.908	2.939	2.894	3.210	3.056	3.205	
0.014	0.002	0.015	0.003		0.009	0.005	0.001		0.002					
0.017	0.014		0.031	0.051	0.030	0.074	0.038	0.069	0.019	0.029				
0.014	0.045	0.070	0.077	0.089	0.079	0.326		0.059	0.050	0.164				
1.841	1.831	1.773	1.823	1.801	1.965	1.781	1.717	1.839	1.636	1.856	1.801	1.883	1.847	
0.005	0.011	0.065	0.013	0.002	0.023			0.003	0.014	0.018				
19.605	19.634	19.617	19.624	19.671	19.790	19.854	19.548	19.692	19.641	19.716	19.576	19.615	19.580	
3.879	3.760	4.000	4.000	4.000	4.000	4.000	4.000	4.000	4.000	4.000	3.624	3.717	3.386	
0.108	0.232										0.376	0.283	0.614	
0.013	0.008													
0.929	0.862	0.853	0.956	0.868	0.811	0.824	0.936	0.814	0.814	0.905	0.987	0.960	1.039	
0.188	0.201	0.211	0.299	0.194	0.270	0.362	0.106	0.202		0.368	0.114	0.172	0.208	
558	503	587	517	528	488	379	481	527	343	464	574	585	542	
1.68	1.95	1.89	1.82	1.71	1.49	1.69	1.91	1.86	1.61	1.71	1.62	1.56	1.35	
816	813	795	802	802	815	790	810	805	781	793	878	883	842	
7.37	6.31	6	6.43	7.98	8.04	6.09	6.08	8	5.08	6.36	9.58	10.82	6.11	

ME FDS-58 B	ME FDS-58 C	ME FDS-58 I	ME FDS-58 I	ME FDS-58 B	ME FDS-58 C	ME FDS-58 I	ME FDS-58 I	ME FDS-58 B	ME FDS-58 C	ME FDS-58 I	ME FDS-58 B									
39.26	39.65	39.36	39.94	39.84	38.78	39.55	39.07	39.65	39.50	39.56	39.42	39.19	39.37	38.48	39.25	39.33	38.97			
1.25	1.34	1.25	1.34	1.25	1.44	1.44	1.54	1.54	1.48	1.36	1.41	1.63	1.42	1.69	1.50	1.39	1.44			
15.17	15.17	15.17	15.36	15.55	15.17	15.46	14.88	15.07	15.05	15.18	15.00	14.81	14.78	14.47	15.46	15.30	15.17			
14.50	15.65	16.32	14.78	15.07	16.70	14.59	15.65	15.26	15.52	15.26	16.07	15.39	16.23	15.44	14.87	15.54	15.49			
0.19	0.19	0.38	0.38	0.19	0.38	0.29	0.29	0.38	0.34	0.30	0.30	0.32	0.21	0.29	0.36	0.18	0.36			
14.69	14.11	14.40	14.59	14.50	14.40	14.30	13.73	13.92	13.78	14.22	13.49	13.34	13.64	13.68	14.05	13.87	13.87			
										0.02		0.10	0.14	0.08		0.06	0.12			
9.22	9.89	9.12	9.60	9.70	9.12	9.60	9.79	9.60	9.52	9.56	9.75	9.53	9.41	9.62	9.25	9.22	9.49			
										0.28	0.17	0.21	0.16	0.11	0.21	0.24	0.18	0.33		
										0.03	0.15	0.10		0.02		0.09	0.15			
1.80	0.70	1.00	0.90	0.50	0.80	0.80	1.20	0.60	0.43	0.13		1.08	0.37		0.45		0.13			
	0.10			0.10	0.10	0.10	0.10	0.10	0.02	0.09	0.07	0.07	0.08	0.04	0.06	0.08	0.03			
-0.76	-0.32	-0.42	-0.38	-0.23	-0.36	-0.36	-0.53	-0.28	-0.19	-0.08	-0.02	-0.47	-0.17	-0.01	-0.20	-0.02	-0.06			
96.07	96.80	97.00	96.90	96.70	96.90	96.13	96.24	96.12	96.01	95.99	96.05	96.02	94.50	96.01	96.01	96.01	96.01	96.01		
5.865	5.865	5.824	5.872	5.858	5.760	5.860	5.855	5.885	5.867	5.854	5.860	5.871	5.867	5.814	5.817	5.822	5.793			
2.135	2.135	2.176	2.128	2.142	2.240	2.140	2.145	2.115	2.133	2.146	2.140	2.129	2.133	2.186	2.183	2.178	2.207			
0.536	0.509	0.470	0.535	0.554	0.415	0.559	0.484	0.522	0.502	0.501	0.487	0.487	0.464	0.391	0.516	0.493	0.451			
0.140	0.150	0.139	0.149	0.138	0.161	0.160	0.173	0.171	0.165	0.152	0.158	0.184	0.159	0.192	0.167	0.155	0.161			
									0.033	0.020	0.025	0.019	0.012	0.025	0.028	0.021	0.038			
1.811	1.936	2.020	1.818	1.854	2.075	1.808	1.961	1.895	1.928	1.889	1.998	1.928	2.023	1.951	1.843	1.924	1.926			
0.024	0.024	0.048	0.048	0.024	0.048	0.036	0.037	0.048	0.042	0.037	0.037	0.040	0.027	0.037	0.045	0.023	0.046			
3.271	3.112	3.176	3.199	3.178	3.188	3.159	3.067	3.080	3.050	3.136	2.989	2.980	3.030	3.082	3.105	3.061	3.074			
									0.003	0.018	0.011		0.015	0.023	0.012		0.009	0.018		
									0.003		0.015	0.023	0.012		0.009		0.018			
1.756	1.866	1.721	1.801	1.819	1.728	1.814	1.872	1.818	1.804	1.805	1.849	1.822	1.788	1.854	1.749	1.740	1.800			
19.537	19.596	19.575	19.548	19.565	19.615	19.537	19.593	19.534	19.544	19.564	19.607	19.599	19.599	19.693	19.602	19.657	19.663			
3.150	3.647	3.532	3.581	3.743	3.599	3.600	3.406	3.693	3.793	3.917	3.982	3.470	3.805	3.990	3.774	3.980	3.931			
0.850	0.327	0.468	0.419	0.233	0.376	0.375	0.569	0.282	0.202	0.061		0.512	0.174		0.211		0.061			
	0.025			0.025	0.025	0.025	0.025	0.025	0.005	0.023	0.018	0.018	0.020	0.010	0.015	0.020	0.008			
1.008	1.061	1.014	1.101	1.086	0.923	1.047	0.979	1.064	1.041	1.047	1.028	0.998	1.023	0.888	0.998	1.010	0.954			
0.140	0.214	0.014	0.185	0.206		0.208	0.188	0.200	0.199	0.170	0.245	0.315	0.223	0.232	0.282	0.223	0.223			
509	514	464	536	485	546	580	594	599	569	532	527	627	533	659	593	533	556			
1.56	1.48	1.49	1.54	1.64	1.52	1.65	1.43	1.46	1.45	1.49	1.43	1.40	1.34	1.28	1.65	1.56	1.52			
865	849	814	829	827	805	819	829	808	801	801	773	819	797	774	785	771	784			
5.98	7.81	4.5	5.8	7.23	4.16	5.81	5.31	4.18	4.37	5	3.69	3.72	3.92	3.81	3.78	4.28	4.01			

ME FDS-58 C	ME FDS-58 B	ME FDS-58 C	ME FDS-58 I	ME FDS-58 I	ME FDS-58 B	ME FDS-58 C	ME FDS-58 B	ME FDS-58 C										
38.68 1.43 15.11 15.17 0.38 14.91 0.09 0.28 9.57	39.54 1.53 15.41 15.33 0.17 13.56 0.18 0.10 9.48	39.31 1.69 15.12 15.45 0.40 13.59 0.04 0.12 9.54	39.71 1.65 15.43 15.27 0.30 13.50 0.05 0.14 9.67	39.39 1.40 15.07 16.00 0.25 13.35 0.05 0.26 9.54	38.43 1.85 14.49 16.20 0.31 13.04 0.11 1.18 9.58	39.41 1.41 15.19 15.75 0.30 13.69 0.09 0.36 9.63	39.64 1.49 14.90 15.24 0.27 13.83 0.14 0.08 9.83	39.94 1.31 14.90 14.83 0.41 14.43 0.07 0.11 9.55	39.00 1.42 15.15 15.77 0.27 14.05 0.33 0.18 9.10	39.09 1.29 14.76 16.92 0.25 13.82 0.52 0.15 8.62	40.03 1.31 14.79 16.92 0.28 14.17 1.21 0.36 9.17	38.65 1.31 15.03 15.59 0.12 14.30 0.34 0.45 8.28	39.54 1.33 14.99 15.04 0.12 13.68 0.43 0.12 9.44	39.35 1.10 14.92 15.04 0.25 14.32 0.40 0.12 9.35	39.66 1.40 15.45 15.11 0.25 13.92 0.30 0.12 9.42	39.53 1.29 15.23 15.02 0.15 14.09 0.30 0.25 9.32	39.85 1.60 14.98 15.39 0.28 14.04 0.18 0.07 9.32	
0.30 0.08 0.38 0.01 0.00	0.29 0.06 0.32 0.07 -0.17	0.32 0.22 0.22 0.06 -0.15	0.28 0.36 0.36 0.05 -0.11	0.42 0.41 0.41 0.02 -0.16	0.15 0.21 0.34 0.05 -0.15	0.15 0.21 0.18 0.03 -0.01	0.21 0.18 0.78 0.05 -0.33	0.18 0.36 0.40 0.36 -0.02	0.36 0.36 0.36 0.31 -0.13	0.40 0.36 0.27 0.31 -0.02	0.36 0.41 0.43 0.12 -0.13	0.27 0.36 0.43 0.12 -0.01	0.21 0.28 0.28 0.04 -0.02	0.21 0.02 0.12 0.05 -0.02	0.28 0.24 0.24 0.02 0.00			
96.00	96.04	96.03	95.99	96.02	96.01	95.99	96.02	96.00	96.03	96.01	96.01	96.01	96.02	96.01	95.70	96.00	96.00	
5.736 2.264 0.378 0.160 0.035 0.034 1.881 0.048 3.296 0.009 0.014 0.080 1.811	5.858 2.142 0.549 0.170 0.034 0.037 1.900 0.022 2.996 0.007 0.029 0.028 1.792	5.840 2.160 0.488 0.189 0.037 0.032 1.919 0.051 3.011 0.007 0.006 0.033 1.808	5.862 2.138 0.547 0.183 0.032 0.050 1.886 0.037 2.971 0.008 0.008 0.041 1.821	5.858 2.142 0.500 0.157 0.050 0.049 1.991 0.031 2.961 0.008 0.008 0.075 1.810	5.776 2.224 0.343 0.209 0.049 0.018 2.037 0.039 2.921 0.017 0.014 0.102 1.837	5.842 2.158 0.496 0.157 0.025 0.018 1.953 0.037 3.025 0.014 0.014 0.022 1.821	5.884 2.116 0.491 0.166 0.021 0.025 1.892 0.034 3.061 0.023 0.023 0.030 1.861	5.882 2.118 0.512 0.145 0.021 0.043 1.827 0.052 3.168 0.011 0.052 0.030 1.795	5.823 2.177 0.419 0.145 0.043 0.047 1.969 0.034 3.128 0.013 0.052 0.044 1.733	5.811 2.189 0.419 0.144 0.047 0.041 1.969 0.031 3.063 0.013 0.083 0.044 1.635	5.905 2.095 0.519 0.144 0.047 0.041 2.103 0.035 3.116 0.013 0.044 0.044 1.725	5.728 2.272 0.346 0.146 0.031 0.049 1.861 0.016 3.160 0.025 0.335 0.102 1.566	5.877 2.272 0.490 0.146 0.031 0.049 1.932 0.016 3.031 0.025 0.054 0.130 1.789	5.817 2.123 0.508 0.123 0.031 0.042 1.870 0.016 3.156 0.002 0.068 0.033 1.763	5.866 2.183 0.521 0.156 0.033 0.042 1.868 0.019 3.069 0.029 0.064 0.072 1.778	5.852 2.148 0.473 0.143 0.031 0.033 1.859 0.019 3.110 0.029 0.047 0.072 1.754		
19.711 3.997 0.178 0.003 0.905 0.060	19.519 3.807 0.150 0.015 1.045 0.285	19.549 3.832 0.103 0.018 1.068 0.196	19.526 4.000 0.015 0.015 1.024 0.285	19.582 3.881 0.171 0.013 0.875 0.275	19.797 3.816 0.160 0.013 1.024 0.342	19.626 4.000 0.160 0.013 1.063 0.273	19.575 3.828 0.160 0.007 1.103 0.294	19.560 3.993 0.368 0.007 0.965 0.233	19.591 3.632 0.024 0.007 0.975 0.157	19.565 3.976 0.145 0.008 1.120 0.094	19.485 3.855 0.202 0.025 0.900 0.248	19.636 3.992 0.056 0.013 1.048 0.396	19.602 3.773 0.017 0.003 1.012 0.394	19.592 3.931 0.017 0.015 1.062 0.267	19.532 3.981 0.009 0.005 1.043 0.305	19.605 3.976 0.009 0.005 1.090 0.265	19.513 3.995 0.005 0.005 1.090 0.197	
577 1.47 785 4.06	586 1.62 814 7.15	646 1.49 792 3.31	630 1.60 799 6.11	522 1.48 786 4.44	684 1.25 805 4.13	535 1.51 795 5.76	579 1.37 811 5.75	516 1.44 781 3.42	550 1.34 820 5.16	465 1.32 785 5.97	507 1.39 817 5.16	503 1.32 784 6.27	515 1.40 804 4.24	411 1.39 792 5.69	547 1.62 792 5.38	489 1.51 788 5.55	621 1.36 789 5.01	

ME FDS-58																				
B	C	B	C	B	C	B	C	B	C	B	C	B	C	B	C	B	C	B	C	
39.69	39.68	39.67	39.69	39.07	39.83	39.48	39.97	39.07	40.10	39.45	39.99	39.58	39.71	40.43	39.96	40.50	39.22			
1.36	1.37	1.37	1.28	1.47	1.34	1.25	1.30	0.93	1.48	1.19	1.28	1.08	1.43	1.45	1.32	1.32	1.40			
14.73	15.24	15.21	14.94	15.11	15.26	14.99	15.12	14.78	14.84	15.21	15.26	14.74	14.84	15.86	14.60	16.05	14.66			
15.33	14.73	14.17	15.29	16.10	14.98	15.24	14.61	16.28	15.00	15.50	14.88	15.71	15.05	14.39	15.22	14.17	16.49			
0.27	0.20	0.20	0.15	0.27	0.23	0.24	0.25	0.32	0.12	0.19	0.37	0.27	0.30	0.22	0.29	0.20	0.26			
13.91	14.09	13.97	14.07	13.80	14.04	13.99	14.40	13.37	14.13	13.76	14.14	14.03	14.20	13.95	14.14	14.11	14.04			
0.55	0.19	1.49	0.11	0.38	0.10	0.41	0.37	1.16	0.39	0.60	0.22	0.36	0.14	0.05	0.14	0.12	0.10			
0.12	0.16	0.21	0.14	0.18	0.30	0.13	0.38	0.29	0.15	0.53	0.10	0.57	0.06	0.15	0.15	0.26				
9.42	9.43	9.24	9.40	9.15	9.49	9.58	9.28	9.33	9.32	9.37	9.48	9.08	9.28	9.45	9.06	9.10	9.39			
0.18	0.37	0.36	0.29	0.36	0.33	0.27	0.31	0.18	0.38	0.19	0.29	0.33	0.31	0.10	0.15	0.23	0.10			
0.01	0.05				0.09	0.07		0.23	0.06		0.07	0.71	0.08		0.94			0.03	0.10	
0.46	0.52	0.02	0.63			0.34					0.07	0.71	0.08							
0.05	0.04	0.03	0.04	0.09	0.03	0.04		0.04	0.02		0.03	0.05	0.05	0.06	0.02	0.02				
-0.20	-0.23	-0.02	-0.27	-0.02	-0.01	-0.15		-0.01	0.00		-0.04	-0.31	-0.04	-0.01	-0.40	0.00				
96.07	96.04	95.99	96.03	95.98	96.01	96.02	96.00	95.99	96.00	95.99	96.01	96.02	95.99	96.00	96.03	95.99	96.01			
5.892	5.870	5.845	5.892	5.801	5.873	5.861	5.879	5.832	5.905	5.841	5.891	5.893	5.870	5.916	5.938	5.909	5.832			
2.108	2.130	2.155	2.108	2.199	2.127	2.139	2.121	2.168	2.095	2.159	2.109	2.107	2.130	2.084	2.062	2.091	2.168			
0.470	0.529	0.487	0.506	0.445	0.525	0.484	0.500	0.434	0.481	0.495	0.541	0.479	0.456	0.652	0.496	0.669	0.401			
0.152	0.153	0.152	0.143	0.164	0.149	0.139	0.143	0.105	0.164	0.133	0.141	0.120	0.159	0.160	0.147	0.145	0.157			
0.021	0.044	0.043	0.034	0.042	0.038	0.032	0.036	0.022	0.045	0.022	0.034	0.038	0.036	0.011	0.018	0.027	0.011			
1.904	1.822	1.746	1.899	1.999	1.847	1.892	1.797	2.033	1.847	1.920	1.833	1.956	1.861	1.761	1.891	1.729	2.051			
0.034	0.025	0.025	0.019	0.034	0.029	0.030	0.031	0.040	0.016	0.024	0.047	0.034	0.037	0.027	0.036	0.025	0.033			
3.079	3.108	3.068	3.115	3.055	3.085	3.096	3.157	2.976	3.102	3.037	3.105	3.113	3.129	3.043	3.132	3.069	3.113			
0.001	0.006			0.010	0.008			0.028	0.007		0.001	0.003		0.003		0.011	0.011			
0.087	0.030	0.235	0.017	0.061	0.015	0.066	0.059	0.186	0.062	0.096	0.035	0.057	0.023	0.008	0.023	0.020	0.015			
0.036	0.047	0.060	0.041	0.053	0.085	0.039	0.110	0.083	0.044	0.152	0.028	0.162	0.016	0.044	0.043	0.075				
1.784	1.779	1.738	1.780	1.733	1.786	1.814	1.741	1.777	1.751	1.770	1.780	1.725	1.750	1.763	1.718	1.694	1.781			
19.566	19.539	19.560	19.552	19.585	19.568	19.599	19.575	19.682	19.518	19.649	19.516	19.551	19.617	19.441	19.508	19.421	19.649			
3.771	3.747	3.983	3.694	3.977	3.993	3.830	4.000	3.990	3.995	4.000	3.960	3.653	3.950	3.985	3.553	3.995	4.000			
0.216	0.243	0.009	0.296			0.160					0.033	0.334	0.037		0.442					
0.013	0.010	0.007	0.010	0.023	0.007	0.010		0.010	0.005		0.007	0.013	0.013	0.015	0.005	0.005	0.005			
1.071	1.066	1.060	1.071	0.970	1.087	1.036	1.108	0.976	1.129	1.029	1.112	1.057	1.069	1.175	1.117	1.183	0.996			
0.336	0.294	0.569	0.255	0.174	0.301	0.322	0.342	0.462	0.312	0.420	0.281	0.247	0.285	0.333	0.232	0.339	0.117			
527	544	550	492	556	523	477	514	276	581	438	496	383	564	573	513	526	527			
1.28	1.53	1.47	1.39	1.48	1.51	1.42	1.41	1.35	1.28	1.51	1.50	1.31	1.31	1.76	1.22	1.83	1.26			
802	815	795	823	770	780	799	794	769	795	797	793	791	780	799	805	797	785			
4.86	5.68	5.16	5.56	4.25	5.57	5.39	5.65	4.16	6.21	6.01	4.81	4.15	3.43	6.34	3.67	6.66	4.47			

ME FDS-58	BG SOS-600A	BG SOS-600A	BG SOS-600A	BG SOS-600A	BG SOS-600A								
B	C	B	C	B	C	B	C	B	C	B	C	B	C
39.63	39.83	39.47	39.63	38.71	38.46	39.18	39.73	39.58	38.05	37.70	38.01	38.08	37.54
1.24	1.44	1.23	1.55	1.65	1.61	1.44	1.58	1.50	1.56	1.47	1.56	1.53	1.51
14.58	14.71	14.81	14.68	14.04	14.25	14.41	14.58	14.91	15.23	15.91	15.38	14.80	15.18
16.10	15.73	16.40	15.80	17.54	18.18	16.89	15.92	15.72	17.61	18.32	17.99	18.52	17.64
0.35	0.29	0.12	0.25	0.22	0.29	0.27	0.36	0.15	0.41	0.42	0.44	0.39	0.34
14.03	14.00	14.33	13.73	12.83	12.77	13.20	13.64	13.70	12.65	12.76	12.55	12.32	11.80
0.19	0.04	0.12	0.04	0.19		0.17	0.21	0.04	0.12	0.08	0.04	0.13	0.53
0.14	0.21	0.10	0.41	0.23	0.02	0.35	0.14	0.06	0.76	0.33	0.15	0.65	1.80
9.44	9.49	8.94	9.47	9.74	10.00	9.42	9.61	9.49	9.51	8.93	9.80	9.54	9.55
0.21	0.16	0.25	0.34	0.36	0.27	0.22	0.17	0.22					
0.01		0.13	0.06		0.05	0.05	0.01	0.13					
		0.01		0.47	0.06	0.38							
0.09	0.10	0.10	0.06	0.04	0.04	0.05	0.04		0.02	0.07	0.07		
-0.02	-0.02	-0.03	-0.01	-0.21	-0.03	-0.17	-0.01		0.00	-0.02	-0.02		
96.00	96.00	96.00	96.00	96.01	95.99	96.02	96.00	95.50	95.92	95.97	95.99	95.97	95.88
5.883	5.897	5.848	5.877	5.843	5.804	5.869	5.895	5.884	5.725	5.661	5.722	5.751	5.687
2.117	2.103	2.152	2.123	2.157	2.196	2.131	2.105	2.116	2.275	2.339	2.278	2.249	2.313
0.435	0.464	0.435	0.443	0.340	0.339	0.414	0.445	0.496	0.425	0.476	0.451	0.386	0.397
0.138	0.160	0.137	0.172	0.187	0.183	0.162	0.177	0.167	0.176	0.166	0.177	0.173	0.180
0.025	0.019	0.029	0.039	0.042	0.032	0.026	0.020	0.026					
1.999	1.948	2.032	1.960	2.214	2.295	2.116	1.975	1.954	2.215	2.300	2.265	2.339	2.236
0.043	0.036	0.014	0.031	0.028	0.037	0.034	0.045	0.019	0.053	0.054	0.056	0.050	0.043
3.104	3.089	3.166	3.035	2.886	2.873	2.948	3.017	3.036	2.837	2.856	2.816	2.773	2.665
0.001		0.016	0.007		0.006	0.006	0.001	0.016					
0.031	0.006	0.020	0.006	0.031		0.028	0.034	0.006	0.020	0.012	0.006	0.022	0.086
0.041	0.061	0.028	0.119	0.067	0.006	0.100	0.041	0.017	0.221	0.095	0.045	0.191	0.530
1.787	1.793	1.689	1.791	1.876	1.926	1.800	1.818	1.800	1.826	1.710	1.882	1.838	1.846
19.604	19.576	19.566	19.603	19.672	19.695	19.633	19.573	19.538	19.773	19.668	19.700	19.773	19.974
3.977	3.975	3.970	3.985	3.765	3.961	3.807	3.990	4.000	3.995	3.982	3.982	4.000	4.000
		0.005		0.224	0.029	0.180							
0.023	0.025	0.025	0.015	0.010	0.010	0.013	0.010		0.005	0.018	0.018		
1.061	1.091	1.033	1.060	0.925	0.884	0.996	1.078	1.055	0.813	0.752	0.806	0.821	0.732
0.208	0.220	0.062	0.251	0.205	0.095	0.236	0.256	0.211	0.211		0.101	0.188	0.560
458	552	453	589	594	571	525	600	572	552	510	550	526	521
1.20	1.25	1.31	1.24	1.04	1.15	1.18	1.20	1.39	1.65	2.00	1.74	1.45	1.68
769	769	792	770	808	806	792	769	811	764	770	773	775	796
3.05	3.31	4.51	3.72	5.14	7.22	4.06	3.38	7.39	3.97	3.94	4	4.23	6.58
													5.49

BG SOS-600A B	BG SOS-600A C	BG SOS-600A B										
38.75	37.82	38.14	38.21	38.28	38.16	38.26	37.99	38.37	38.10	38.17	38.15	37.81
1.52	1.49	1.47	1.55	1.50	1.75	1.41	1.61	1.55	1.62	1.68	1.77	1.82
16.20	16.00	15.20	15.68	16.35	15.97	16.18	16.13	15.88	15.64	15.96	15.68	16.15
16.78	17.81	18.37	18.42	17.02	17.35	17.09	17.33	17.11	17.68	17.68	18.03	17.70
0.27	0.25	0.36	0.42	0.38	0.25	0.26	0.26	0.38	0.39	0.36	0.33	0.36
12.80	12.62	12.34	12.17	12.50	12.23	13.11	12.32	12.33	12.45	11.98	11.86	11.75
0.10	0.16	0.15	0.12	0.11			0.02	0.11			0.04	0.01
0.13	0.42	0.38	0.27	0.15	0.27	0.28	0.43	0.36	0.21	0.16	0.29	0.19
9.43	9.41	9.48	9.02	9.60	9.69	9.26	9.70	9.86	9.81	9.82	9.82	10.13
			0.06			0.33						
0.03		0.03	0.07		0.01	0.04	0.04	0.02	0.02			0.03
-0.01		-0.03	-0.02		-0.14	-0.01	-0.01	0.00	0.00			-0.01
95.99	95.99	95.99	95.94	95.89	96.00	95.89	95.82	95.95	95.93	95.82	95.95	95.96
5.760	5.673	5.747	5.737	5.718	5.727	5.707	5.700	5.747	5.724	5.733	5.737	5.690
2.240	2.327	2.253	2.263	2.282	2.273	2.293	2.300	2.253	2.276	2.267	2.263	2.310
0.598	0.502	0.446	0.512	0.596	0.553	0.551	0.553	0.550	0.493	0.560	0.516	0.554
0.170	0.168	0.166	0.175	0.168	0.197	0.158	0.182	0.174	0.183	0.190	0.200	0.206
2.086	2.234	2.315	2.313	2.126	2.177	2.132	2.175	2.143	2.222	2.221	2.268	2.228
0.034	0.032	0.047	0.054	0.049	0.032	0.033	0.033	0.049	0.050	0.045	0.042	0.046
2.836	2.822	2.771	2.725	2.783	2.736	2.916	2.755	2.752	2.788	2.683	2.658	2.636
0.015	0.026	0.025	0.020	0.017			0.003	0.017			0.006	0.002
0.039	0.123	0.112	0.078	0.044	0.078	0.081	0.126	0.103	0.062	0.048	0.084	0.056
1.788	1.800	1.823	1.728	1.829	1.854	1.763	1.856	1.883	1.880	1.882	1.884	1.944
19.565	19.706	19.705	19.604	19.612	19.629	19.634	19.682	19.671	19.679	19.628	19.657	19.672
3.992	4.000	3.964	3.982	4.000	3.841	3.990	3.990	3.995	3.995	4.000	4.000	3.992
		0.029			0.157							
0.008		0.008	0.018		0.003	0.010	0.010	0.005	0.005			0.008
0.918	0.772	0.829	0.838	0.846	0.829	0.840	0.800	0.863	0.820	0.831	0.829	0.773
0.192	0.134	0.159	0.085	0.197	0.191	0.091	0.215	0.283	0.142	0.199	0.209	0.220
545	521	504	528	531	616	506	570	547	572	584	608	629
2.07	2.04	1.65	1.88	2.19	2.03	2.09	2.11	1.96	1.86	2.03	1.89	2.15
787	807	772	765	808	822	779	779	787	775	800	803	806
6.01	7.07	4.63	4.1	5.54	7.71	5.63	6.06	5.54	4.85	6.22	7.05	7.55

BG SOS-600A C	BG SOS-600A B	BG SOS-600A C	BG SOS-600A B	BG SOS-600A C	BG SOS-600A B	BG SOS-600A C	BG FDS-11 C	BG FDS-11 C	BG FDS-11 I	BG FDS-11 I	BG FDS-11 I	BG FDS-11 I	BG FDS-11 B	BG FDS-11 C
37.85	38.42	38.23	38.49	38.41	38.13	37.94	38.69	38.40	38.40	38.40	38.50	38.30	38.88	38.86
1.78	1.72	1.63	1.42	1.64	1.69	1.62	1.15	1.63	1.73	1.82	1.92	1.73	1.73	1.66
15.72	15.96	15.87	15.97	15.86	15.96	16.02	16.03	15.94	16.13	15.65	15.84	15.65	16.51	15.88
17.96	17.43	17.43	16.93	17.70	17.99	17.60	17.76	18.24	17.95	18.14	17.95	18.34	17.28	17.05
0.44	0.29	0.32	0.39	0.29	0.31	0.25	0.38	0.29	0.38	0.38	0.19	0.38	0.29	0.24
12.03	11.88	12.44	12.48	12.14	12.30	12.59	12.38	11.81	11.81	11.90	11.90	11.81	11.90	12.26
0.05	0.03	0.07	0.27		0.06									0.09
0.13	0.40	0.08	0.70		0.11	0.20								0.18
9.89	9.73	9.67	9.28	9.82	9.25	9.69	9.60	9.70	9.60	9.70	9.60	9.89	9.50	9.47
														0.20
														0.12
		0.20			0.03			0.20	0.30	0.50	0.50	0.40	0.70	0.70
0.03	0.02	0.01	0.06		0.02					0.10		0.10		
-0.01	0.00	-0.09	-0.01		-0.02			-0.08	-0.13	-0.21	-0.23	-0.17	-0.32	-0.29
95.89	95.89	95.94	96.00	95.87	95.84	95.90	96.20	96.30	96.50	96.60	96.30	96.90	96.80	96.00
5.704	5.757	5.734	5.747	5.758	5.718	5.689	5.782	5.755	5.742	5.761	5.764	5.754	5.777	5.794
2.296	2.243	2.266	2.253	2.242	2.282	2.311	2.218	2.245	2.258	2.239	2.236	2.246	2.223	2.206
0.497	0.577	0.539	0.558	0.561	0.538	0.521	0.606	0.570	0.585	0.528	0.560	0.525	0.669	0.585
0.201	0.194	0.184	0.160	0.185	0.191	0.183	0.129	0.184	0.194	0.206	0.216	0.195	0.193	0.186
														0.014
2.264	2.185	2.187	2.115	2.220	2.256	2.207	2.220	2.286	2.245	2.277	2.248	2.304	2.147	2.126
0.056	0.037	0.040	0.050	0.037	0.039	0.032	0.049	0.037	0.049	0.049	0.024	0.049	0.036	0.030
2.702	2.653	2.782	2.778	2.714	2.749	2.813	2.759	2.638	2.632	2.662	2.657	2.644	2.637	2.725
0.008	0.005	0.011	0.043		0.009									0.014
0.039	0.117	0.022	0.203		0.031	0.059								0.053
1.901	1.861	1.850	1.768	1.878	1.770	1.853	1.830	1.854	1.831	1.855	1.833	1.895	1.801	1.800
														0.012
19.668	19.628	19.615	19.674	19.594	19.582	19.667	19.592	19.580	19.558	19.577	19.539	19.612	19.484	19.544
3.992	3.995	3.903	3.985	4.000	3.981	4.000	3.905	3.858	3.764	3.737	3.811	3.642	3.671	4.000
		0.095			0.014		0.095	0.142	0.236	0.237	0.189	0.333	0.329	
0.008	0.005	0.003	0.015		0.005					0.025		0.025		
0.781	0.871	0.840	0.879	0.870	0.824	0.792	0.913	0.868	0.866	0.869	0.883	0.854	0.940	0.940
0.140	0.287	0.149	0.322	0.176	0.067	0.109	0.194	0.160	0.142	0.130	0.141	0.156	0.221	0.265
616	597	578	500	572	588	575	363	555	591	625	656	589	598	586
1.93	2.01	1.97	1.99	1.96	2.01	2.05	2.03	2.00	2.08	1.85	1.94	1.87	2.23	1.93
787	780	814	770	811	780	806	816	826	839	818	860	833	853	804
5.32	6.46	6.32	4.72	7.76	5.59	7.3	5.94	7.63	6.34	5.47	9.62	6.32	7.65	7.83

BG FDS-11 I	BG FDS-11 I	BG FDS-11 B	BG FDS-11 C														
37.35	37.84	38.27	37.71	37.99	38.36	37.96	38.64	37.86	37.80	37.48	37.27	37.55	38.08	38.01	38.40	37.05	37.97
1.56	1.73	1.68	2.49	2.16	2.34	1.30	1.86	2.23	2.05	2.39	0.08	2.35	2.34	1.34	1.24	1.90	1.60
15.77	15.81	16.05	16.46	16.86	17.03	16.36	15.96	15.50	15.21	15.03	15.33	15.10	15.80	15.57	15.77	15.25	15.78
14.76	17.25	17.31	18.42	17.33	17.03	18.38	16.95	17.85	18.27	18.07	17.51	18.28	17.83	18.30	18.13	18.70	17.73
0.26	0.37	0.24	0.35	0.30	0.38	0.43	0.29	0.31	0.37	0.38	0.36	0.41	0.38	0.32	0.25	0.32	
12.04	12.16	12.26	10.28	10.14	10.54	11.35	12.36	11.95	11.88	11.45	11.60	11.51	10.75	12.56	11.74	11.62	12.43
0.73	0.13	0.23	0.08	0.09	0.12	0.15	0.21	0.12	0.12			0.10	0.18	0.09	0.09	0.33	0.17
4.49	1.01	0.14	0.14	1.07	0.40	0.46	0.12	0.24	0.27	0.29	1.47	0.59	0.78	0.36	0.76	1.07	0.36
8.64	9.54	9.59	9.57	9.40	9.36	9.35	9.34	9.64	9.57	9.32	9.11	9.69	9.28	9.04	9.13	9.44	9.19
0.18	0.06	0.20	0.34	0.58	0.36	0.11	0.17	0.15	0.29	0.94	0.14	0.29	0.35	0.18	0.17	0.09	0.26
0.07	0.03		0.08	0.06		0.10	0.02	0.11	0.12	0.02	2.51	0.04		0.07	0.05	0.12	0.16
0.07	0.02		0.03	0.02	0.01	0.01	0.05			0.25	0.10	0.09	0.06	0.15	0.13		
	0.03				0.06					0.48		0.10					
	-0.01				-0.01					-0.11		-0.02					
95.93	95.99	95.97	95.94	95.97	96.01	95.95	95.97	95.95	95.96	95.38	95.74	95.93	95.99	95.96	95.95	95.93	95.98
5.617	5.687	5.728	5.687	5.712	5.730	5.713	5.761	5.698	5.710	5.716	5.688	5.690	5.739	5.714	5.771	5.630	5.699
2.383	2.313	2.272	2.313	2.288	2.270	2.287	2.239	2.302	2.290	2.284	2.312	2.310	2.261	2.286	2.229	2.370	2.301
0.412	0.488	0.560	0.614	0.700	0.729	0.614	0.564	0.449	0.418	0.418	0.446	0.388	0.546	0.474	0.565	0.362	0.491
0.177	0.195	0.189	0.282	0.244	0.263	0.147	0.209	0.252	0.233	0.274	0.009	0.268	0.265	0.152	0.140	0.217	0.181
0.008	0.003		0.009	0.007		0.011	0.002	0.013	0.014	0.002	0.302	0.005		0.008	0.006	0.014	0.019
1.857	2.168	2.167	2.324	2.179	2.128	2.314	2.114	2.246	2.308	2.304	2.235	2.317	2.247	2.301	2.279	2.377	2.226
0.033	0.048	0.030	0.044	0.038	0.049	0.055	0.036	0.039	0.048	0.050	0.046	0.053	0.049	0.040	0.032	0.040	
2.698	2.725	2.735	2.312	2.272	2.347	2.546	2.746	2.681	2.676	2.604	2.638	2.601	2.415	2.814	2.630	2.631	2.782
0.008	0.002		0.003	0.002	0.001	0.001	0.006			0.031	0.012	0.010	0.007	0.019	0.016		
0.118	0.022	0.037	0.012	0.014	0.020	0.025	0.034	0.019	0.020		0.016	0.029	0.014	0.014	0.053	0.028	
1.310	0.294	0.042	0.042	0.311	0.117	0.134	0.036	0.070	0.079	0.085	0.435	0.172	0.227	0.106	0.221	0.314	0.106
1.657	1.829	1.831	1.841	1.803	1.783	1.795	1.776	1.850	1.844	1.813	1.774	1.873	1.784	1.734	1.750	1.829	1.759
0.011	0.003	0.012	0.020	0.034	0.021	0.006	0.010	0.009	0.017	0.056	0.009	0.017	0.020	0.011	0.010	0.005	0.015
20.288	19.777	19.603	19.504	19.603	19.458	19.649	19.534	19.628	19.657	19.607	19.877	19.713	19.598	19.670	19.675	19.851	19.647
4.000	3.992	4.000	4.000	4.000	3.985	4.000	4.000	4.000	4.000	3.876	4.000	3.974	4.000	4.000	4.000	4.000	4.000
	0.008				0.015					0.124		0.026					
0.695	0.777	0.845	0.757	0.802	0.859	0.798	0.903	0.782	0.775	0.727	0.691	0.733	0.820	0.805	0.870	0.651	0.797
1.103	0.313	0.231	0.231	0.556	0.393	0.294	0.204	0.121	0.125	0.132	0.587	0.173	0.353	0.078	0.323	0.238	0.143
588	610	592	779	702	758	410	658	750	698	788	-1249	773	758	454	392	645	563
1.94	1.96	2.05	2.34	2.52	2.56	2.26	1.97	1.80	1.67	1.66	1.83	1.64	1.97	1.83	1.94	1.75	1.93
801	774	809	804	813	782	802	810	801	792	785	795	787	772	794	794	795	804
7.69	4.56	8.42	6.6	6.94	5.4	4.97	7.08	6.51	4.95	4.44	5.43	4.71	4.95	4.85	5.86	6.71	5.98

| BG
FDS-11 |
|--------------|--------------|--------------|--------------|--------------|--------------|--------------|--------------|--------------|
| C | C | C | C | C | C | C | C | C |
| 37.85 | 38.19 | 37.80 | 39.31 | 34.92 | 38.89 | 39.08 | 38.22 | 37.86 |
| 1.71 | 1.71 | 2.41 | 2.18 | 0.84 | 1.13 | 1.10 | 1.59 | 1.73 |
| 15.86 | 15.92 | 15.53 | 15.69 | 12.36 | 15.28 | 15.74 | 15.83 | 15.80 |
| 17.77 | 17.36 | 18.55 | 17.33 | 0.23 | 17.24 | 16.49 | 17.75 | 17.17 |
| 0.43 | 0.40 | 0.32 | 0.36 | 0.12 | 0.28 | 0.17 | 0.37 | 0.26 |
| 12.44 | 12.62 | 11.58 | 10.58 | 9.97 | 12.76 | 13.26 | 12.20 | 11.90 |
| 0.01 | 0.11 | 0.01 | 0.07 | | | 0.09 | 0.12 | 0.18 |
| 0.29 | 0.26 | 0.23 | 0.15 | 4.49 | 0.30 | 0.36 | 0.20 | 1.25 |
| 9.36 | 9.16 | 9.22 | 9.83 | 8.55 | 9.59 | 9.32 | 9.52 | 9.50 |
| 0.17 | 0.08 | 0.18 | 0.19 | | 0.21 | 0.24 | | |
| 0.06 | 0.13 | | 0.03 | 3.12 | 0.21 | 0.10 | 0.09 | 0.25 |
| | | | 0.08 | 0.01 | 16.20 | 0.02 | 0.02 | 0.04 |
| | | | | | | 5.27 | | |
| | | | | | | -1.19 | | |
| 95.95 | 95.93 | 95.90 | 95.73 | 96.09 | 95.91 | 95.98 | 95.90 | 95.95 |
| 5.685 | 5.709 | 5.697 | 5.891 | 5.705 | 5.823 | 5.810 | 5.732 | 5.690 |
| 2.315 | 2.291 | 2.303 | 2.109 | 2.295 | 2.177 | 2.190 | 2.268 | 2.310 |
| 0.492 | 0.514 | 0.457 | 0.661 | 0.086 | 0.520 | 0.569 | 0.531 | 0.490 |
| 0.193 | 0.192 | 0.273 | 0.246 | 0.103 | 0.128 | 0.123 | 0.180 | 0.195 |
| 0.007 | 0.016 | | 0.003 | 0.403 | 0.025 | 0.011 | 0.010 | 0.030 |
| 2.232 | 2.170 | 2.338 | 2.172 | 0.031 | 2.159 | 2.051 | 2.227 | 2.159 |
| 0.055 | 0.051 | 0.040 | 0.046 | 0.017 | 0.035 | 0.022 | 0.048 | 0.033 |
| 2.785 | 2.813 | 2.601 | 2.363 | 2.429 | 2.848 | 2.938 | 2.728 | 2.667 |
| | | | 0.009 | 0.001 | 2.128 | 0.002 | 0.002 | 0.005 |
| 0.002 | 0.017 | 0.002 | 0.011 | | | 0.014 | 0.020 | 0.029 |
| 0.084 | 0.075 | 0.067 | 0.045 | 1.423 | 0.086 | 0.105 | 0.059 | 0.364 |
| 1.793 | 1.746 | 1.772 | 1.879 | 1.782 | 1.832 | 1.768 | 1.822 | 1.822 |
| 0.010 | 0.004 | 0.011 | 0.011 | | 0.012 | 0.014 | | |
| 19.653 | 19.599 | 19.569 | 19.438 | 20.403 | 19.647 | 19.618 | 19.624 | 19.793 |
| 4.000 | 4.000 | 4.000 | 4.000 | 2.541 | 4.000 | 4.000 | 4.000 | 4.000 |
| | | | | 1.459 | | | | |
| 0.778 | 0.831 | 0.773 | 1.019 | 0.308 | 0.948 | 0.973 | 0.838 | 0.780 |
| 0.076 | 0.092 | 0.016 | 0.465 | | 0.277 | 0.285 | 0.173 | 0.404 |
| 601 | 608 | 782 | 714 | 1039 | 368 | 369 | 555 | 606 |
| 1.98 | 1.97 | 1.83 | 1.87 | 0.68 | 1.64 | 1.83 | 1.95 | 1.95 |
| 801 | 808 | 797 | 812 | | 791 | 804 | 799 | 805 |
| 4.49 | 4.65 | 6.08 | 6.7 | | 6.26 | 7.22 | 5.56 | 6.84 |